Spirit of Amelia

Purdue University

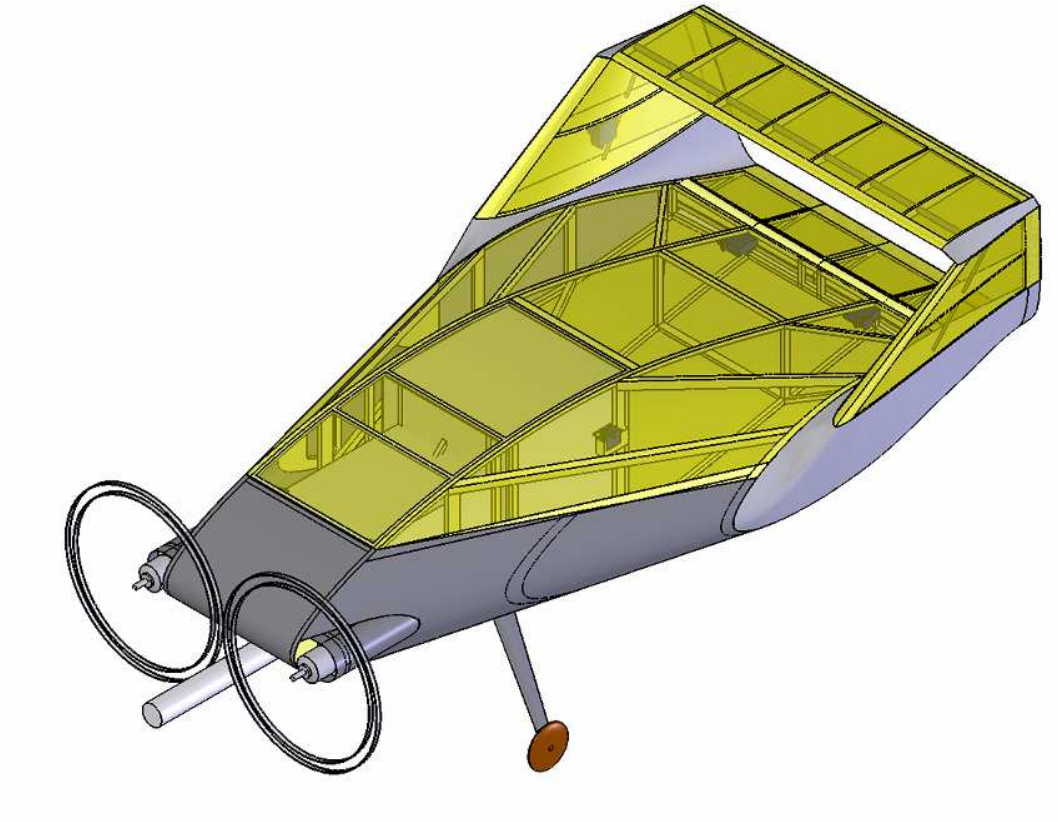

AIAA Design, Build, Fly
2006-2007

Design Report

1. Executive Summary

This report describes the design, manufacturing, and testing techniques used for development of Purdue University's entry to the 2006-2007 AIAA Student Design/Build/Fly Competition. A spiral design approach was used to systematically design and optimize an aircraft to yield the highest total score which is a combination of the written report score, total flight score, and rated aircraft cost (RAC).

1.1 Design Spiral One

The first design spiral was accomplished in four stages; conceptual design, preliminary design, manufacturing, and testing. During conceptual design, the competition rules and requirements were integrated into a mission modeling and scoring analysis program, concluding that the primary scoring factor was the minimization of wingspan. This analysis was used to identify and properly weight figures of merit (FOM). Selection matrices based on the FOM were used to narrow aircraft selection to three general wing types; biplane, lifting body, and faceted-lifting body. Next, preliminary design focused on refining the three aircraft to identify an optimal configuration. By minimizing the span and allowing it to fit in the box, the aircraft was sized to maximize total score. With the aircraft sized at a span of 2.4 ft, a more detailed wing analysis was performed to investigate wing sizing. As a result of this analysis, winglets were added to the Lifting Body and the span was shortened to 2 ft. yielding a 44% increase in total score. The three aircraft were refined to include the aircraft sizing and, as a means of comparison, were scored in a performance analysis. All three aircraft were then built and wind tunnel tested. Additionally, the Facet and Lifting Body were flight tested and studied with computational fluid dynamics. The actual construction and testing of the aircraft provided valuable data that served two functions. First, it demonstrated that the unconventional designs could be successfully built and flown. Second, the results of the testing validated computer models and led to the selection of a single configuration, the Lifting Body.

1.2 Design Spiral Two

The second design spiral consisted of four stages; preliminary design, detail design, manufacturing, and testing. The optimization of the Lifting Body in preliminary and detail design was emphasized. First, airfoil, sweep, and winglet analyses ensured the selection of the optimal wing geometry. A propulsion systems analysis selected an optimum motor, which was purchased with two others for testing. The airframe was lightened through structural analysis. Spiral one flight testing and a stability analysis illustrated the need to stabilize the aircraft. This was accomplished by adding a horizontal stabilizer. Furthermore, the aircraft's motor was changed from a single pusher to a twin tractor, counter-rotating configuration. This removed the motor from a high mounting location, eliminated left-turning tendencies, and allowed for yaw control with differential thrust. During spiral one flight testing, the tail-dragger configuration of the Facet was observed to takeoff in a short distance and was thus adopted for use on

the Lifting Body. Figure 1.1 illustrates the design process and aircraft evolution. The final aircraft configuration is shown in Figure 1.2.

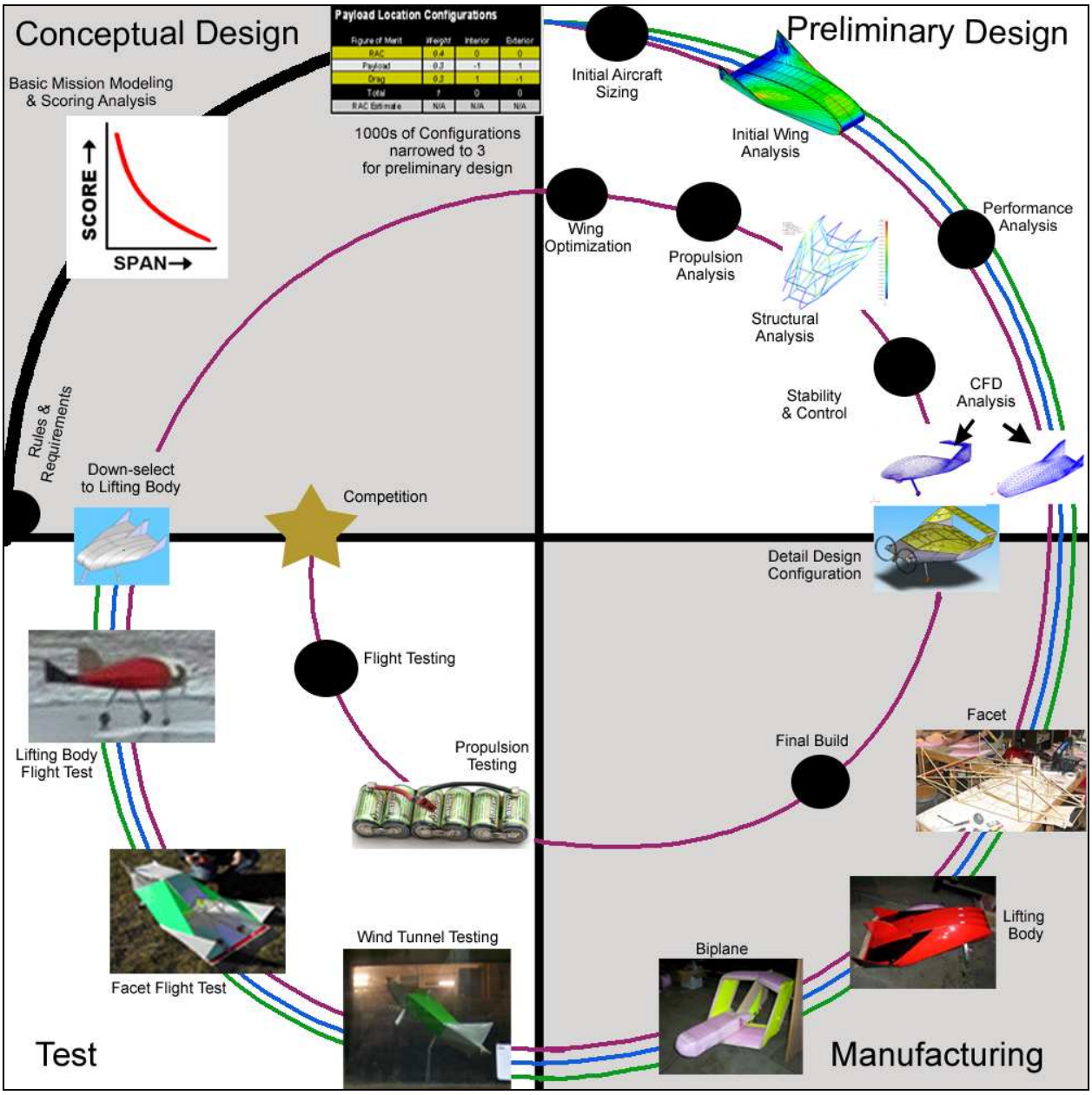

Figure 1.1 – Spiral Design Process and Aircraft Evolution

Aircraft Walk Around

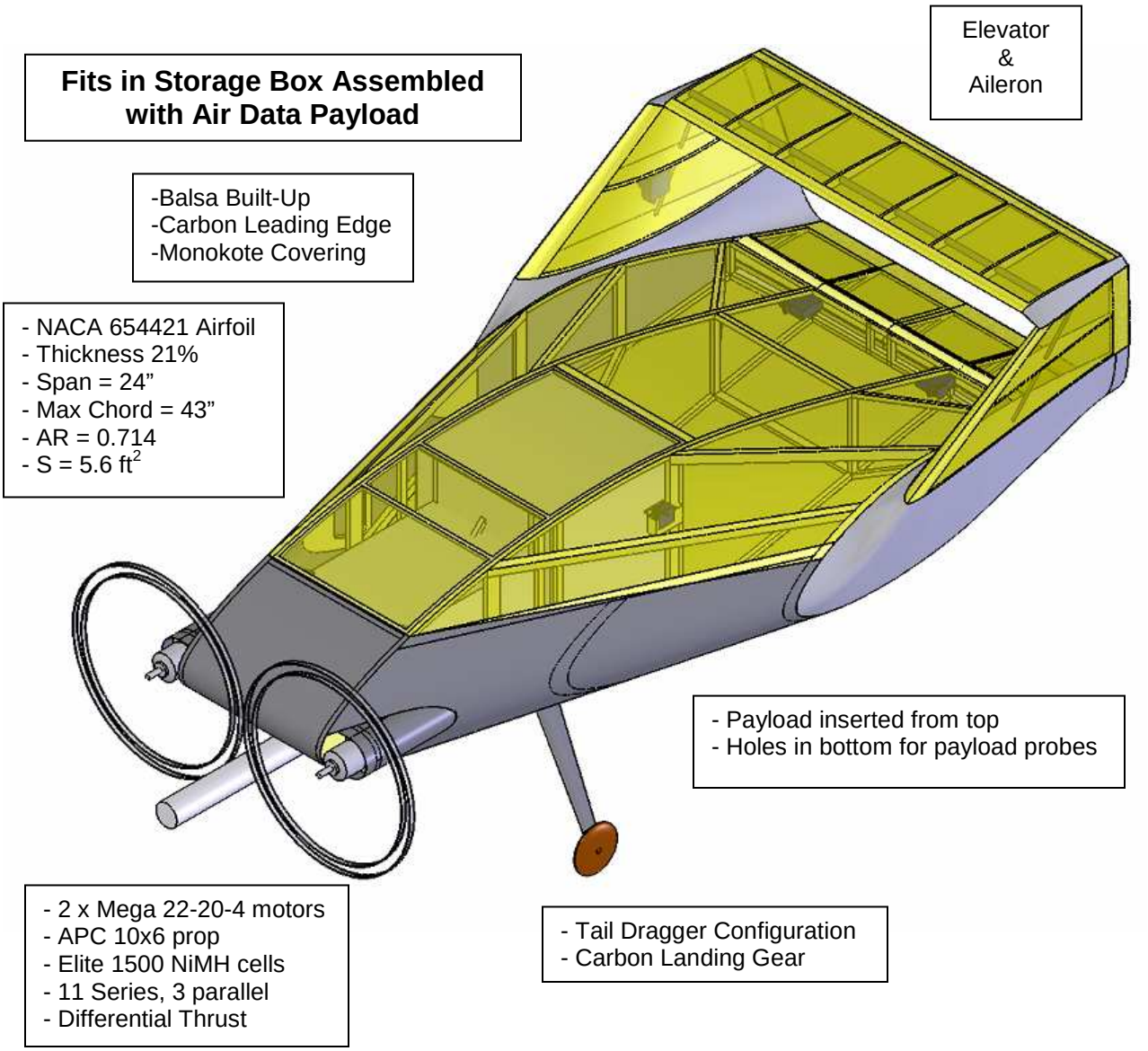

Figure 1.2- Final Aircraft Configuration

2. Management Summary

The successful design, construction, and testing of an aircraft is a complex task that requires a well managed team. The first step, therefore, was to organize a team and develop a project schedule. The project schedule with actual progress denoted follows below (Figure 2.1).

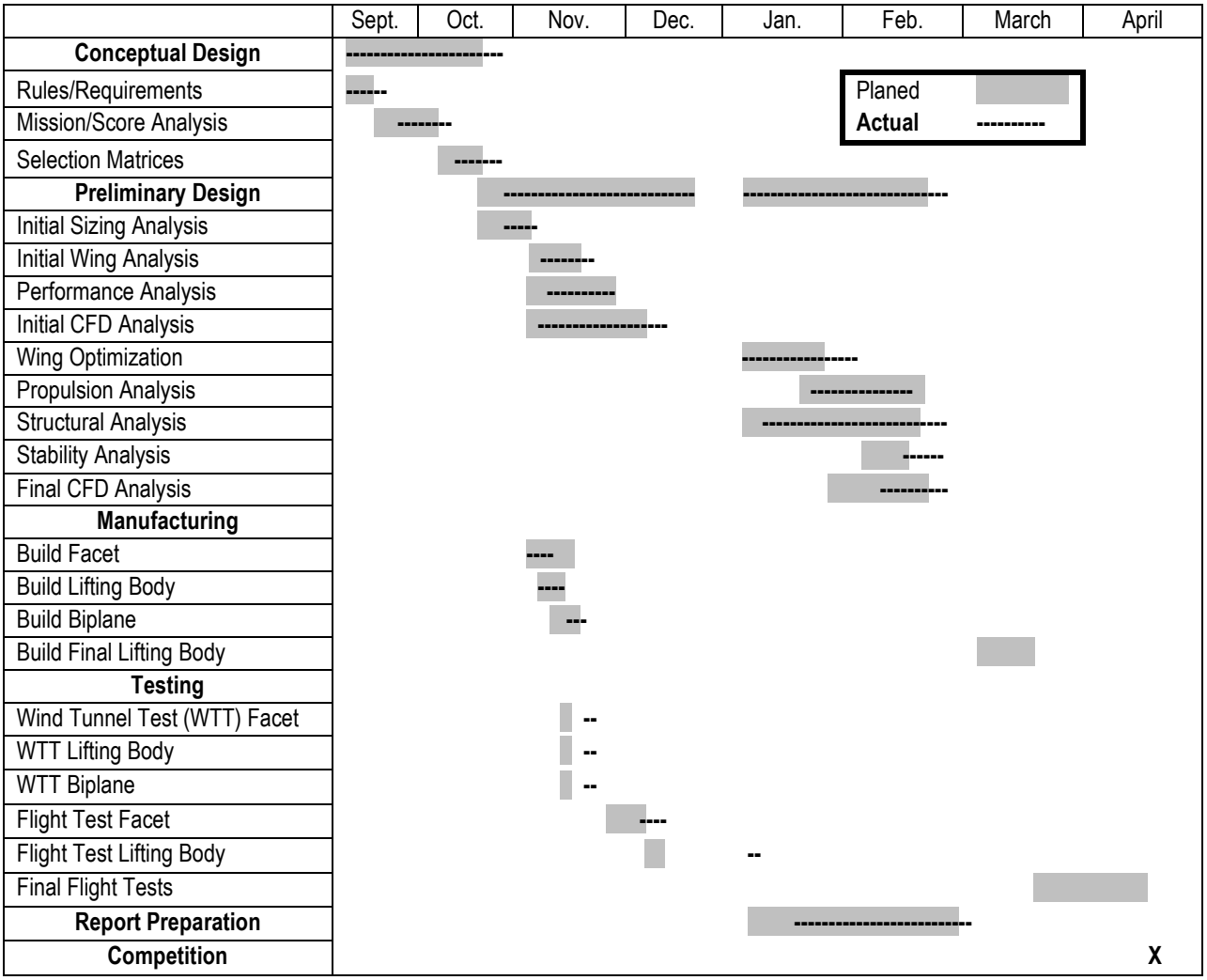

Figure 2.1 – Milestone Chart of Design Progress

2.1 Team Organization and Assignments

During the first design spiral the team initially divided in half, creating equally balanced subgroups that operated independently so that no ideas were overlooked. Each team analyzed the rules, scoring factors, and brainstormed aircraft configurations with the goal of maximizing the score. The teams rejoined after design reviews and selected aircraft configurations for further investigation. The second spiral concentrated on optimization. Team members were assigned a sub-team in the areas of structures, aerodynamics, stability, and propulsion. This allowed for a more efficient and detailed analysis of the aircraft. Table 2.1 lists the team members and their primary areas of responsibility.

Table 2.1 - Team Members and Responsibilities

Name	Responsibilities	Name	Responsibilities
Aaron Wypyszynski	Team Leader/CAD	Stefan Oechsner	Propulsion/Programming
Jessica Schoenbauer	Propulsion/Structures	Jonathan Huseman	Construction/Propulsion
Matt Conrad	CAD/ Weight & Balance	Laura Markee	Aerodynamics/CFD
Paulina Rabczak	Stability and Control	Pritesh Mody	Aerodynamics/CFD
Mark Kannen	Construction/Report	Liaquat Iqbal	Graduate Student Mentor
Kyle Noth	Aerodynamics/CFD		

3. Conceptual Design

The goal of conceptual design was to identify aircraft configurations that would yield the highest score. This was accomplished in three phases. First, the competition rules and mission requirements were thoroughly analyzed. Next, a computer program was written to identify important relationships between aircraft performance and scoring. Results from these two steps were used to further investigate potential aircraft configurations. Three configurations were finally chosen for further analysis and refinement in the preliminary design.

3.1 Mission Requirements and Profiles

The aircraft must fit into a box of 2 ft x 4 ft x 1.5 ft, and other important limitations include a 100 ft takeoff limit and a maximum battery weight of 3 lbs. The competition includes four missions and two payloads; air sampler and camera ball systems. Two of the four missions require flying a payload around a rectangular course. The two ground missions involve reconfiguration and deployment of the aircraft.

3.1.1 Payloads

Air Sampler – The air sampling system consists of an 18 in. “L” shaped tube and a processor unit. The processor unit is an 8 in. x 8 in. x 8 in. cube weighing 3 lbs (Figure 3.1.a).

Camera Ball – The camera ball consists of a 12-inch softball and a processor unit. If the aircraft is configured as a tail-dragger the camera ball must be located forward of the landing gear and if tricycle landing gear is used the ball must be located behind the landing gear. The processor unit is a 4 in. tall, 6 in. wide and 15 in. long box weighing 5 lbs (Figure 3.1.b).

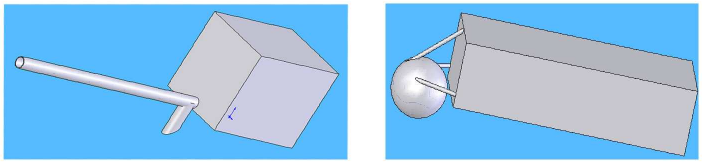

A B

(a) Air Sampler (b) Camera Ball

Figure 3.1 – Payloads

3.1.2 Mission Profiles

The four missions are described below and the scoring equations are shown in Table 3.1. The course layout is shown in Figure 3.2.

- **Dash** – The aircraft flies two timed laps of the course with the air sampler payload installed. Time begins when the throttle is advanced and ends when the aircraft passes over the starting line in the air.
- **Loiter** – The aircraft flies two laps, each 2 minutes long, with the camera ball system installed. Time begins when the throttle advances and ends when the aircraft passes over the starting line in the air.
- **Reconfiguration** – The aircraft is preconfigured with the camera ball system and the installation of the air sampler payload is timed.
- **Deployment** – The team is timed for deploying the aircraft for flight with the air sampler payload installed. The aircraft and both payloads must initially be inside the storage box.

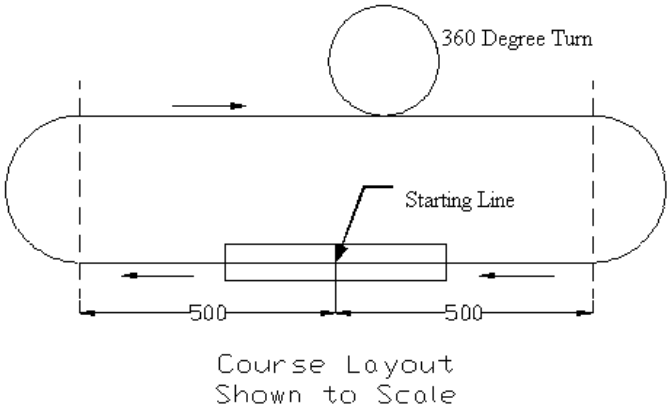

Figure 3.2 – Course Layout

Table 3.1 – Mission Scoring Equations

	Dash	Loiter	Reconfiguration	Deployment
Scoring Equation*	$\frac{1}{\text{Total Lap Time}}$	$\frac{1}{\text{RAC}^{**}}$	$\frac{1}{\text{Time}}$	$\frac{1}{\text{Time}}$

*All scores are normalized to the best score for each mission

** RAC = Manufacturer's Empty Weight (MEW) x Wing Span (SPAN) (3.1)

The highest score from each of the four missions is summed to compute the Total Flight Score. The overall score is calculated by;

$$\text{Score} = \frac{\text{Written Report Score} \times \text{Total Flight Score}}{\text{RAC}} \quad (3.2)$$

3.2 Mission Modeling and Scoring Analysis

Conceptual design continued by identifying relationships between aircraft capabilities and flight score by developing a program to analyze parameters for the flying missions. The inputs to the program included aspect ratio (AR), number of wings, and maximum velocity (V_{max}). The program iterated V_{max} over a range of wing loadings to determine what velocity resulted in the highest score. The program output three mission constraint diagrams; the power loading required, the energy required per pound, and the battery weight for each mission. Each constraint diagram was based on wing loading. A final graph showed the flight score with respect to wing loading. To generate graphs for this section the program was run for an AR of 1 and a V_{max} of 103 ft/s to demonstrate the methodology, unless otherwise noted.

For the Dash mission, the program divided the mission into takeoff, climb, cruise, and turn sections. Landing was not included because the mission ends with the aircraft still in the air. Time, distance, and energy & power per pound were calculated for each of the sections.

The Loiter mission was analyzed in a similar iterative manner, by minimizing the power[1] by calculating the optimal value of C_L. This allowed the calculation of an optimal loiter velocity. The program calculated the time required for the two 1000 ft straight legs and adjusted the radius of the turns so that each lap took 120 seconds to complete. This analysis was performed twice because the first lap includes the takeoff and climb, so the turns will have a smaller radius than the turns of the second lap. The results of these analyses can be seen in Figure 3.3 and illustrates the difference in power requirements for each mission.

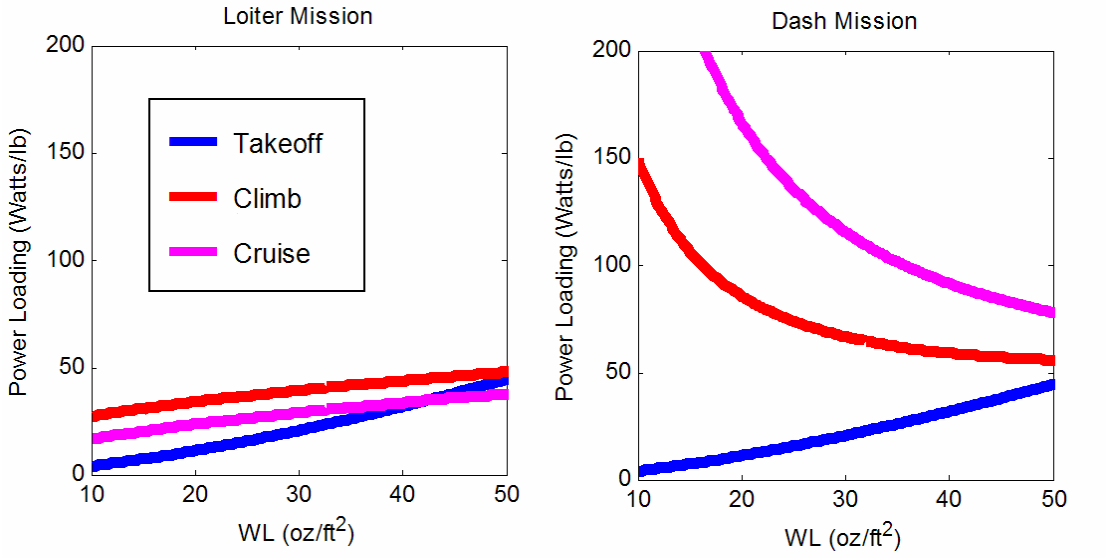

Figure 3.3 – Power Loading Comparison between Loiter and Dash Missions

The program then calculated the battery and aircraft weight for each mission. The weight of the heaviest payload determined the base empty weight of the aircraft, since that mission requires more energy per pound. The program iterated to converge on the final battery weights and total weight of the empty

aircraft for each mission. The historical data used to determine the battery weights and the energy requirements for each mission are shown in Figure 3.4.

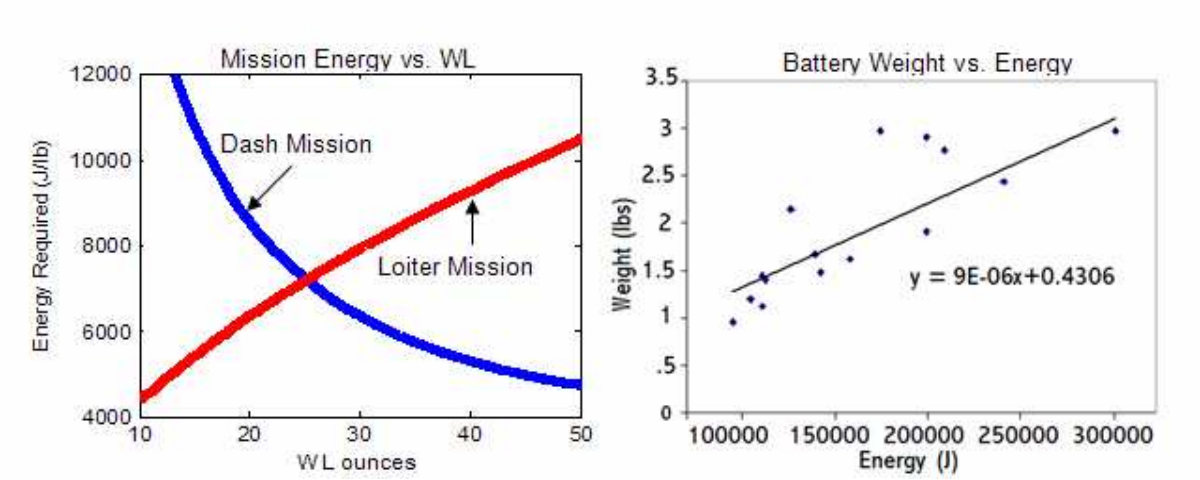

Figure 3.4 – Energy Requirements and Historical Battery Weights

The battery weights for the two missions, the airframe weight, and the total empty weight were then plotted for the range of wing loading values. In the graph below, the plot used to determine battery weight and the following calculated weights are shown (Figure 3.5).

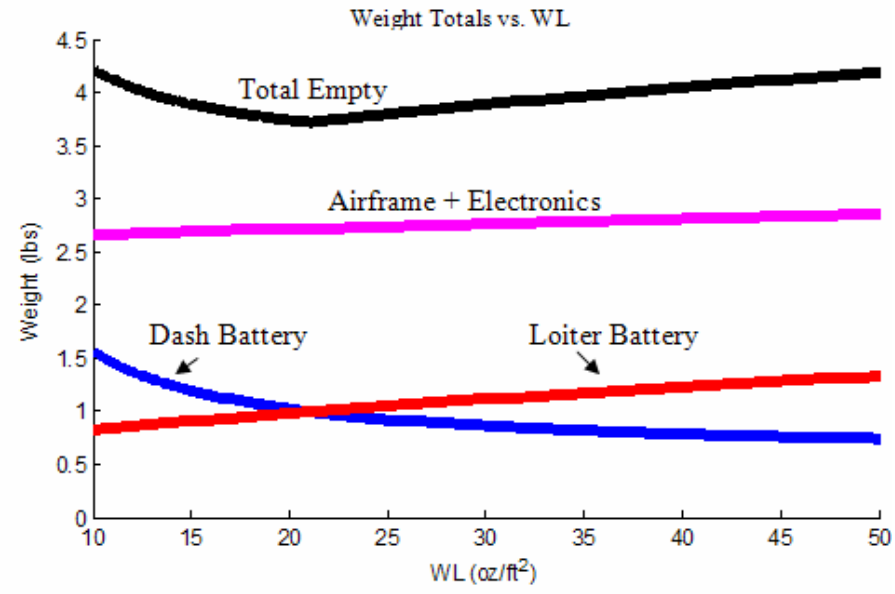

Figure 3.5 – Aircraft Weight Breakdown

The program finally output the flight score based on the wing loadings. For a fixed AR, the wing area was used to find the span of the aircraft, which, combined with the empty weight of the aircraft, determined the flight score (Figure 3.6).

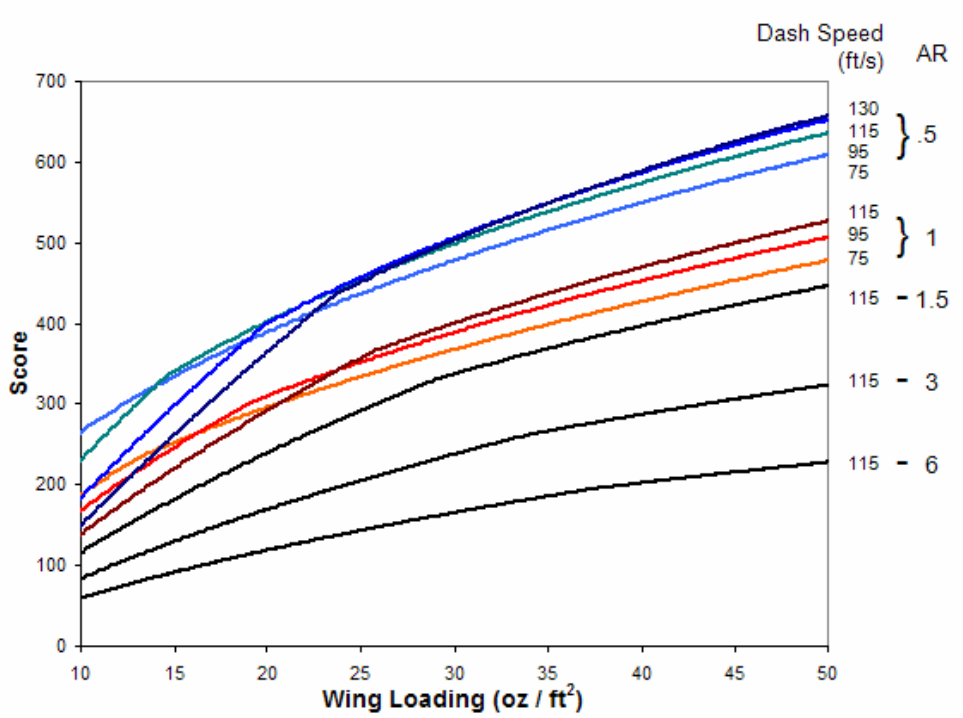

Figure 3.6 – Aircraft Parameters as they Relate to Flight Score

The final output indicated that a maximum flight score was achieved with a high wing loading on a low aspect ratio wing. This analysis laid the groundwork to determine the configuration of the aircraft.

3.3 Initial Design Concepts

The mission modeling analysis and careful study of the rules showed that maximizing the score depended on several design requirements, the primary being the aircraft's span. Figure 3.5 showed that as the aircraft's wingspan increased, score decreased dramatically. Furthermore, the overall scoring equation rewarded a small span. The aircraft's size also affected its performance in the two non-flying missions. To perform best in these two missions, the plane should fit fully assembled in the box, allowing for the absolute minimum deployment time, as verified with time trials (Table 3.2). It was calculated that assembling an aircraft would decrease the total score by 10%. These design requirements established a maximum size of the aircraft, with the air data probe installed, as 4 x 2 x 1.5 ft, the size of the box it must fit within.

Table 3.2 – Deployment Time Trials

Time to Deploy	Time (sec)
No assembly required	8
Assembly required	16

3.3.1 Figures of Merit

Six figures of merit (FOMs) were chosen based upon the results of the initial mission modeling & scoring analysis, qualitative reasoning, and experience. The FOMs and their description are listed below in order of importance.

1. **RAC**: The main focus was weight, with wingspan only being considered for wing type selection. RAC was weighted highest because of its effect on score.
2. **Payload**: The configuration affected the placement of the payload and greatly effects the load time of the payloads. It was weighted second only to RAC.
3. **Drag:** Drag greatly affects aircraft weight and the max speed attainable in the two flight missions. In some areas it was broken down into loiter speed, affected by induced drag, and max speed, affected by parasite drag. Because this played a role in the Dash mission, as well as indirectly effecting RAC, it was determined to be of equal importance to the payload placement.
4. **Stability:** An unstable aircraft is difficult or impossible to fly, so stability was an important consideration. However, a marginally stable aircraft can still be flown through augmentation such as gyros and pilot training, so it was not weighted higher.
5. **Construction:** Complexity of the airframe and supporting elements increases the complexity of assembly and can increase weight, so simple designs were emphasized.
6. **Risk:** The unknowns of a design can lead to wrong assumptions and unexpected problems. This can cause delays and increase weight, leading to redesign.

3.3.2 Numerical Selection Matrices

Selection matrices were used as means to numerically evaluate FOMs. Only configuration options that were deemed feasible to integrate into the aircraft design were included in the matrices. A parafoil wing, for example, was excluded due to its slow speed and narrow flight envelope. Each FOM was given a numerical value. If a configuration was beneficial, it was assigned a value of 1, if it was neutral a value of zero, and if it had a negative effect a value of -1 was assigned. Not all FOMs were used for each type of configuration and the weight of the FOM changed from one matrix to the next. However, the overall trend was maintained as far as what aspects were considered most important. The last row of each matrix contains a RAC estimate.

3.3.3 Wing Configuration

Table 3.3 – Wing Configurations

Figure of Merit	*Weight*	Monoplane	Biplane	Blended	Lifting Body	Faceted Lifting Body
RAC	*0.3*	-1	0	-1	1	1
Max speed	*0.2*	0	-1	1	0	0
Loiter speed	*0.2*	0	1	0	-1	-1
Construction	*0.2*	0	0	-1	0	0
Risk	*0.1*	0	0	-1	-1	-1
Total	*1*	-0.3	0	-0.4	0	0
Span (inches) / Weight (lbs)	N/A	48 / 4.5	24 / 4.7	36 / 5.0	24 / 3.75	24 / 3.60
RAC Estimate	N/A	216	112.8	180	90	86.4

The monoplane is a single wing used as the basis for the wing type selection. It is versatile, reliable, and easy to build. The biplane's primary aerodynamic advantage is decreased induced drag, with a corresponding increase in wetted area, and therefore parasite drag. Due to several fuselage intersections, the biplane will suffer from higher parasite drag and will not perform as well in the Dash mission. A blended wing body can decrease parasite drag, increasing performance for the Dash mission, but the complex, smooth geometry makes construction and optimization difficult. A lifting body has a shorter wingspan, as the entire aircraft surface is devoted to lift. Lifting bodies often have lower aspect ratios however, negatively impacting the loiter speed. The unusual design was rated as a higher risk factor. The facet is essentially the same as the regular lifting body, but is constructed with simple geometry, allowing weight savings with a penalty of increased drag. This selection matrix (Table 3.3) proved inconclusive about a wing selection because the biplane, lifting body, and facet each had unique strengths and weakness.

3.3.4 Tail Configuration

Table 3.4 – Tail Configurations

Figure of Merit	*Weight*	Conventional	V-tail	T-tail	Canard	Tailless
RAC	*0.3*	0	-1	-1	0	1
Drag	*0.25*	0	1	0	1	1
Stability	*0.25*	0	0	0	-1	-1
Construction	*0.1*	0	-1	-1	-1	0
Risk	*0.1*	0	-1	-1	-1	-1
Total	*1*	0	-0.25	-0.5	-0.2	0.2
RAC Estimate (lb)	N/A	.55	.65	.70	.45	.2

Meeting the requirements of reasonable drag, high stability, and easy construction, a conventional design was used as the basis for comparison between the tail types. The V-tail was considered to be slightly more aerodynamic than a conventional tail due to less area. However, the concentrated loads it encounters requires more structure and induces roll with rudder inputs. The T-tail is normally used to provide extra ground clearance, or to keep the tail from being blocked by the wing, and is heavier due to structural requirements for the vertical component of the tail. A canard offers more flexible CG location and can possibly reduce drag. The decrease in drag is a result of the canard being able to provide a

positive component of lift. However, the canard is complicated to design to avoid problems such as fatal deep stall. A tailless configuration is defined as only containing the vertical appendage of a tail and no control surfaces. Its main disadvantage is a complicated design, so care must be taken to achieve stability naturally. However, these factors are outweighed by the decrease in drag and RAC. The selection matrix (Table 3.4) favored a tailless configuration.

3.3.5 Landing Gear Configuration

Table 3.5 – Landing Gear Configurations

Figure of Merit	*Weight*	Tail Dragger	Tricycle	Bicycle
RAC	*0.4*	1	0	0
Drag	*0.2*	1	0	-1
Stability	*0.2*	-1	1	0
Payload	*0.1*	0	0	0
Takeoff Distance	*0.1*	1	0	-1
Total	*1*	0.5	0.2	-0.3
RAC Estimate (lb)	N/A	.35	.51	.47

Depending on the landing gear chosen, the camera ball system was required to be placed either in front or behind the landing gear – a major consideration. A tail dragger configuration allows for both the air data boom and the camera ball to protrude from similar locations on the aircraft. It also allows for decreased drag due to a much smaller 3rd wheel when compared to a tricycle configuration and takeoff rotation is easier. However, it is harder to have a pusher design due to propeller clearance issues. The tail wheel is also less stable, though the stability issues are easily overcome with pilot skill. The tricycle gear is heavier than a tail wheel configuration and has slightly more drag due to the larger 3rd wheel. It is more stable and can accommodate a pusher prop configuration without running into clearance problems. However, the aircraft cannot rotate as easily. A bicycle gear has a tandem main pair of wheels with wheels at the wingtips. This configuration is heavier because it has 4 wheels and heavy reinforcement in the wings, leading to a heavier airframe and more drag. The takeoff distance is also affected because the rear wheel in the tandem configuration tends to be far back, making it harder to rotate. Table 3.5 indicated that a tail dragger configuration might be the best option.

3.3.6 Motor Placement and Number

Table 3.6 – Motor Location Configurations

Figure of Merit	*Weight*	Single Tractor	Single Pusher	Pod Mounted	Twin Tractor
RAC	*0.45*	0	0	-1	-1
Payload	*0.35*	-1	1	0	1
Risk	*0.2*	1	-1	-1	1
Total	*1*	-0.15	0.15	-0.65	0.1
RAC Estimate (lb)	N/A	2.10	2.10	2.50	2.25

Primary factors again were RAC, payload placement, and risk of prop strikes and off center thrust lines. The evaluation is shown in Table 3.6. A single tractor provides the lightest weight and good prop

clearance. However, it does not allow for the air data probe to be mounted on the center-line of the aircraft. A single pusher has the benefit of a lightweight power system with the ability for center-mounted, interchangeable payloads. However, the pusher leads to problems with prop clearance, requiring either heavier tricycle gear or mounting the propulsion system higher up on the back of the plane, increasing weight for the supporting structure. A pod mounted power system achieves the needed clearance and protection for the propeller and allows for uniform placement of the payloads on the center line. However, the increase in the weight and decreased stability make pod mounting an unfavorable option. A twin tractor may be heavier than a single engine configuration, but allows for a center mounted air data probe and a tail dragger landing gear. This matrix proved inconclusive in selecting a motor number and location, so single pusher and twin tractor configurations were both considered.

3.3.7 Payload Location

Table 3.7 – Payload Location Configurations

Figure of Merit	*Weight*	Interior	Exterior
RAC	*0.4*	0	0
Payload	*0.3*	-1	1
Drag	*0.3*	1	-1
Total	*1*	0	0
RAC Estimate	N/A	N/A	N/A

Payload had to be easily accessible, and compatible with the landing gear &motor placement. To maintain balance about the lateral axis with a short wingspan, the air data probe had to be placed on the centerline. This also allowed it to be attached directly to the processor for quick reconfiguration with little change in CG. The actual placement of the payload was left to be a function of the landing gear selection. The remaining factor was an internal versus external payload (Table 3.7).

3.3.8 Configuration Selection

It was concluded there was insufficient data to narrow the configuration selection to a single design. Therefore, it was decided to carry 3 different configurations to the preliminary design stage for further investigation and analysis (Table 3.8). The Lifting Body and Facet are similar in shape, so their configurations were varied slightly as means of further evaluation. The Lifting Body incorporated tricycle landing gear and a single pusher, whereas the Facet utilized twin tractor motors and tail dragger landing gear. This would allow the optimal final configuration to be later selected.

Table 3.8 – Configurations Selected for Preliminary Design

Wing Configuration	Tail Configuration	Landing Gear	Motor Location	Payload Location
Biplane	Tailless	Tail Dragger	Single Pusher	External
Lifting Body	Tailless	Tricycle	Single Pusher	Internal
Facet	Tailless	Tail Dragger	Twin Tractor	Internal

3.4 Conceptual Design Conclusion

Conceptual design began by evaluating the mission rules & requirements and developing an initial mission modeling & scoring analysis program. These analyses concluded that wingspan was the primary scoring factor and the maximum size of the assembled aircraft was constrained to the dimensions of the storage box. FOMs were then evaluated, and ranked, according to the results of the mission modeling & scoring analysis. Numerical selection matrices were used to narrow thousands of design configurations to three conceptual designs; the Biplane, the Lifting Body, and the Facet.

4. Preliminary Design

The goal of preliminary design was to refine the three aircraft and identify an optimal configuration. The aircraft was first sized to maximize score, resulting in a span of 2.4 ft. An initial wing analysis investigated the use of winglets on the Lifting Body and their addition shortened its span to 2 ft, resulting in a 44% increase in its final score. The three aircraft were then flown and scored in a mission simulation and performance program. Data was insufficient for a down selection at this state, so all three designs were built and wind tunnel tested. Concluding the first design spiral, the Facet and Lifting Body were also flight tested, providing valuable data. The testing results verified computer models and led to the selection of the Lifting Body configuration. Design then focused on optimization, beginning with an optimization of airfoil, sweep, and winglets. A propulsions system analysis optimized the motor and battery selection. Next, a structural analysis led to the selection of materials that would result in the lightest airframe. Flight testing in the first design spiral illustrated the need to stabilize the aircraft and a stability analysis led to refinement of the final aircraft configuration.

4.1. Aircraft Sizing and Mission Analysis

The selection of design parameters was based upon the configurations chosen and scoring relationships identified by the preliminary mission model, with the overall goal of maximizing the total score. The initial design parameters included planform areas, wing span, and static thrust. The aircraft sizing and mission analysis program, Figure 4.1, iterated through a range of planform areas, spans, and static thrusts to converge on optimal values that would yield the maximum score. This sizing analysis did not distinguish

between the three aircraft, but rather sought to calculate the optimum size. The range of planform areas, spans and static thrust values are included within the flowchart of Figure 4.1.

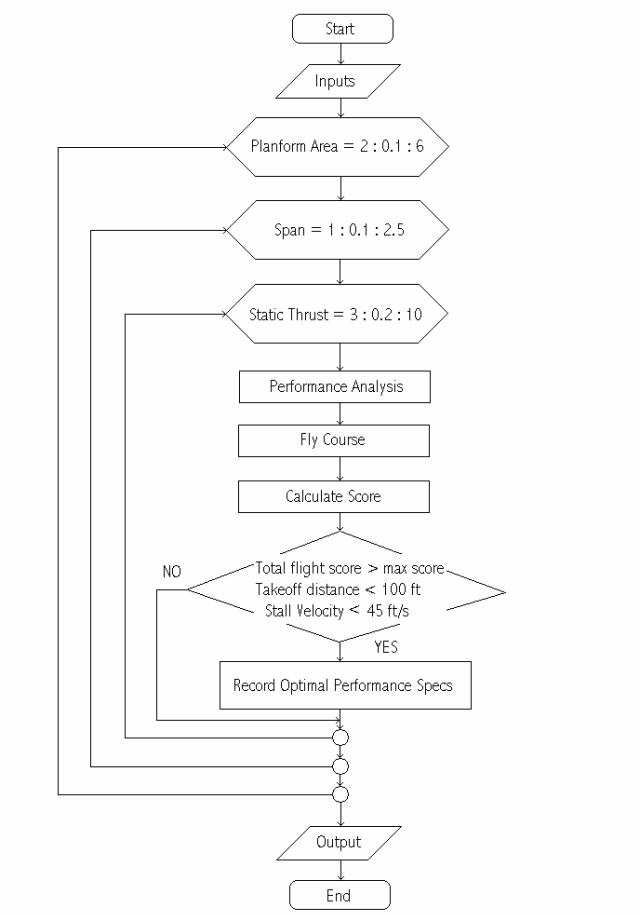

Figure 4.1 – Aircraft Sizing and Mission Analysis Program Flowchart

As the program iterated through the range of values it calculated aircraft performance. Based on the performance, the course was flown and scored. If the current configuration achieved a new high score, satisfied a takeoff distance of less than 100 ft, and had a stall velocity less than 45 ft/s, it was saved as the new optimal aircraft. The following sections explain the program in detail.

4.1.1 Optimization

The range of planform areas was based on the goal of having the aircraft fit in the box flight-ready. A planform area smaller than 2 ft^2 and a wingspan less than 1 ft were chosen as preliminary lower bounds. Static thrust was based on historical values of static thrust for aircraft of similar size. To optimize, structural weight and wetted surface areas were calculated as functions of planform area. This ensured that a larger aircraft would have a larger structural weight and wetted surface area.

4.1.2 Performance Calculations

In the performance portion of the program, the parasite drag, induced drag, total drag, thrust available, $V_{max\ endurance}$, $V_{max\ climb}$, maximum rate of climb, battery cells required, battery weight, takeoff distance, stall velocity, V_{max} and $(L/D)_{max}$ were calculated[2].

Drag

For parasite drag, an equivalent skin friction drag coefficient (C_{fe}, = 0.014[2]) and the aircraft's wetted surface area yielded a parasite drag coefficient of 0.035. Further analysis of the parasite drag was conducted in wind tunnel testing later in the design process. For induced drag, Oswald's efficiency factor was used. It was recognized that the proposed aircraft did not fall in the optimum range for the Oswald's calculation, but it was chosen to keep the initial analysis simplistic.

Thrust Available

In Figure 4.2 thrust available was plotted with total, parasite and induced drag. The thrust available was calculated for a motor of similar performance to previous competition aircraft.

Flight Velocities

Maximum velocity, velocity for best rate of climb, and velocity for maximum endurance were found using the curves in Figure 4.2.

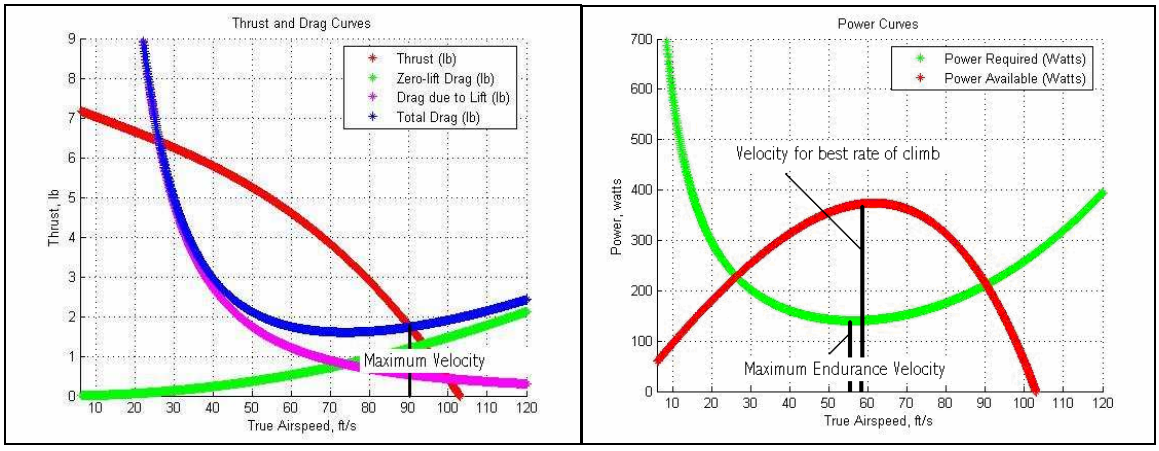

Figure 4.2 – Thrust, Drag and Power for the High Score Configuration

Stall Velocity

The primary importance of a low stall velocity is that it results in a lower landing velocity. This reduces the risk of damage to the aircraft and increases the ease of landing for the pilot. A maximum of 45 ft/s was placed on stall velocity due to pilot preference.

Takeoff Distance

The takeoff distance was calculated with the assumption that takeoff occurred at 1.2 times stall velocity[2]. The takeoff distance was one of the major constraints placed on the aircraft. The calculated distance of 91.9 ft gave a fair margin of safety to takeoff considering this was a no headwind scenario.

Number of Batteries Required and Battery Weight

To meet the requirements for the Loiter mission, maximum endurance velocity had to be attained for a time of 5 minutes, allowing for a 1 minute safety margin. Using the maximum endurance velocity and the required thrust at that velocity the required wattage was found. A 2400 mAh battery was assumed based on a historical analysis of previous competition aircraft. Using a 2400 mAh cell for a 5 minute endurance gave the required amperage. Using the required wattage, amperage, and required volts the initial estimate of the number of batteries required was found. Using the fact that each cell weighed 0.101 pounds and had a voltage of 1.2 volts, the weight of the battery pack was found. With a 12 cell count being the output, the weight of the battery pack was 1.22 pounds.

4.1.3 Mission Modeling

After each variable was iterated to calculate performance, the two flight missions were simulated. For the Dash mission, on the upwind leg 90% of V_{max} was used to account for slower groundspeed during takeoff and climb. For all turns, 75% of V_{max} was used because a slower velocity would allow for sharper turns and at 75% of V_{max} the aircraft was reasonably far from the stall velocity. V_{max} was used for the downwind legs because of the simplification that there will be negligible time required to accelerate and decelerate.

The Loiter score is only based on completing the two 2-minute laps. If the laps are completed in the correct amount of time, the score is a factor of RAC and independent of mission performance. Previous battery calculations ensured that the aircraft would have the appropriate endurance.

The score was calculated at each iteration point using self-normalized scores as a basis for evaluation.

4.1.4 Results

The specifications of the optimum aircraft are tabulated Table 4.1. The results show that the highest score is attained by an aircraft with a low AR, a small span, and a large thrust to weight ratio.

Table 4.1 – Optimum Outputs

Optimized Factors	Value	Optimized Factors	Value
Span	2.4 ft	Number of Batteries	12
Planform Area	3.80 ft^2	Structural Weight	3.42 lbs
Thrust to Weight Ratio	0.70	Propulsion Weight	1.78 lbs
Static Thrust	7.4 lbs	Takeoff Weight	10.62 lbs
V_{stall}	44.76 ft/s	C_{D0}	0.035
$V_{max\ climb}$	59.9 ft/s	$(L/D)_{max}$	5.93
V_{max}	90.3 ft/s	Maximum Rate of Climb	969 ftpm
$V_{min\ pwr}$	56 ft/s	Takeoff Distance	91.9 ft
Predicted Mission Performance			
Endurance	5 min	Dash Time	1.18 min

4.2 Wing Study

The sizing program provided an optimal aircraft size to maximize score, but was limited by its assumptions and simplicity. Therefore, an analysis was performed using the low order panel code CMARC. One goal of this analysis was to determine if the wing spans could be shortened through the use of winglets. A decrease in span might result in a decrease in score, but the effect of changes in parasite and induced drag has to be considered. In order to provide a scoring benefit, the increase in score due to the decreasing wingspan must outweigh the changes winglets will cause in battery weight and structural weight. Three models were analyzed; a lifting body with a 2.4 ft span, a lifting body with a 2 ft span and winglets, and the biplane with end plates joining the wings. It should be noted that the total wing area is larger than calculated optimum because the chord was increased so that the payload could fit inside the wing with a reasonable thickness ratio. The biplane, now actually a joined wing aircraft, is still referred to as the biplane to keep continuity within the report. Figure 4.3 shows the three models with pressure distributions. All models are shown at the same angle of attack with the same pressure scales and approximately the same scale.

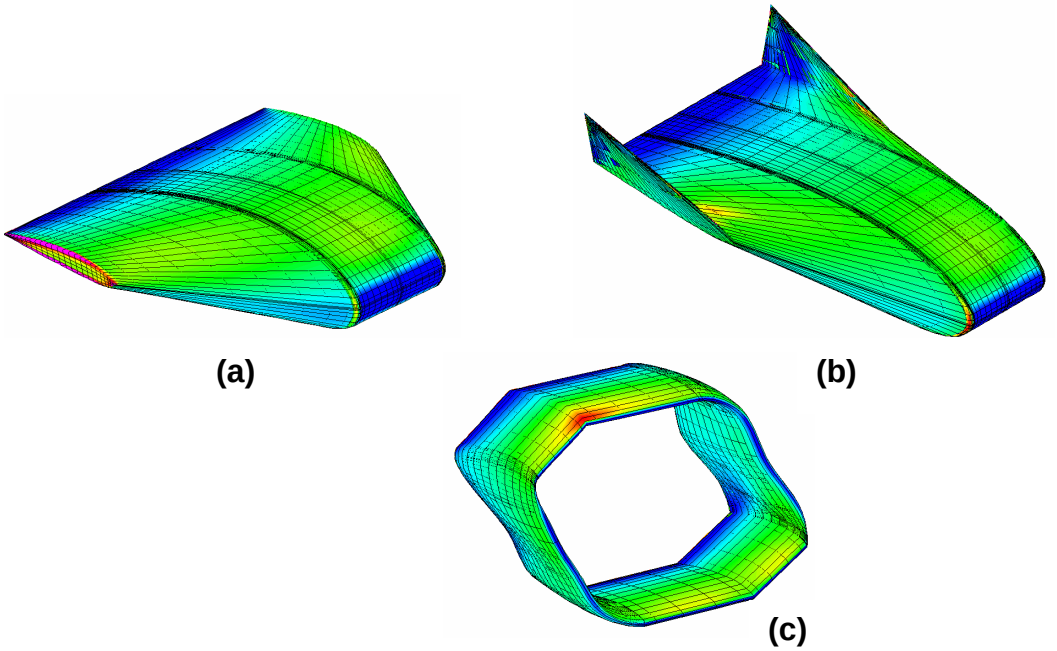

Figure 4.3 – CMARC Analysis Result
(a) Lifting Body, (b) Lifting Body with Winglets, and (c) Biplane

Decreasing the span and adding winglets slightly increased pressure on the wing, allowing it to produce nearly the same lift as that of the wider span. The biplane, even with only 2/3 the lifting area, produced nearly the same life due to higher pressures created due to less loss of lift.

Once the lift and drag values were determined for each of the aircraft, a standard zero lift drag was determined using coefficients of friction based on wetted area. These drag values were then used to predict the performance of each of the aircraft for the two flight missions (Table 4.2). The same gross weight of 8 and 10 lbs, for the Dash and Loiter missions respectively, were used for all three aircraft.

Table 4.2 – Extracted Drag Data from CMARC

	Biplane	Lifting Body	Lifting Body with Wingtips
Drag Loiter	1.31 lbs	1.39 lbs	1.42 lbs
Drag Dash	3.88 lbs	4.04 lbs	2.93 lbs

As can be seen, the biplane performed best in the Loiter mission, but only by a few percent. In comparison, due to the external payload, its Dash drag was more than 30% higher.

Most importantly, it was found to be advantageous to drop the wing span from 2.4 feet to 2 feet. During the loiter mission, the drag is 2% higher. This approximately increases the battery weight by the same

percent, but because the battery is only about ¼ of the weight, this leads to a small increase in RAC. By decreasing the wingspan, the RAC decreases by 25%, leading to approximately a 24.5% gain. The analysis showed that by decreasing the wing spans to 2 feet and adding winglets translated to a 44.2% increase in final score. The refined configurations are shown in Figure 4.4 below.

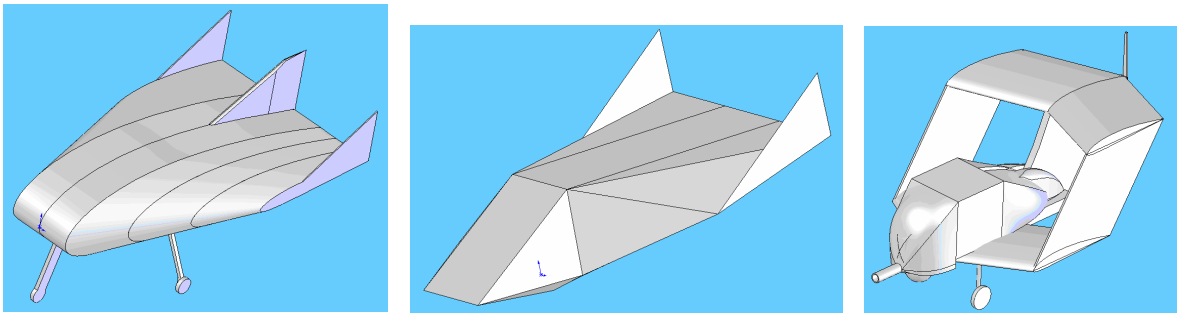

Lifting Body Facet Biplane

Figure 4.4 – Refined Configurations

4.3 Performance Analysis and Detailed Mission Modeling

A performance analysis was conducted for each aircraft design and each was compared in a detailed mission modeling program. The configuration that yielded the greatest overall score could then be selected for further design and optimization.

The performance analysis was highly dependent on aircraft properties and engine specifications. The aircraft geometry used as input for the analysis code was determined from CAD models of the refined designs and used in the calculations of lift, drag, and performance parameters. A standard engine was used for all three aircraft designs to ensure standardized comparisons. The program analyzed the aircraft performance over a range of velocities, from 0 to 150 ft/s. The thrust available data was obtained from historical MotoCalc data. The inputs to the program are shown in Table 4.3.

Table 4.3 – Analysis Code Inputs for Dash and Loiter Missions

	Facet & Lifting Body		Biplane	
Mission	**Dash**	**Loiter**	**Dash**	**Loiter**
Wingspan (ft)	2	2	2	2
Planform Area (ft^2)	6.03	6.03	3.56	4.11
Wetted Area (ft^2)	15.77	15.94	20.06	21.19
Weight (lb)	10	10	8	8

4.3.1 Drag Calculations

A skin friction coefficient, C_{fe}, of 0.014 was again considered a reasonable approximation. Using the inputs displayed in Table 4.3, a drag curve was created for each aircraft, for each mission (Figure 4.5). The Facet and Lifting Body were designed with the same parameters; only their shapes differ, so only one drag curve was produced for each mission to reflect the performance of both aircraft.

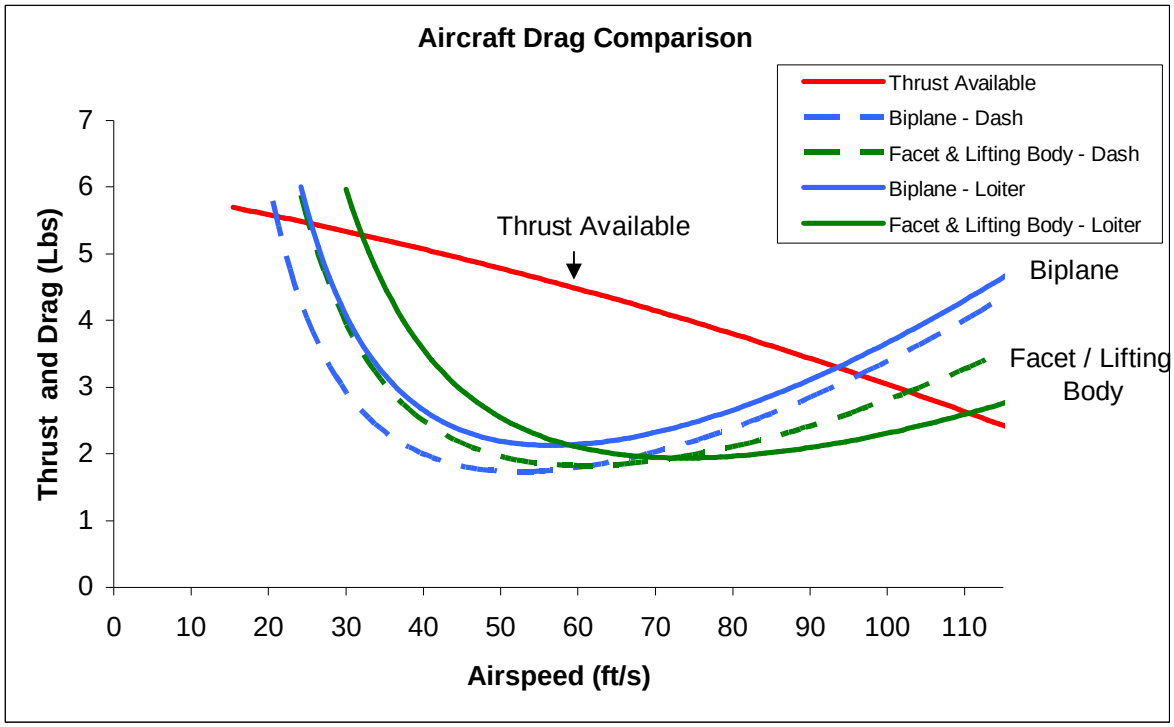

Figure 4.5 – Aircraft Drag Comparison

4.3.2 Turn Analysis

An analysis of turn radius and velocity in the Dash mission was necessary to ensure the optimum turn velocity of the aircraft. The turn analysis calculated the lap times at a given velocity, taking into account the turn radii when computing lap distance. Given that the radius of a turn is proportional to velocity squared, an interesting compromise was observed. Although traveling at higher velocity on straight-aways decreased lap time, it increased turn radii and caused the aircraft to travel a farther difference. The turn analysis allowed a reduced turn velocity, reducing the turn radii. A bank angle of 30° was chosen, due to the large amount of lift lost and increase in g-loading at greater bank angles. The turn analysis proved that higher speed turns decrease score by increasing lap time, due to the greater radii required. It was calculated that a speed decrease of 15 ft/s less than cruise speed was optimal for turns, as a greater decrease in velocity resulted in velocity not being sufficiently regained on straight-aways.

4.3.4 Mission Analysis Results

With the takeoff distance & speed, climb rate, turn radius & speed, and cruise speed calculated[2], the missions were flown with each aircraft design to determine which aircraft would theoretically yield the best score as seen in Table 4.4.

Table 4.4 – Performance Specifications and Mission Scores

	Facet & Lifting Body		Biplane	
	Dash	**Loiter**	**Dash**	**Loiter**
Wing Loading (oz/ft^2)	20.08	25.80	33.91	37.22
Empty Weight (lbs)	2.72	2.72	2.68	2.68
Battery Pack Weight (lbs)	0.8489	1.0039	0.8608	0.8999
Span (ft)	2	2	2	2
AR	0.66	0.66	1.77	1.77
Cruise Speed (ft/s)	122.2	-	96.1	-
Loiter Speed (ft/s)	-	55.7	-	42.5
Stall Speed (ft/s)	27.9	31.5	34.4	35.9
T/O Speed (ft/s)	33.7	37.5	41.4	42.2
T/O Distance (ft)	42.6	67.5	64.3	87.2
Rate of Climb (ft/min)	1242	1056	1100	978
	Dash	**Loiter**	**Dash**	**Loiter**
Mission Time (s)	89.2	240	78.5	240
Energy Consumed (kJ)	46.48	63.7	47.8	52.14
Flight Mission Scores	**89.69**	**80.56**	**101.91**	**83.72**
Total Score	**403.2**		**444.8**	

4.3.5 Conclusions

The Biplane resulted in the highest score, but the Lifting Body and Facet were close in score (Table 4.4). It was concluded, therefore, that the performance and mission analysis did not provide conclusive evidence as to which configuration to select. Additionally, the mission analysis program could not accurately simulate all the differences between the three designs. Therefore, it was decided to perform additional CFD analysis and build representative models for wind tunnel testing and flight testing to accurately develop a detailed drag polar for each aircraft.

4.4 CFD Analysis

The goal of the CFD analysis was to develop a tool for continued accurate and versatile aerodynamic performance analysis. The CFD analysis was later validated with wind tunnel testing. Only the analysis of the Lifting Body is described.

A 3-D model of the Lifting Body was constructed with the following CFD modeling methodology (Figure 4.6). The full-scale aircraft geometry was simplified by removing the landing gear. A symmetry plane was used so only half of the fluid domain was needed in the CAD package to improve the CFD solver run-

time. The 'clean' CAD model was imported into the meshing package GAMBIT. The flow solution was obtained using FLUENT and post processed using Tecplot.

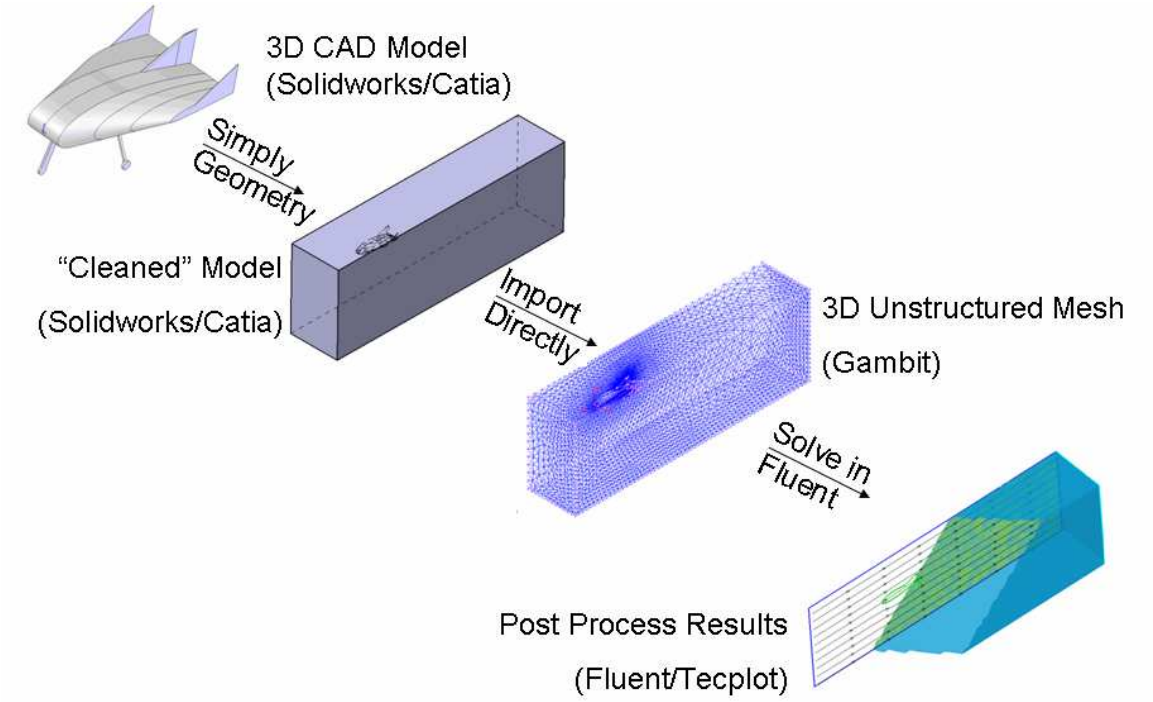

Figure 4.6 – 3D CFD Analysis Methodology

The CFD mesh consisted of a triangular surface mesh on the faces of the aircraft and an unstructured tetrahedral volume mesh as shown in Figure 4.7.

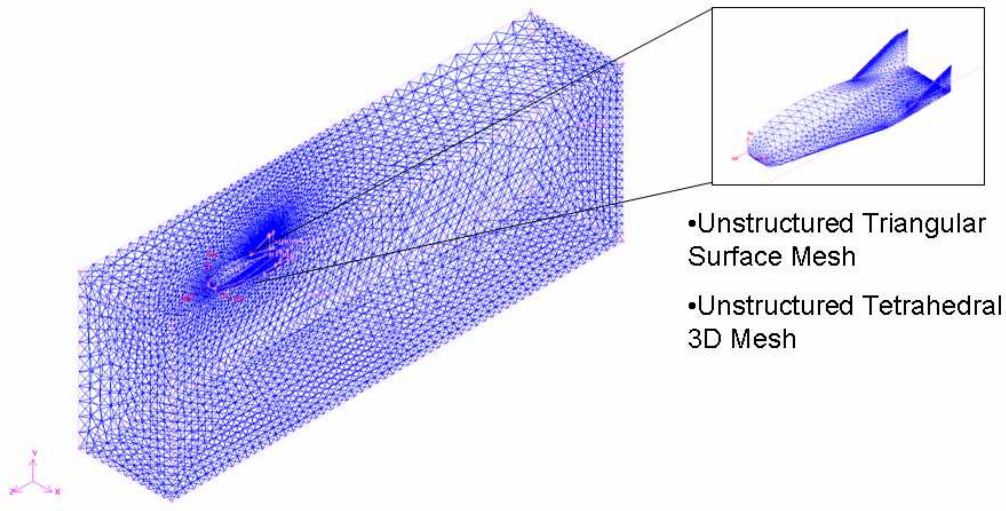

Figure 4.7 – Lifting Body 3-D Mesh

This mesh was loaded into FLUENT and a viscous steady state flow solution was obtained for the same free stream velocity as present during wind-tunnel testing. A convergence study evaluated the solution accuracy. Different mesh densities, turbulence models, and solver settings were evaluated at zero angle of attack to evaluate the trade between solution accuracy and run-time. The final selection was evaluated at a series of angles of attack to generate the drag polar as shown in Figure 4.8.

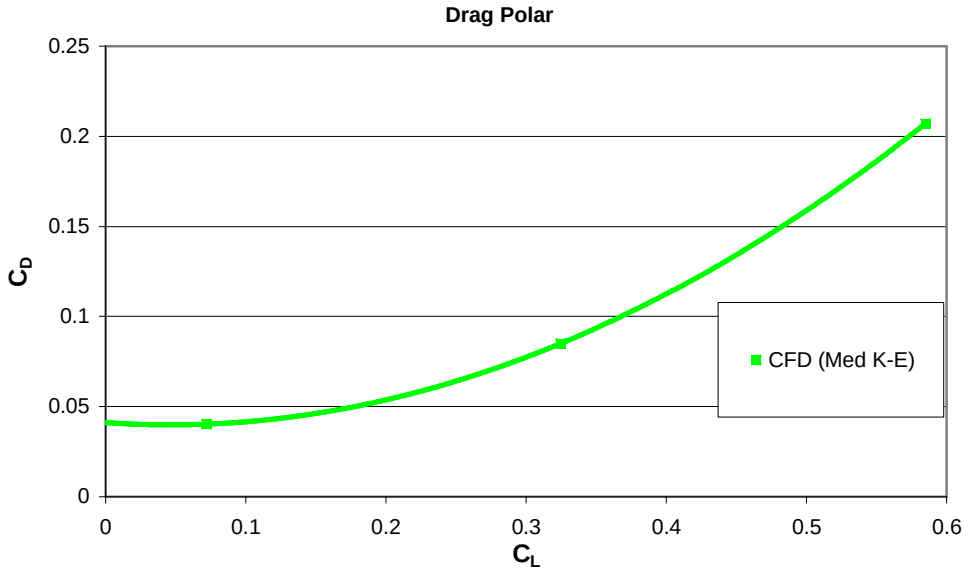

Figure 4.8 – Lifting Body Drag Polar

In order to validate the drag polars calculated by the initial CFD analysis, prototypes of the three aircraft configurations were constructed for wind tunnel and flight testing.

4.5 Prototype Construction

All three aircraft were constructed during the first iteration spiral, each with a different construction technique. Construction experience gained from these designs was applied to the final aircraft design.

The entire frame of the Facet was built using hardwood dowels, glued and tied together with thread, to form faceted surfaces. Iron-on covering was applied to the frame, greatly increasing its torsional rigidity. This combination resulted in a light-weight rigid aircraft that accommodated internal payloads and was easy to build.

The Lifting Body used hardwood dowels to join together plywood root ribs, foam intermediate ribs, and plywood tip ribs. Balsa stringers maintained curvature across the surface of the wing and served as tacking point for iron-on covering. A plywood vertical stabilizer, buttressed with hardwood dowels, functioned as a motor mount. The large plywood root ribs and vertical stabilizer added significantly to the aircraft's weight, making it much heavier than the Facet without being significantly stronger.

The Biplane's wings employed hot-wire cut foam, joined together at the root with a large sheet of balsa. While this yielded a strong, rigid, and easy to construct airframe, it was also much heavier than the Facet. This was accounted for by the large balsa plate and glue needed to join the wings, as well as the additional structure required to mount the payloads externally. The three finished models are shown in Figure 4.9.

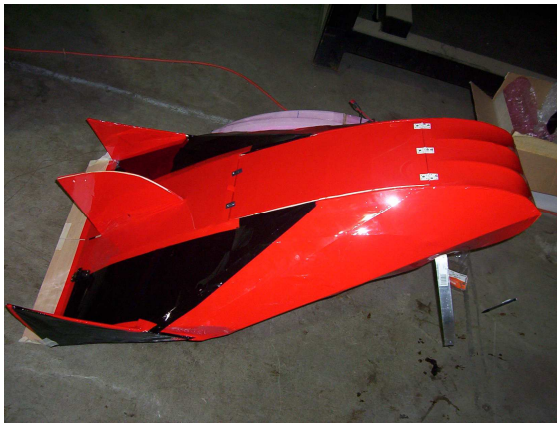

Lifting Body (a)

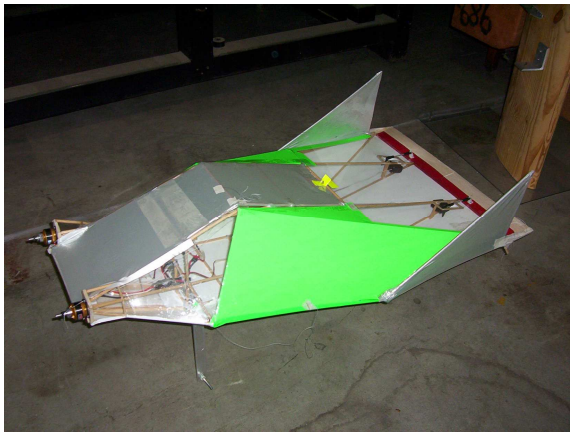

Facet (b)

Biplane (c)

Figure 4.9 – Photographs of Test Aircraft

4.6 Wind Tunnel Testing

Wind tunnel tests were performed with each aircraft. Because the Biplane has external payloads, it was run once with each payload to account for the significant difference in profile drag. Each test was conducted at 37.5 ft/s. Shown in Figure 4.10 is the drag vs. lift curve obtained directly from the data.

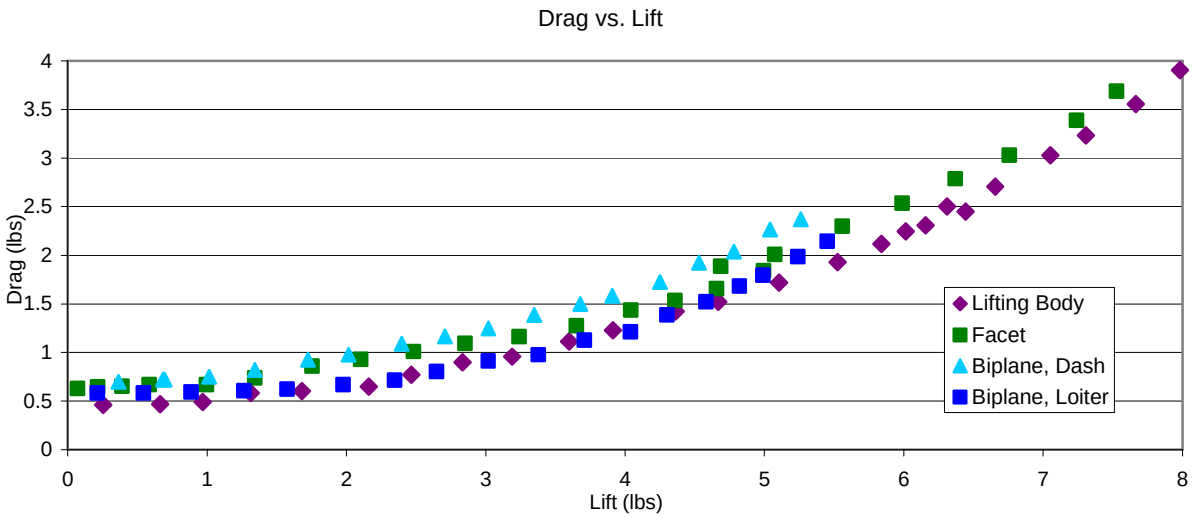

Figure 4.10 – Wind Tunnel Data Results of Drag vs. Lift for All Aircrafts

With this data, the tunnel velocity, planform area, and standard atmospheric density, the drag polars were created. Added to these plots are the theoretical values calculated for the Dash and Loiter missions displayed in Figures 4.11 and 4.12. The Facet was approximated as a lifting body because of a lack of historical data. The error in the theoretical values is attributed to the atypical designs of the aircraft and their low aspect ratios, for which many of the calculations breakdown.

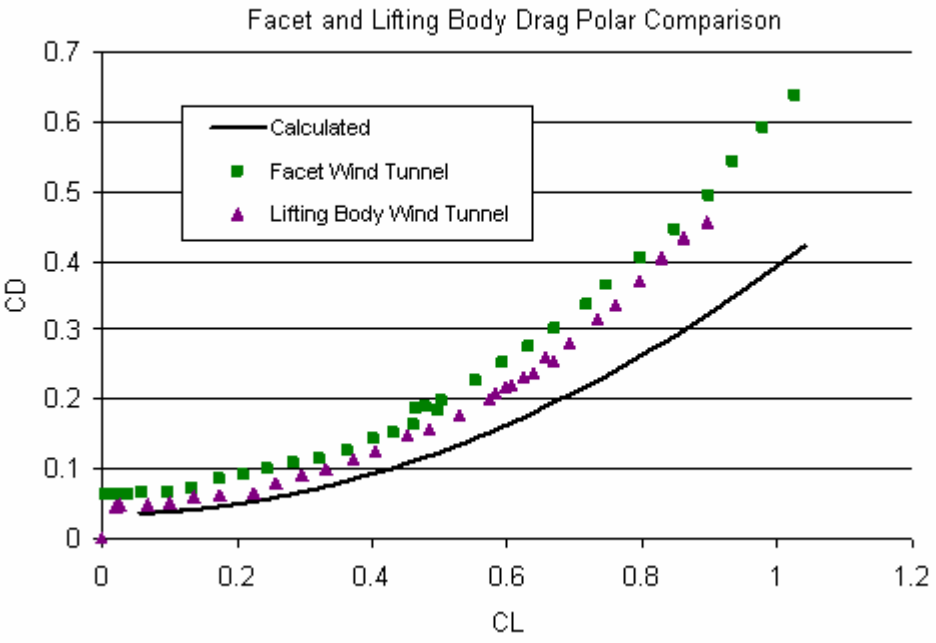

Figure 4.11 – Drag Polar Comparison between Wind Tunnel Data and Theoretical

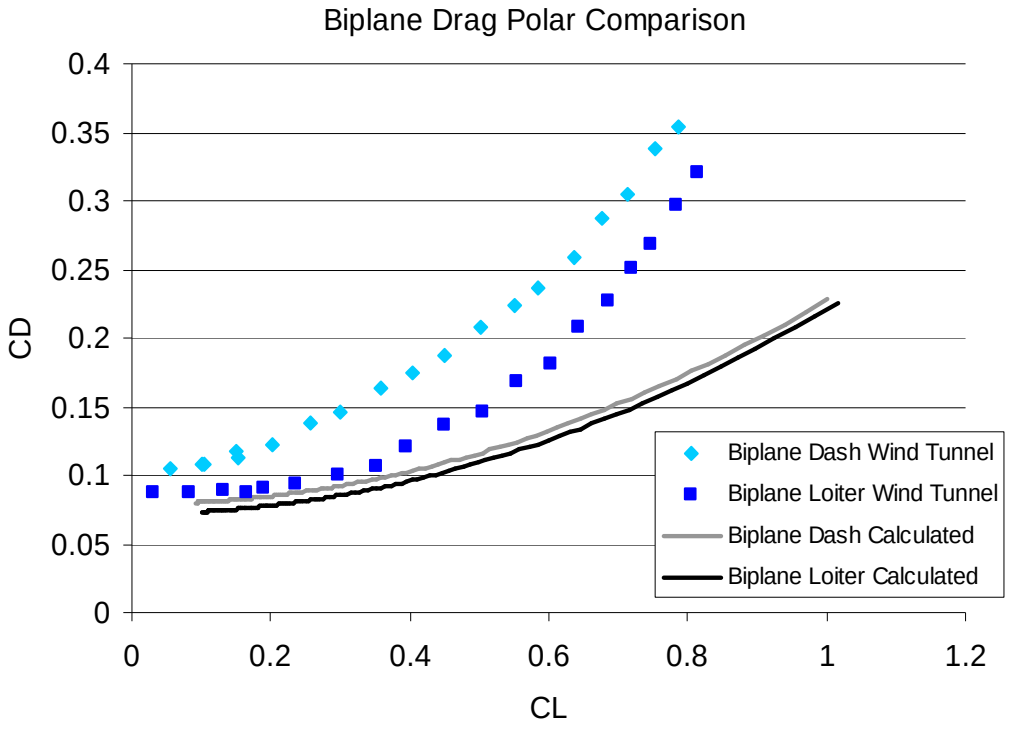

Figure 4.12– Drag Polar Comparison between Wind Tunnel Data and Theoretical

The lift coefficients were then plotted against the angle of attack, shown in Figure 4.13.

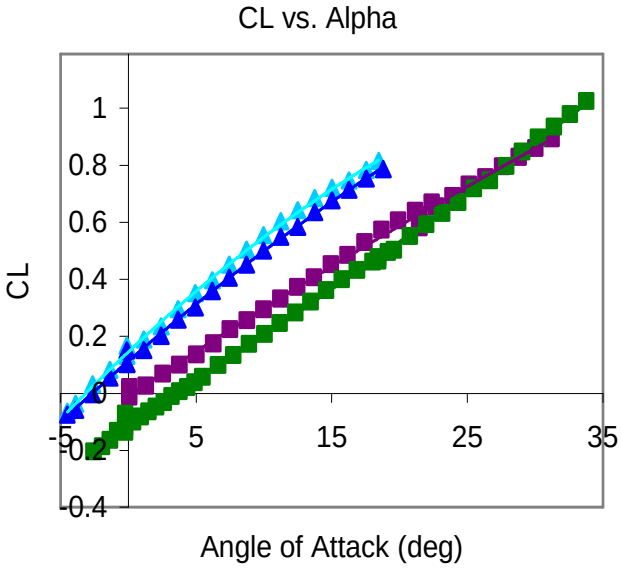

Figure 4.13 – Coefficient of Lift vs. Angle of Attack

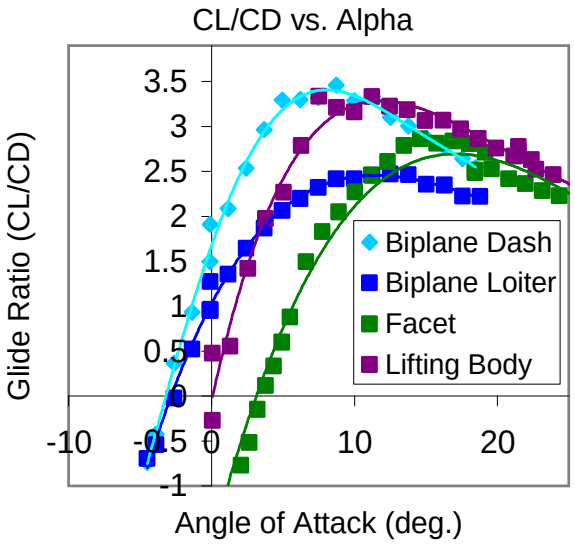

Figure 4.14 – CL/CD vs. Angle of Attack

Combining Figures 4.12 and 4.13, the ratio of lift to drag coefficients versus the angle of attack can be plotted, shown in Figure 4.14.

The prototypes were not built to their optimal weights, thus the analysis of drag required the assumption that the actual weights of each aircraft would be 8 pounds for Dash with the air data probe payload and 10 pounds for Loiter with the camera ball payload. Using the coefficients of drag obtained from the wind tunnel, the drag was found as a function of speed, shown in Figure 4.15. The dashed and solid lines represent the Dash and Loiter missions, respectively.

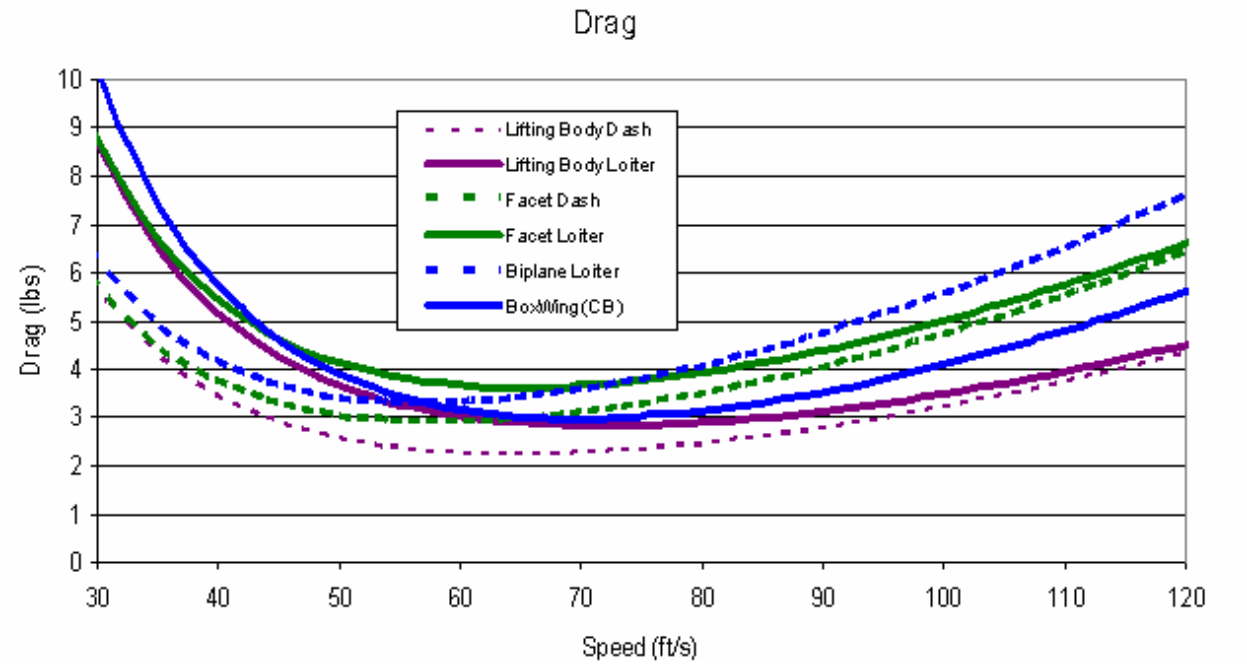

Figure 4.15 – Drag as a Function of Speed

In a similar manner, the power required was determined as a function of speed shown in Figure 4.16. As before, the dashed lines correspond to the Dash mission and the solid lines correlate to the Loiter mission. Figure 4.16 gives the optimal speed for the Loiter mission where the minimum power is consumed, listed in Table 4.5.

Table 4.5 – Optimal Speed for the Lowest Power Requirement

	Lifting Body	Facet	Biplane
Speed (ft/s)	55.7	48.4	57.2

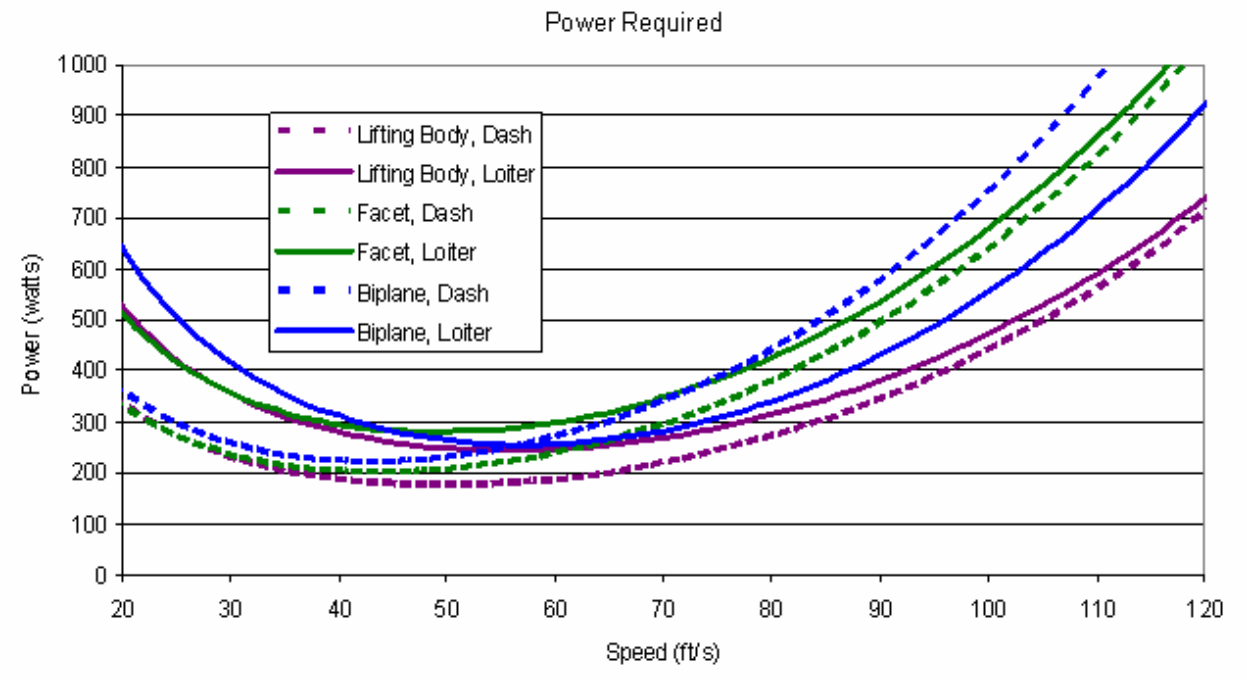

Figure 4.16– Power Requirements as a Function of Speed

4.6.1 Scoring Analysis with Wind Tunnel Data

With the optimal speed determined, the Loiter mission score could be fully calculated. For the two ground missions, the timed trials for reconfiguration and deployment were used as the basis for score. The performance analysis code was improved to account for changes in both battery and motor weight at varying dash speeds, providing a Dash mission score for a range of cruise speeds. Thus, the total score could be calculated as a function of the dash speed, illustrated in Figure 4.17. As the dash speed increases, the scores of the Facet and the Biplane climax and begin to decrease, while the Lifting Body score remains consistently high.

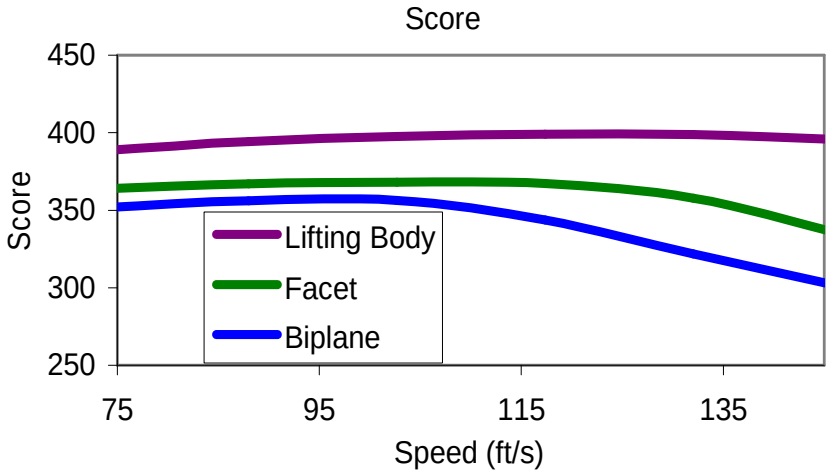

Figure 4.17 – Total Score as a Function of Speed

4.7 Flight Testing

The Facet was flown twice, each time with a different pilot. The pilots both agreed the Facet was neutrally stable in roll. Handling on the ground was also a problem because the differential thrust for taxing did not respond as expected. The differential throttle control will need to be tested more thoroughly. Landing was difficult, as the tail touched down first and was used to bring the plane to a halt. In the second landing the throttle was reduced to zero. The Lifting Body was flown once. The aircraft was unstable in roll and the pitch control was very sensitive. Within 3 seconds of takeoff the aircraft rolled and dove into the ground, destroying most of the aircraft. This reiterated the need to examine roll stability. It also showed that too much pitch control could be harmful. The ratings for the flight tests can be seen in Table 4.6. The Cooper-Harper Pilot Rating system was used to evaluate flight testing.

Table 4.6 – Rating of Test Flights

	Facet #1	Facet #2	Lifting Body
Takeoff	6	5	6
Flight	5	4	8
Max speed	N/A	N/A	N/A
Landing	6	5	10
Stability in Roll	Neutral	Neutral	Unstable
Stability in Pitch	Very Stable	Stable	Very Sensitive

4.8 Design Selection

The Lifting Body met the mission requirements at each stage of its design and consistently performed well. It was ultimately selected as the final aircraft design based upon the scoring calculation in Figure 4.18. It should be noted that the Lifting Bodying scored much higher than the other two designs at all speeds, allowing for an acceptable margin of error since the aircraft were not optimized.

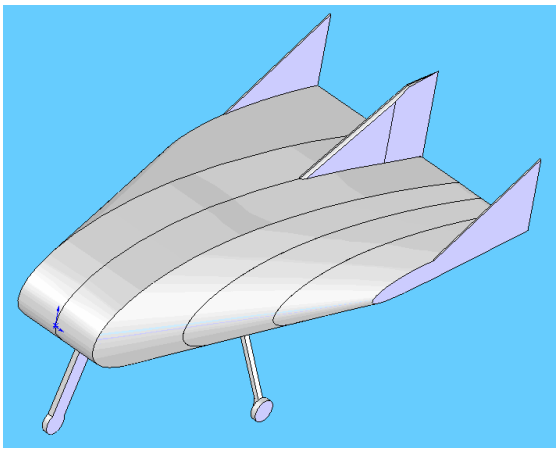

Figure 4.18 – Lifting Body Configuration Selected for Optimization

4.9 Configuration Optimization

The preliminary design now focused on aircraft optimization. Wing optimization was divided into three sections; airfoil, sweep, and winglet optimization. Additional optimization was conducted for the propulsion system, structures, and stability.

4.9.1 Airfoil Optimization

Selection of the airfoil for the Lifting Body was primarily driven by the thickness required to accommodate the payload. The dimensions of the storage box set maximum chord length of the airfoil at 43 inches. Seventeen NACA airfoils[1],[4] were found to match the minimum thickness requirement and each was run through XFOIL at dash and loiter (Re = 1260000 and Re = 680000 respectively). Plots of C_l vs C_d were created with the results of XFOIL and all of the airfoils were compared using these plots. Through a process of elimination, the three airfoils with the lowest drag coefficients were selected. These were the NACA 634221, 654221, and 654421, each with a thickness of 21%. Their drag polars are given below (Figure 4.19).

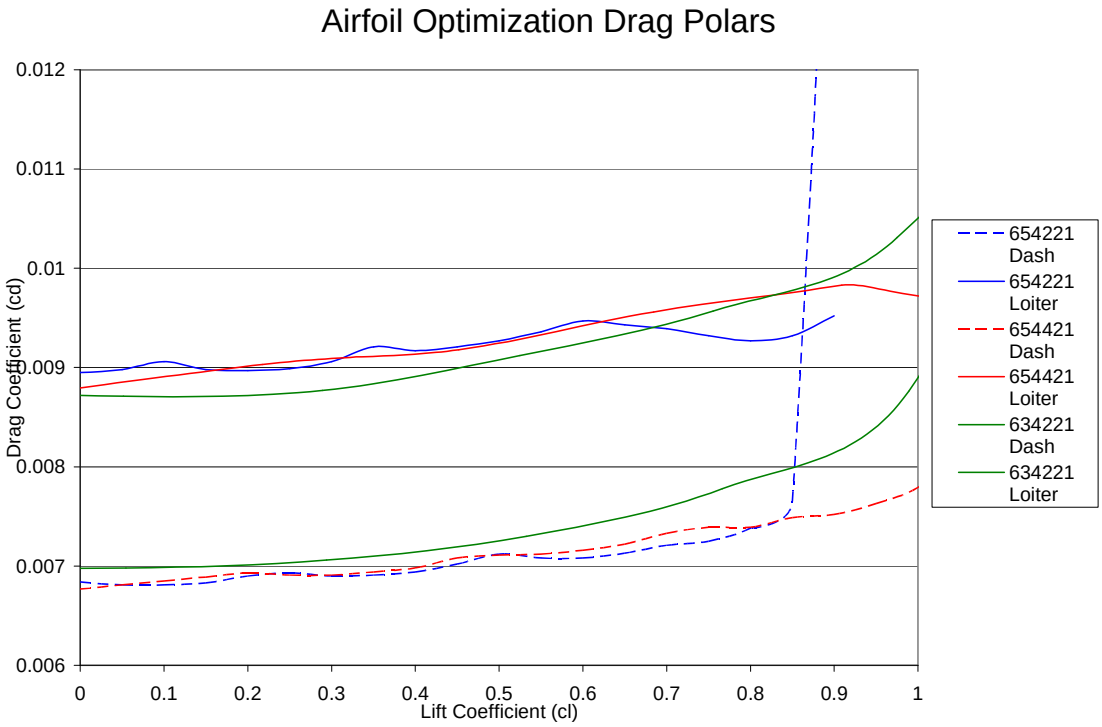

Figure 4.19 – Airfoil Optimization Drag Polars

As a final check, the ability of the payloads to fit within the airfoils was confirmed. All three airfoils were very similar, but NACA 654421 was chosen for its lower drag coefficients at higher lift coefficients.

Reflexed airfoils were considered as part of the airfoil optimization for use in pitch control. However, options were limited by the required thickness of the aircraft and the reflexed airfoils available resulted in significantly higher drag coefficients. Three reflexed airfoils were designed from the chosen NACA 654421, but these also resulted in higher drag and lower maximum lift. Thus, the decision to use NACA 654421 airfoil was confirmed.

4.9.2 Sweep Optimization

Sweep optimization was performed by varying the length of the tip chord, defining the sweep angle as that between the leading edges of the root and tip chords. Three different sweep options were explored to optimize the aircraft's performance: tip chords of 12, 18, and 24 inches (sweep angles of 75.5˚, 72.3˚, and 67.2˚, respectively). These three models were analyzed in CMARC. The induced drag did not vary significantly with each model. The 24 inch chord configuration resulted in higher skin friction drag due to the increase in surface area of the lifting body. The 12 inch tip chord configuration was eliminated due to the loss of lift-producing area and difficulty in constructing the leading edge of the aircraft. The 18 inch tip chord was selected as our optimal configuration, providing the necessarily lift with the least cost in skin friction drag.

4.9.3 Winglet Optimization

The primary purpose of the winglets was to provide lateral stability for the aircraft as will be discussed in the stability section. Due to the low AR of the wing it was decided to try and optimize the winglet to minimize induced drag. First, the wing wake was input to a vortex lattice code, which used Monk's theorem to determine the optimal span loading. This analysis yielded an optimal span efficiency factor for Loiter to be 1.68, versus 1.00 without the winglet. However, the geometry of the wing had already been determined to minimize both structural weight and the skin friction drag. To obtain the optimal span loading with the high sweep wing, C_ℓ values greater than one were required at the small chord sizes near the wing tip and at the base of the winglet, which is not typically possible without stall on small, low Reynolds number airfoils. Several winglets were tried at various angles of leading edge toe out in CMARC to determine which resulted in the highest span efficiency factor due to its direct relation to induced drag. One problem noted during this analysis was that due to the strong vortex formed on the wing, the winglet would be likely to stall at low toe out angles. The PSU-94097 airfoil, developed by Penn State University for gliders, provided the best span efficiency, without the risk of the winglet stalling, at a leading edge out angle of 6 degrees. This yielded a span efficiency factor of 1.28, which decreased induced drag by 28%.

4.10 Propulsion Analysis

The following section documents the analysis and design of the propulsion system. The propulsion system consists of batteries, a speed controller, an electric motor, a gear box and a propeller, as illustrated in the block diagram shown in Figure 4.20.

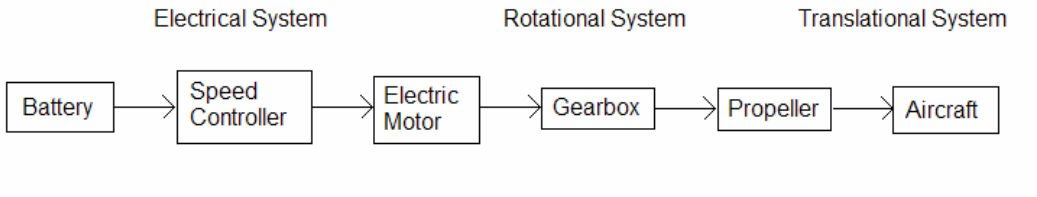

Figure 4.20 – Propulsion System Block Diagram

The propulsion system analysis code begins with the aircraft subsystem. Using wind tunnel data yielded the minimum power required and its corresponding velocity. The velocity for minimum power required is the maximum endurance velocity. With the performance requirements known, historical data research revealed propeller pitch to diameter ratios and the corresponding thrust coefficients, C_T, power coefficients, $C_{P,}$ and advance ratios, J. Using this propeller data, the propeller diameter and propeller RPM that provide maximum propeller efficiency were found. Also, the power output by the propeller and the power required by the propeller were calculated.

Given a specific motor, the power required by the propeller and the gear box efficiency, if one is used, the gear ratio that resulted in maximum motor efficiency was calculated. Additionally, the corresponding motor RPM, motor output horsepower, motor efficiency and the amperage, voltage and power required by the motor were determined. Knowing the voltage, amperage and power required by the motor, along with the required endurance and individual battery cell properties the battery subsystem was analyzed. The battery subsystem analysis resulted in the number of cells, the battery pack voltage & weight, the actual endurance and the overall aircraft efficiency.

Using the propulsion system analysis code, 8 different motors with several different propeller diameters were analyzed. In running these propulsion systems through the code, the Loiter mission endurance of 5 minutes and 100 ft takeoff power requirement were verified. Along with these verifications, the propulsion analysis code output the overall propulsion system efficiency and the battery weight. Using the wind tunnel measurements the total takeoff power required was calculated to be 294 Watts. Each propulsion system analyzed met this takeoff power requirement.

In Figures 4.21 and 4.22, the horizontal axes represent 24 propulsion configurations consisting of several combinations of motors and propellers. Some propulsion systems were deemed invalid because of an

insufficient endurance or because of a propeller that exceeded the air sampler payload constraint of a 10 inch diameter propeller.

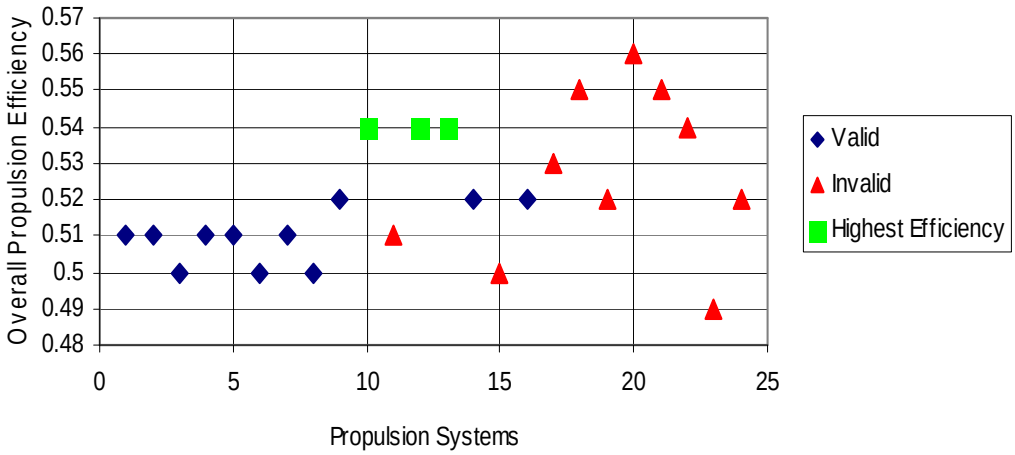

Figure 4.21 – Propulsion System Efficiency

The overall system efficiencies for each configuration analyzed are shown in Figure 4.21. The systems that satisfied the propeller clearance restraint and the endurance requirements with the highest overall efficiency were the Hacker A30/10L, the Hacker A30/8XL and the Mega 22-20-4. Each motor was mounted with a 10 inch diameter propeller.

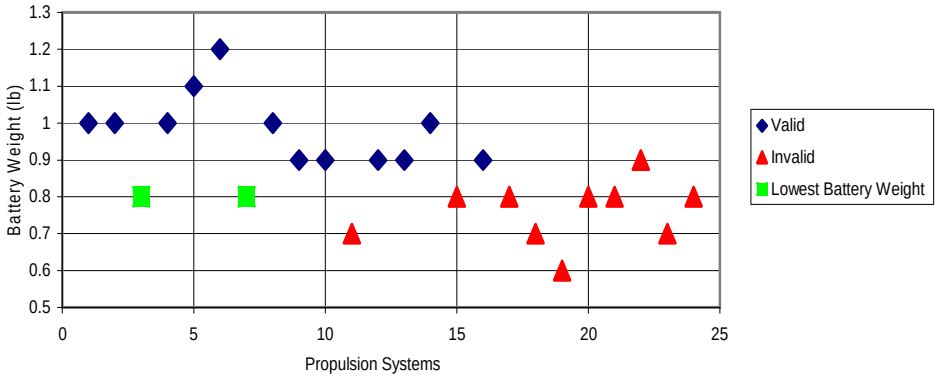

Figure 4.22 – Propulsion System Battery Weights

Figure 4.22 compares the battery weights of each system analyzed. The systems that satisfied the propeller payload restraint and the endurance requirements with the lowest battery weight were the AXI 2820/8 and the Mega 22-20-4. Each motor was equipped with a 9 inch diameter propeller.

The propulsion analysis code resulted in a down-select to the Hacker A30/8XL, the Mega 22-20-4 and the AXI 2820/8. These motors were considered for further analysis and testing.

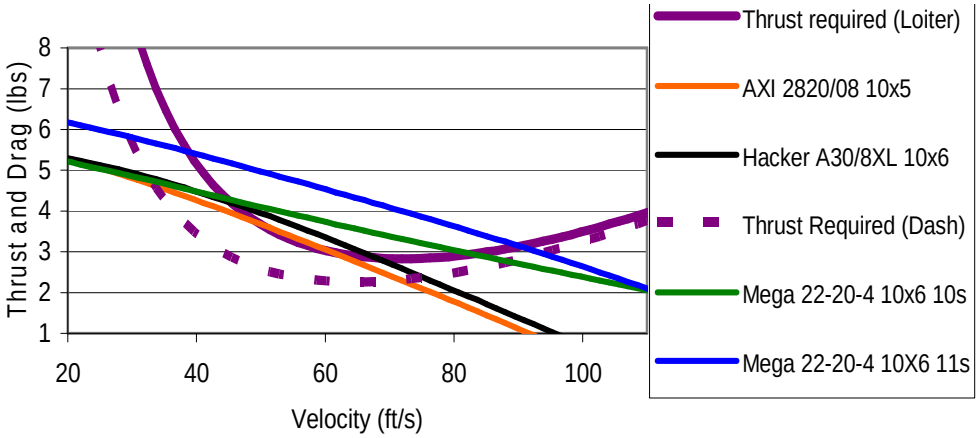

Figure 4.23 – MotoCalc Propulsion System Analysis for 3 Down-Selected Motors

MotoCalc calculated the thrust available for the Hacker A30/8XL, the Mega 22-20-4 and the AXI 2820/8. Figure 4.23 shows that the Mega 22-20-4 with Elite 1500 cells outperforms the Hacker A30/8XL, the AXI 2820/08 and the Mega 22-20-4 with GP 3300 cells.

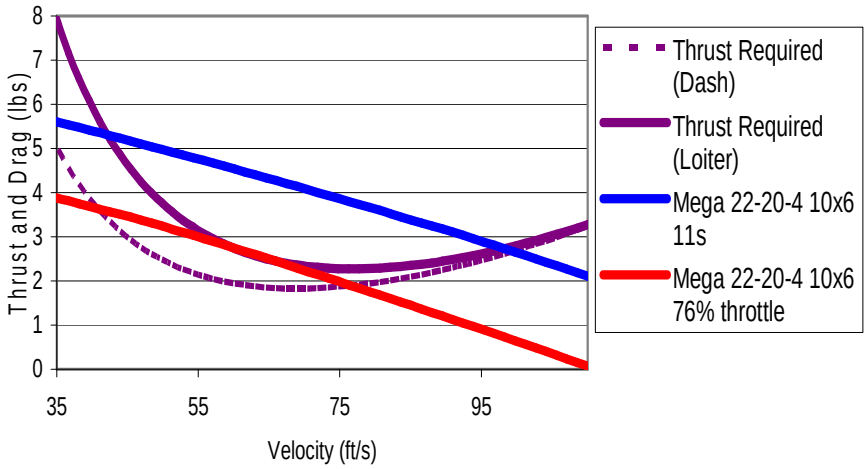

Figure 4.24 – MotoCalc Propulsion System Analysis for Down-Selected Motors

The Mega 22-20-4 with the Elite 1500 cells was selected due to its superior performance. Figure 4.24 shows the Mega 22-20-4 thrust available and the Mega 22-20-4 at 76% throttle along with the thrust required for the Loiter and Dash missions. At 76% throttle the thrust available corresponds to the thrust required for the maximum endurance velocity.

The final motor configuration stemming from this analysis is the Mega 22-20-4 using 11 Elite 1500 cells in series with 3 Elite 1500 cells in parallel and a 10x6 APC propeller. A Castle Creations Phoenix 45 speed controller was chosen due to budget constraints and because it was on-hand.

Testing these motors will yield which motor, propeller and battery combination will result in the highest score but because the Mega 22-20-4 with the Elite 1500 cells showed the best theoretical performance, it was used for the theoretical performance analyses in the sections preceding the motor testing.

4.11 Structural Analysis

I-deas software was used to analyze the airframe by modeling it with beam elements. The cross section of the beams was a solid box of quarter inch balsa material. The leading edge was modeled as shell elements of 0.005" thick carbon fiber. The motor, servos, batteries, battery receiver, and payload were modeled using lumped masses. The Monokote covering was not modeled. Although it will add torsional rigidity, this model focused primarily on beam bending elements and the leading edge. For the first loading case, restraints were placed at the wing tips and the aircraft was loaded to max gross weight, simulating the 2.5g load done at tech inspection. The stress results for the leading edge and balsa frame for these boundary and loading conditions are plotted below in Figure 4.25.

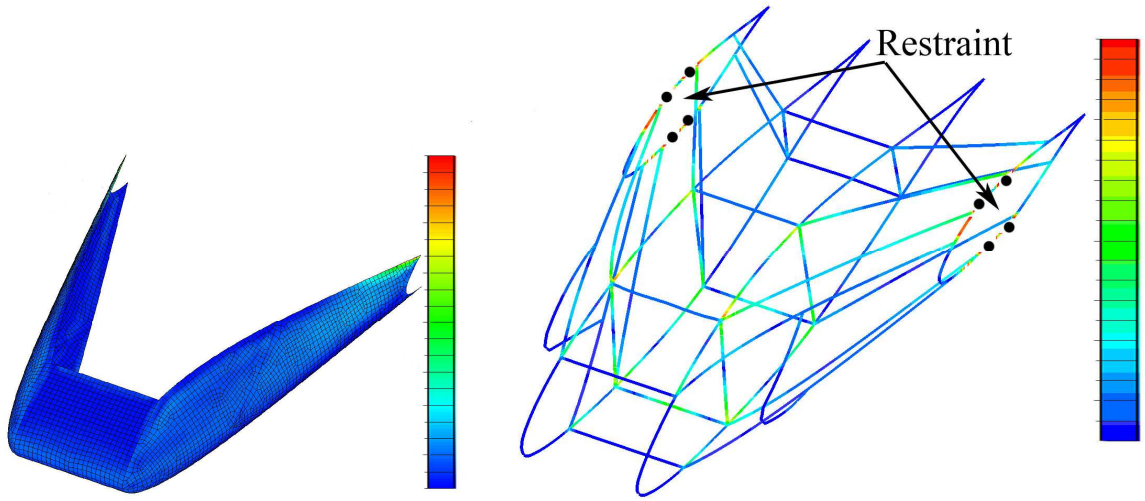

Figure 4.25 - Stress Due to 1g Load Restrained at Wingtip

Red colors represent the yield stress of the respective materials. Peak stress occurs in the wing tip because the aircraft's center of gravity causes it to pitch down. This creates a large moment at the wing tip, particularly in the restraint locations. Since the aircraft would actually have to be provided some support at the nose of the aircraft during the structural integrity check, the moment would not be nearly as severe and the high stresses in the wing tips would not be present.

For the second loading case restraints were placed in the fuselage at the payload mounting location. The structure was then analyzed using a 2.5g vertical up load to simulate lift on the aircraft. The stress results for the leading edge and for the frame for these boundary and loading conditions are plotted below in Figure 4.26.

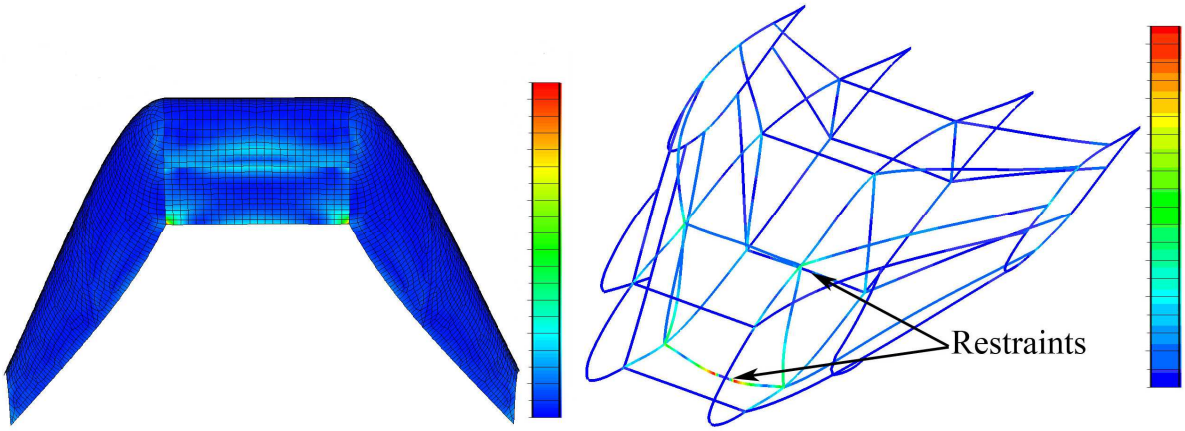

Figure 4.26 - Stress Due to 2.5g Load Restrained at Payload (Red is Yield Stress)

The peak values are localized in the front section of the leading edge where it connects into the frame. Small gussets could be added in the corners to alleviate the concentrated stress. Maximum stress occurs in the frame at the payload restraint location. Although this area is of concern, the payload housing structure has not been modeled with this frame and therefore the stress is not distributed exactly as it will be in the actual structure. Also the landing gear will be placed at this location further strengthening it. The main structure of the airframe was thus concluded to have adequate strength.

As a result of the structural analysis, the structural beam elements of the frame could be properly sized to reduce the weight of the airframe. The initial weight of the aircraft was reduced by nearly 20% by identifying overbuilt areas. Additionally, areas of structural concern were identified for reinforcement.

4.12 Stability and Control

Stability and pilot feedback were evaluated with *X-Plane*[5], a FAA certified flight simulator that uses aircraft geometry to create a flight model by utilizing blade element theory and a combination of theoretical and empirical methods. The program accurately models the space shuttle and B-2 bomber which are two unconventional designs similar to the Lifting Body. A number of configurations were tested and their progression is shown below (Figure 4.27).

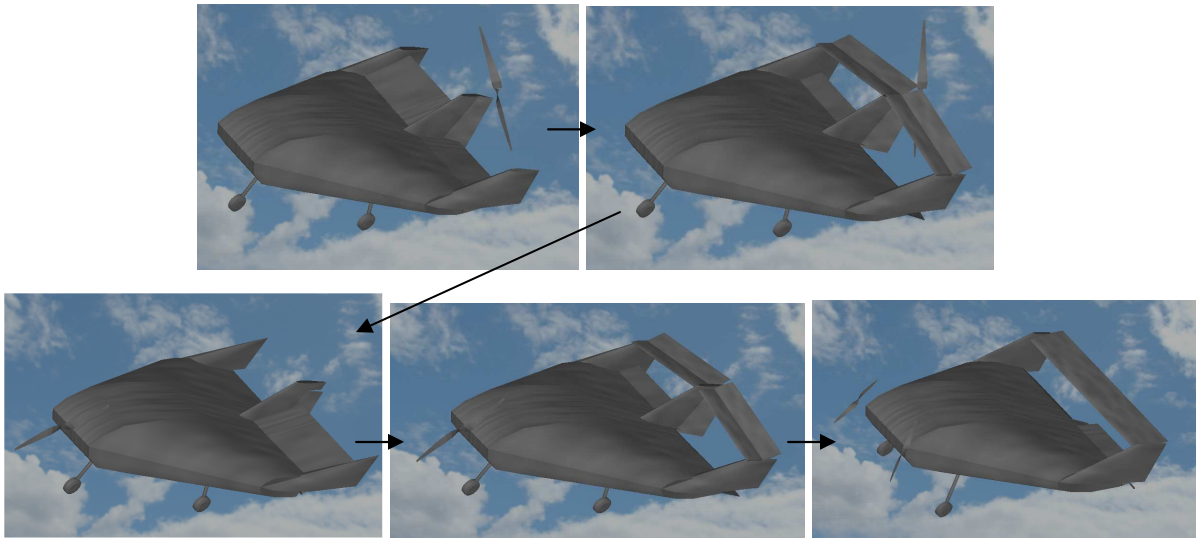

Figure 4.27 - X-Plane Aircraft Progression from Upper Left to Lower Right

Four areas were studied, pitch, yaw, roll control, and motor location. The following results were seen.

Pitch: The lifting body design was sensitive to CG and required significant elevator input to balance the differing flight conditions. A horizontal stabilizer reduced this tendency and allowed for easier trim of the aircraft. The stabilizer's size was iterated and adequate pilot control was experienced with a 6 inch tail. Elevons were considered, but were observed to adversely affect aircraft performance and add drag.

Yaw: Yaw control was observed to only be required at landing speeds and was addressed with motor location.

Roll: Roll stability was a concern due to the short wingspan and led to a crash of a prototype aircraft. It proved difficult to improve the roll characteristics through aerodynamic design, so the addition of a rate gyro was explored in X-plane. The results showed a dramatic increase in pilot control.

Motor Location: The original configuration was a pusher and testing showed that left turning tendencies were amplified at takeoff and landing. The motor's height created large pitching moments, resulting in takeoff distances of up to 50% more. Instead, a single motor was placed at the nose, which reduced yawing tendencies. However, the single tractor engine posed payload mounting issues. The motor configuration was thus changed to a twin tractor. The use of a counter rotating setup eliminated left turning tendencies and allowed for differential thrust, eliminating the need for rudders and allowing the payload to be easily mounted.

As a result of the X-Plane analysis, the aircraft configuration was changed slightly. A horizontal stabilizer was added to improve pitch control and trim. A rate gyro will be used to dampen rolling caused by the small wingspan and low rolling moment. The engine was moved from a single pusher configuration to a twin tractor to improve control, eliminate the need for rudders, and allow for payload mounting.

The vertical tail size was driven more by the placement of the horizontal stabilizer than anything. To ensure that it was large enough to provide adequate stability, a simple tail volume method was used, presented in Raymer[3]. Due to the unconventional aircraft design, along with the fact that it is a remote control aircraft with no rudder, the largest presented vertical tail coefficient of .09 was used. This yields a required tail area of .664 ft^2. The wing will have two winglets that act as vertical stabilizers, and thus should have an area of at least .332 ft^2 each. Due to taper from the wing to the winglet, and the height requirements for the horizontal stabilizer to be above the majority of the wing turbulence, each vertical ended up with a size of .42 ft^2. This is slightly over the minimum value determined, however there is no rudder and this is a remotely controlled aircraft, thus the extra area provides a safety margin to make sure the aircraft is stable in yaw.

The unconventional design of the aircraft poses concerns in pitch stability. An initial attempt at using empirical methods was tried, however due to the complex geometry of the aircraft, it was determined to be easier and more accurate to use CFD data. A value of 5% was chosen for the static margin as that is the lowest value recommended for a normal aircraft. $C_{M\alpha}$ and $C_{L\alpha}$ from the Fluent model were used to determine the moments about the CG and then the CG was varied. It was found that 16 inches from the leading edge produced a static margin of 5.28% with a $C_{M\alpha}$ = -.00133 (1/deg) and a $C_{L\alpha}$ =.0246 (1/deg). The final step in the pitch stability was to determine the trim diagram. Due to the large forces needed to balance out the change in pitching moment, it was decided to use a full flying tail as had been found in the X-Plane results. A NACA 0008 was used for its small thickness, low drag, and symmetry allowing for a large variation in trim angles. It was noted that at the tail Reynolds number, the flying tail could attain +/-8 degrees. A pitch trim diagram was then completed to determine the flight envelope of the aircraft as seen in Figure 4.28.

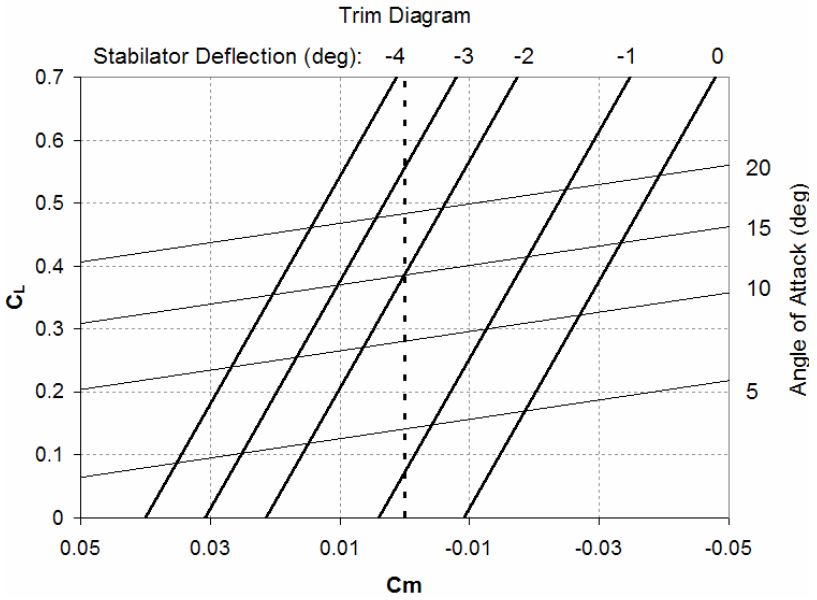

Fig. 4.28 - Pitch Trim Diagram

It can be seen that 4 degrees of deflection is required to trim the aircraft at the stall C_L, requiring only half of the available elevator deflection and thus the aircraft is able to be trimmed all the way to stall with adequate control authority remaining.

4.13 Preliminary Design Conclusion

Through preliminary design, an optimal configuration was identified through the three aircraft configurations. The wing span was reduced to 2 ft, resulting in a 44% increase in final score. The three aircraft were flown in a mission simulation and performance program. Through calculations, wind tunnel testing, and flight testing, the design was down selected to the Lifting Body. Design then focused on optimization of aerodynamics, propulsion, structures, and stability, resulting in the finalized aircraft configuration.

5. Detail Design

Detailed design further analyzed the final aircraft model. Focus was placed on additional CFD analysis to determine the final performance characteristics. The design of the payload was also studied to determine its interaction with the aircraft and its effects on score. The weight and balance of the aircraft was calculated to verify proper CG location for stability as well as final performance calculations. The selected systems, weight, and performance were summarized in a concise table. Finally, a detailed drawing package was created to illustrate the aircraft's final geometry.

5.1 Final CFD Model

After the completion of several design iterations, the final detailed aircraft model's aerodynamic performance was evaluated directly using the validated CFD from the Lifting Body prototype model. The final CAD model included an updated and fully detailed airfoil, winglets, external payload geometry, simplified engine nacelles and landing gear geometry. The model was meshed using the same mesh sizing parameters as implemented for the baseline model (Figure 5.1).

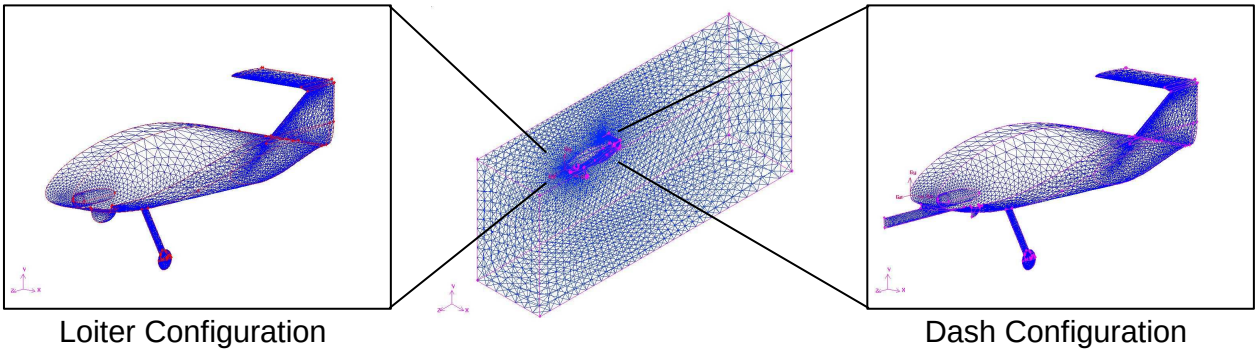

Figure 5.1 – Detailed Surface and Volume CFD Mesh

The viscous flow solution was obtained using a realizable k-epsilon turbulence model and a coupled – implicit solver with 2nd order discretization for the two critical design points (Loiter and Dash) based on the two aircraft missions. Corresponding drag polars were created as shown below (Figure 5.2).

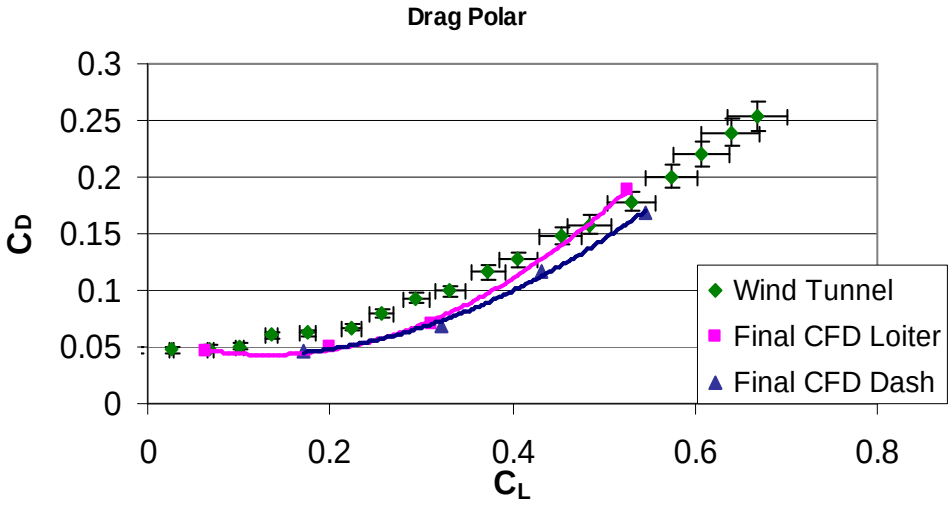

Figure 5.2 – Detailed CFD Drag Polar

Deviations seen from the original wind tunnel results can be attributed to the changeover to an optimized airfoil, winglets and the addition of the engine nacelles and the horizontal stabilizer. Despite additional drag created by the engine nacelle and horizontal stabilizer, winglet and airfoil optimization has helped reduce aircraft drag. As expected, the addition of external payload geometry resulted in a reduction of the available lifting area on the wing, which corresponds with the lower lift coefficients obtained for the detailed CFD models.

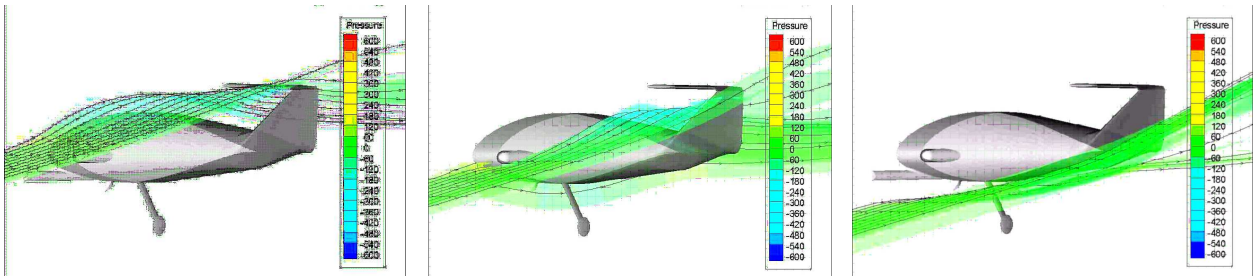

(a) (b) (c)

Figure 5.3 - Flow Contours of Aircraft (Dash Configuration)

Airflow visualization around the aircraft was accomplished through post processing the CFD results in Tecplot. The three slices above in Figure 5.3 represent the flow over the top of the aircraft and horizontal stabilizer (a), around the aircraft and winglets (b), and underneath the aircraft and around the landing gear (c). Smooth streamlines around the aircraft confirm that no separation effects are disturbing the flow. Post processing of the CFD results yielded detailed information on the airflow around the aircraft's

geometry and pressure distributions. The CFD data verified the evolution of several design features since the prototype wind-tunnel testing. In conclusion, the CFD results are representative and are within the error bounds of wind tunnel testing.

5.2 Payload

The reconfiguration mission makes payload restraints an integral part in the aircraft and scoring. Several configurations were analyzed to determine which would provide the fastest reconfiguration time while minimizing weight gained. The following figures of merit were used to determine which payload restraint was the optimal configuration: loading time, aircraft gross weight, RAC (empty weight only), and complexity. Each payload configuration was rated below (Table 5.1) based on the figures of merit. This scale is based from -5 to 5, with -5 being disadvantageous, 0 being neutral, and 5 being the most advantageous.

Table 5.1 – Payload Restraint Configuration

Figure of Merit	Weight	Spring Loaded Pin	Payload mounted servo	Fuselage mounted servo	Pivot latch	Screw
Time	.6	0	5	5	-2	-5
Weight	.2	0	-5	0	0	0
RAC	.1	0	0	-5	0	0
Complexity	.1	-5	-3	0	3	5
TOTAL	**1**	**-.5**	**1.7**	**2.5**	**-.9**	**-2.5**

- Spring Loaded Pin: A pin is mounted on the payload insert held in place by a spring. When removed, a hand on each side of the payload insert depresses a flap, compressing the spring and freeing the payload. This mechanism is fast because the payload can be unlatched while it is being grasped for removal.
- Payload Mounted Servo: A servo is mounted on the payload insert, allowing for the payload to be unlatched while the loader is approaching it. All they have to do is remove the payload. This keeps the servo from being added to the empty weight, but requires its own receiver and power supply, greatly increasing the insert's weight. Also, size constraints of the insert limit where the servos can be placed.
- Fuselage mounted servo: This servo is mounted on the fuselage and counts toward the empty weight, increasing the RAC. However, servos as light as ¼ oz. can be used, which is a small increase in weight. It also allows for more flexible mounting positions and can run off the onboard receiver and power supply.
- Pivot Latch: A simple latch is turned by a handle on the top surface of the payload insert, fostering low weight and simple construction. However, the handle must be very small to remain aerodynamic, and thus difficult to operate. Opening the latch and displacing the payload are two separate actions, taking extra time.

- Screw: This most simplistic latching mechanism requires a solid mounting point on the insert and a screw that requires a tool.

The fuselage mounted servo method was chosen as the fastest way to secure and release the payload inserts. To then remove the inserts, a simplistic string handle would be used that would lay flat on the fuselage in flight.

5.3 Weight and Balance

A table of all the major components of the aircraft was made to determine the center of gravity and moments of inertia of the aircraft. This took into account batteries, motors, servos, frame, control surfaces, and skin weights and location. The location is based off of an XYZ coordinate system centered at the nose of the aircraft. X being the roll axis, Y being the pitch axis, and Z being the yaw axis, with Z pointed in the upward direction. The CAD model in SolidWorks was used to find the CG of the fixed components, such as the airframe, motors, etc. The CG of the batteries and payload was allowed to be movable to balance the aircraft. The payload CG did however need to stay within the constraints of the payload box. This was then used to find the CG of the aircraft as a whole by calculating the moments of each component. The moments of inertia were calculated using SolidWorks for most of the components of the aircraft. SolidWorks was used because it did not assume point masses and therefore was more accurate. The batteries and payloads however were calculated in Excel, assuming point masses. This was done because the batteries were not modeled in the CAD file and the payload was determined to not have constant density. This image below shows the CG for the aircraft and the local CG of the major components (Figure 5.4).

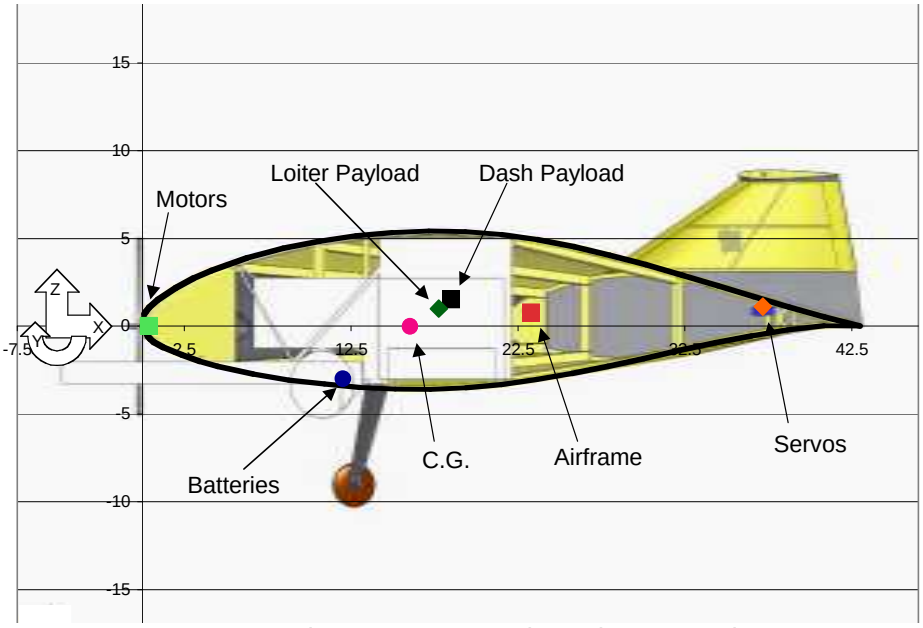

Figure 5.4 – CG and Local C.G Locations

Table 5.2– Moments of Inertia

Moments of Inertia	Ixx	Iyy	Izz	Ixy	Ixz	Iyz	
Dash	1.796	18.491	19.909	0.000	0.437	0.000	lb ft^2
Loiter	1.803	22.088	23.499	0.000	0.459	0.000	lb ft^2

Table 5.3 – CG Locations

CG	X	Y	Z	
Dash	1.33	0	0	ft
Loiter	1.34	0	0	ft

From the inertia and moments tables (Tables 5.2 and 5.3) the components of the aircraft can be moved around easily. This is very important for making sure the aircraft is balanced properly. After the final build the tables make finding the final locations for the different components simple.

5.4 Configuration and Performance Predictions

Table 5.4 – Performance and Configuration Specifications

Weight	
MEW (lb)	4.287
RAC	102.89

Geometry	
Fuselage/Wing	
Airfoil	NACA 654421
Chord (in)	43
Span (in)	24
Area (ft^2)	5.6
AR	0.714
Horizontal Stab	
Airfoil	NACA 0008
Chord (in)	6
b_t (in)	24
S_t (ft^2)	1
AR	4
Winglets	
Airfoil	PSU 94097
C root (in)	15
C tip (in)	6
h_v (in)	6
AR	0.57

Performance		
CL max	0.7	
L/D max	4.49	
	Gross Weight Performance	
	Dash Configuration	**Loiter Configuration**
(Rate of Climb) max (ft/min)	784.8	469.2
Stall Speed (ft/s)	43.44	48.39
Maximum Speed (ft/s)	98.27	--
Loiter Speed (ft/s)	--	66.00
Take off Distance (ft)	54.23	96.23
Weight and Balance		
Airframe (lb)	1.281	
Propulsion (lb)	2.485	
Avionics (lb)	0.521	
Empty weight (lb)	**4.287**	
	Dash Configuration	**Loiter Configuration**
Payload Weight (lb)	3 (4 with support and probes)	5 (6 with support and probes)
Total (lb)	**8.287**	**10.287**
Systems		
Motor	Mega 22-20-4	
Batteries	Elite 1500, 11s3p (NiMH)	
Servos	HS-81 x 3 (surfaces) HS-55 x 2 (payloads)	
Receiver	Berg 7P	
RX battery	4.8V 650 mAh	
ESC	Castle Creations Phoenix 45	
Propellor	APC 10x6 counter-rotating	

5.5 Drawing Package

6. Manufacturing Plan

A manufacturing plan was developed through the use of five Figures of Merit to determine how the aircraft would be constructed. Material properties and Figures of Merit were evaluated for each structural component. Cost, team abilities, and a schedule were also established.

6.1 Manufacturing Figures of Merit

For materials and technique selection, several figures were important to the construction of the aircraft.

- **RAC**: Since the aircraft was already sized, only the weight was a factor.
- **Payload Integration**: The structure must accommodate internal payloads.
- **Ease of Construction**: How quickly and reliably the part can be built.
- **Reparability**: Includes the durability of the structure and how easily it can be replaced.
- **Team Ability**: The team's familiarity with using the method, leading to better quality.

6.1.1 Lessons Learned from First Manufacturing Iteration

Features from each of the constructed aircraft were analyzed according to the FOMs for integration into second iteration spiral. Due to the Facet's light weight, a structure of curved balsa beams forming the outer frame was chosen. This method's little internal structure easily accommodated payloads. Additionally, stringers were extended from root to tip to maintain the airfoil shape across the wingspan, similar to the original Lifting Body. However, due to the complexities at the leading edge, it was decided to make the leading edge out of composites. Foam, as used in the biplane, was chosen to form the transisition between the wing and winglets. Twin, tractor motors, as in the Facet design, eliminated the need for a large, heavy vertical stabilizer/motor mount.

6.1.2 Construction Methods

- **Balsa Build Up:** A balsa lattice holds the body shape, leading to a lightweight structure. However, many ribs are needed to hold a complex shape, leading to excess weight. Though the method can be difficult to repair it is straightforward and team members are experienced with it.
- **Composite Mold:** A mold and composite material holds aerodynamic shape well. However, few team members are knowledgeable in method, and it is heavy and time consuming.
- **Foam Core:** A CNC machine creates a foam shape. The foam holds shape well, but the entire volume is filled with excess weight that provides little or no structural support.
- **Composite/Balsa:** A balsa build up holds the majority of the structure and areas are reinforced with composites to maintain an aerodynamic shape and distribute loads. Many team members can work on the balsa structure while those knowledgeable can focus on composite techniques.
- **Composite/Core:** This method consists of a balsa or foam core laminated with composites. This technique is heavy, but it provides a strong structure for areas experiencing high stresses.

6.1.3 Winglet/Horizontal Tail

Table 6.1- Winglet / Tail Construction Matrix

Figure of Merit	Weight	Balsa Build Up	Composite Mold	Foam Core	Composite/ Balsa
RAC (weight)	0.55	1	-1	-1	1
Ease of Construction	0.2	0	-1	1	0
Reparability	0.15	-1	0	-1	-1
Team Ability	0.1	1	-1	0	-1
Total	**1**	**0.5**	**-0.85**	**-0.5**	**0.3**

The winglet and horizontal tail both consist of small size airfoils where the leading edge is small enough that a balsa strip can form its shape. This allows for the light-weight balsa build up method to be used for the entire surface. This is verified as seen in Table 6.1.

6.1.4 Landing Gear

Table 6.2 – Landing Gear Construction Matrix

Figure of Merit	Weight	Composite Mold	Composite/ Core
RAC (weight)	0.5	0	0
Ease of Construction	0.2	-1	0
Reparability	0.15	0	1
Team Ability	0.15	-1	0
Total	**1**	**-.35**	**0.15**

The landing gear is subjected to high forces and requires a strong construction. In order to minimize weight and optimize the structure, commercial options were not explored. Combining a composite external structure, capable of handling bending moments, with a stiff inner core allows for a strong landing gear structure. This is verified in Table 6.2.

6.2 Analytical Analysis

6.2.1 Required Skills

The skills required to build each component of the aircraft were analyzed in Table 6.3. A value of -1 indicates a difficult skill and 1 indicates a skill that can be quickly learned. Skills not required are denoted NR.

Table 6.3 – Required Skills for Construction

Skill	Body Balsa	Body Leading Edge	Winglet Transition	Winglet/Horizontal	Landing Gear
CAD	-1	-1	-1	1	-1
CNC	NR	2	-1	NR	1
Balsa Work	-1	NR	NR	1	1
Assembly	1	-1	1	1	1
Covering	1	NR	-1	1	NR

6.2.2 Airframe Construction Cost Analysis

The following chart (Figure 6.1) itemizes the cost to build the airframe per aircraft. Costs of electronics are not included because of their likelihood to survive crashes. It is expected to build 2-4 airframes depending on time constraints and the number of crashes.

Item	Cost	Color
Balsa	$125.00	
Carbon	$0.00	
Foam	$25.00	
Covering	$70.00	
Mold Material	$85.00	
Control Surface supplies	$25.00	
Glue	$35.00	
Total:	**$365.00**	

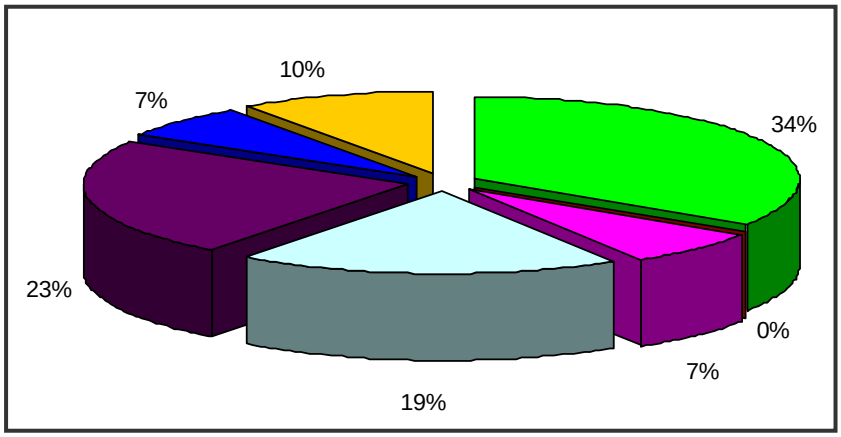

Figure 6.1 – Construction Cost Analysis

6.2.3 Manufacturing Timeline

	January 1	2	3	4	Febuary 1	2	3	4	March 1	2	3	4	5	April 1	2	3
WING CONSTRUCTION										FINAL REPORT						COMPETITION
Airfoil Shaping of Wood											======					
Reinforce Airfoils											======					
LEADING EDGE																
Creating Mold											======					
CNC Mold												======				
Layup Mold												======				
SWEEP WING CONSTRUCTION																
Create Foam Airfoils												===				
Connect Chord to Tip												======				
Create Control Surfaces													===			
WINGLET CONSTRUCTION																
Create Foam Integration												===				
Make and Assemble Parts											======					
HORIZONTAL STABILIZOR																
Make and Assemble Parts											======					
Foam Fillets												===				
Final ASSEMBLY													===			

=== Actual
=== Planned

Figure 6.2 – Manufacturing Timeline

7. Testing Plan

7.1 Test Objectives

Based on experiences learned in the first design spiral, testing was considered an integral part in verifying the design process. Four areas will be explored: structural, propulsion, ground mission, and flight testing. Objectives will be to verify the structural integrity of the airframe & landing gear, the motor & propeller combination, the reconfiguration & deployment methods, and the flight model. The competition missions will be practiced by the pilots and ground crew for familiarity.

7.2 Structural Testing

The aircraft will be loaded to max gross weight and the structural test performed during tech. inspection will be verified by lifting the aircraft by its wingtips. Also, landing gear will be tested by means of drop tests from fixed heights. The height is determined by a maximum rate of decent value of 500 ft/min - a reasonable speed for a hard approach. This translated to a drop height of 13 inches. Several landing gear models will be constructed and each will be dropped with 10 lbs to simulate the hardest landing at max gross weight. The lightest gear that is able to withstand 10 simulated landings will be chosen. Ten was chosen because the maximum possible number of landings at the competition will be 5, allowing a safety factor of two.

7.3 Propulsion Testing Plan

The propulsion testing has yet to be conducted due to delays in motor acquisition. The propulsion testing will consist of a static motor endurance test and two dynamic motor tests for several propulsion configurations. For the static motor endurance test the motor will be run at 100% throttle for the duration of the battery life. The two dynamic motor tests will simulate the Loiter and Dash missions. Throughout each test the wattage, voltage, current and thrust will be logged. The necessary equipment will be an Eagle Tree Watt Logger, a thrust stand, USB cables, a laptop computer and a propulsion system to be tested.

7.4 Ground Mission Testing

This portion of testing will consist of testing the payload mechanisms, refining the box, and allowing the ground crew to practice for the competition. The payload restraint mechanisms will be refined to minimize time required to actuate them. The restraints will be tailored to the ground crews needs. For the deployment mission, the box will be tailored so that the ground crew can most easily remove the aircraft. During these ground tests a single ground crew will be selected based on time trials.

7.5 Flight Testing

Flight testing will consist of three phases; control calibration, flight model confirmation, and competition mission analysis. The first phase, control calibration, will consist of several flights with minimal avionics

onboard. The purpose of the flight will be to determine the actual handling qualities of the aircraft compared to predictions. In the flight model confirmation phase, an avionics package will be installed to record in-flight data to match to wind tunnel testing. The lift over drag ratio will be found from making several glides at different trimmed speeds. The drag polar build-up will be accomplished by determining the lift over drag ratio. By combining these, the drag will be compared to that predicted by the wind tunnel. The final stage of flight testing will focus on mission analysis. In this stage of testing each mission will be run through several times to determine the optimal take off and climb profiles, cruise speed, turn radii, and landing approaches. The flight testing timeline is shown below (Table 7.1).

FLIGHT TESTING	April															
	01	02	03	04	05	06	07	08	09	10	11	12	13	14 15-	21 22-	28
	1							2							3	4
FLIGHT CALIBRATION																
Handling Qualities	=========															
Trim Settings		=========														
Gyro Calibration			==========													
FLIGHT MODEL CONFIRMATION																
Eagle Tree Data Collection						======										
Flight Test Data Comparison							======									
COMPETION PRACTICE																
Dash and Loiter Missions										==========						

Actual
=== Planned

COMPETITION

Table 7.1 – Flight Testing Timeline

A flight test card was used to evaluate and compare flights. A consistent set of procedures was used to evaluate the flight tests according to the Cooper-Harper pilot rating system (Figure 7.1).

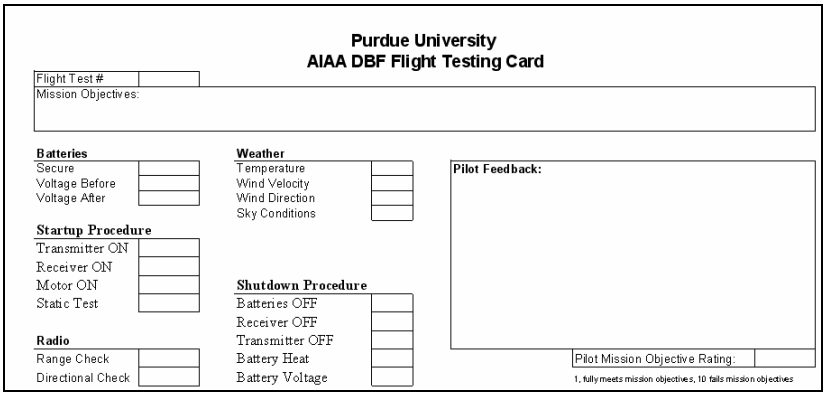

Purdue University
AIAA DBF Flight Testing Card

Flight Test #
Mission Objectives:

Batteries
Secure
Voltage Before
Voltage After

Weather
Temperature
Wind Velocity
Wind Direction
Sky Conditions

Pilot Feedback:

Startup Procedure
Transmitter ON
Receiver ON
Motor ON
Static Test

Shutdown Procedure
Batteries OFF
Receiver OFF
Transmitter OFF
Battery Heat
Battery Voltage

Radio
Range Check
Directional Check

Pilot Mission Objective Rating:
1, fully meets mission objectives, 10 fails mission objectives

Figure 7.1 – Flight Test Card

8.0 References

[1] Abbott, I.H., Von Doenhoff, A.E. *The Theory of Wing Sections*. 1st Ed. Dover Publications, Inc. New York, NY. 1959.

[2] Brandt, S.A., Stiles, R.J., Bertin, J.J., Whitford, R. *Introduction to Aeronautics: A Design Perspective*. 5th Ed. American Institute of Aeronautics and Astronautics, Inc. Reston, Virginian. 1997.

[3] Raymer, D.P. *Aircraft Design: A Conceptual Approach*. 4th Ed. American Institute of Aeronautics and Astronautics, Inc. Washington, DC. 2006.

[4] UIUC Airfoil Coordinate Database; http://*www.ae.uiuc.edu/m-selig/ads/coord_database.html*

[5] X-Plane Flight Simulator; *http://www.x-plane.com*

9. Post Report Submission Work

This section highlights the project from the time of the competition report submission to after the competition.

9.1 Construction and Manufacturing

The final aircraft was built for the most part out of ¼" balsa, with a bit of carbon fiber and plywood for reinforcement where needed. The main ribs of the aircraft were formed by steaming wood in a form so they would retain the curvature of the airfoil, and the airframe was assembled on a full-sized jig to ensure straight, accurate construction. The leading edge of the aircraft was a single sheet of 1/32" balsa, glued to the ribs and stringers to maintain its shape.

The elevons were built as a modular assembly, hinged about an aluminum tube running from one side of the aircraft to the other. This design feature allowed the elevons to survive each crash undamaged, and for them to be quickly mounted on the next airframe for flight.

On the original aircraft, airfoiled winglets were used, and were built out of balsa with a sheeted D-box construction for strength, as they had to support the full-flying horizontal stabilizer. The horizontal stabilizer was built around an aluminum tube, with balsa ribs, a balsa leading edge, and a thin carbon trailing edge. The aluminum tube also functioned as the hinge, rotating in nylon bushings attached to the winglets.

The final aircraft design did away with the canted, airfoiled winglets and the horizontal stabilizer, adding a central vertical stabilizer and rudder, and large, flat-plate winglets. The winglets were comprised of a balsa stick frame laminated on the outer side with 1/32" balsa. The vertical stabilizer and rudder were made up of a built-up balsa stick structure.

The original landing gear was a commercial carbon fiber product. Over the course of a number of crash landings and a crash on takeoff, it was determined that the carbon gear was too rigid, and was prone to destroying the bottom of the aircraft rather than absorbing the impact. Replacement gear were bent from aluminum stock purchased at the hardware store, and we found that the aluminum would bend much more than the carbon on landing (and stay bent), absorbing the impact and greatly increasing the survivability of the airframe.

9.2 Motor and Battery Selection and Testing

Of the two motors chosen to test (the AXI 2820/08 and Mega 22/20/4), we decided on the AXI for a few different reasons. Testing on the thrust stand showed that with the APC 9"x6" and 10"x5"

props the AXI produced more thrust at a given voltage than the Mega with both ten and eleven cell packs. The AXI also ran noticeably cooler (more efficiently), and was lighter than the Mega (5.3 vs. 5.8 ounces each). For these reasons, the AXI was the final choice.

The batteries chosen were the Elite 1500mAh cells. In comparing many different brands and capacities, we found that the Elite 1500mAh had a very high energy density, and was shown to hold voltage under load very well when compared to similar battery cells. Through our own testing on the thrust stand, we decided that an 11s3p (3 parallel packs of 11 cells in series) provided the needed thrust and endurance for the lowest weight. During testing, we determined that the batteries required being cycled a few times to allow them to provide the required current and their full capacity, and that they ran best when warm off the charger.

9.3 Wind Tunnel Testing

After the first flight test, it became apparent that lateral directional stability problems existed. In order to solve this and other control questions, the aircraft underwent a series of tests in the 4x6 foot Boeing wind tunnel. A full report on the wind tunnel testing can be found in the AAE 520 Spring 2007 report by Aaron Wypyszynski entitled “Stability and Control of Lifting Body Remote Controlled Aircraft”.

Initial studies focused on changing the winglet size and shape to try and minimize the amount of rolling moment generated by sideslip. The winglets studied can be seen below.

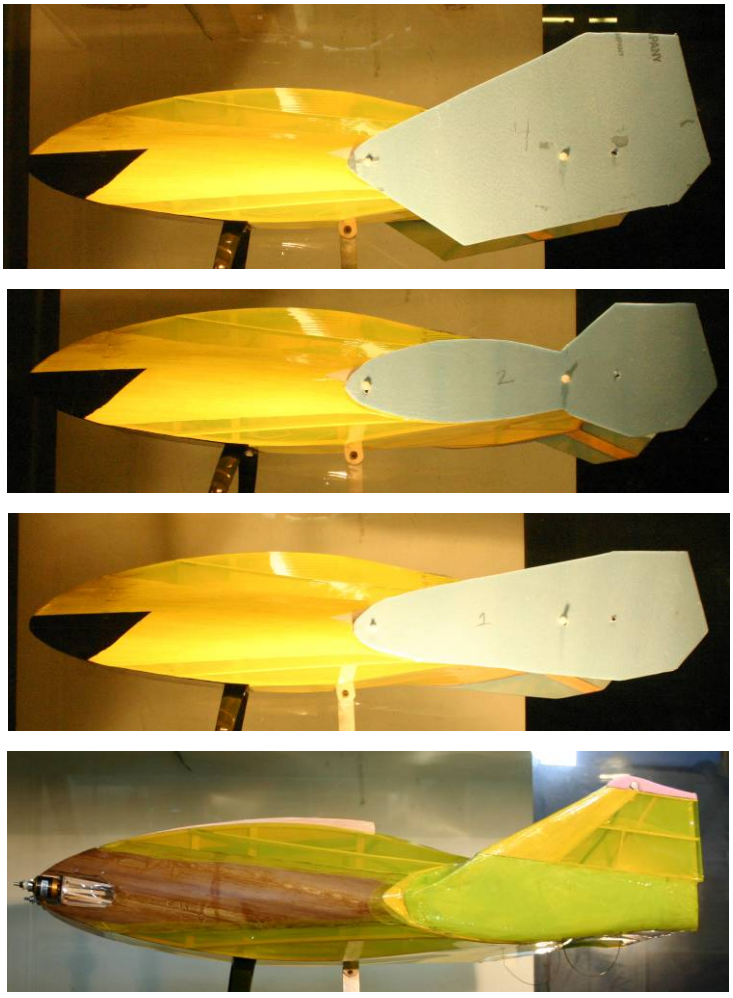

(a)

(b)

(c)

(d)

Figure 9.1 - Winglets Studied

(a) Winglet 4, (b) Winglet 2, (c) Winglet 1, (d) Original Winglet

It became apparent that winglet size had only a small effect on this rolling moment and although a smaller winglet provided less rolling moment at low angles of attack, the moment increased sharply with angle of attack. On the other hand larger winglets produced more rolling moment at low angles of attack, but had less change with angle of attack. An example of this can be seen in the graph below.

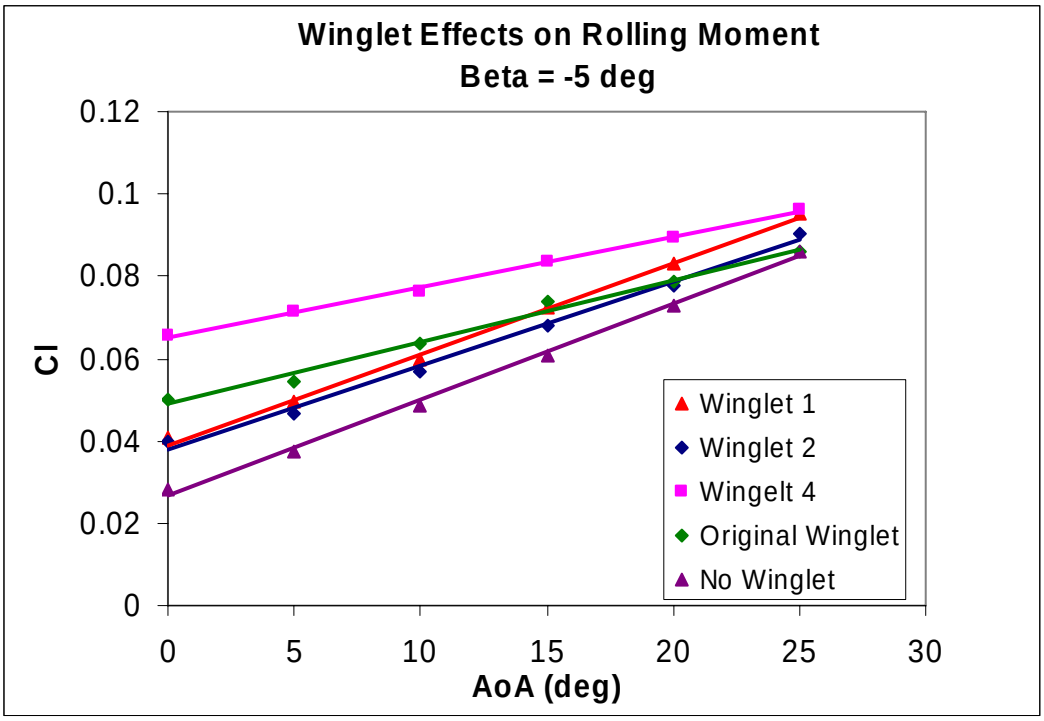

Figure 9.2 - Rolling Moment at -5 degrees Sideslip

Due to rolling moment not being able to be changed on the model, it became necessary to keep rolling moment to a minimum. In order to do so, sideslip would need to be kept small by means of increasing yawing moment generated by sideslip. The effects showed what was expected, that larger winglets produced greater yawing moment as seen in the figure below.

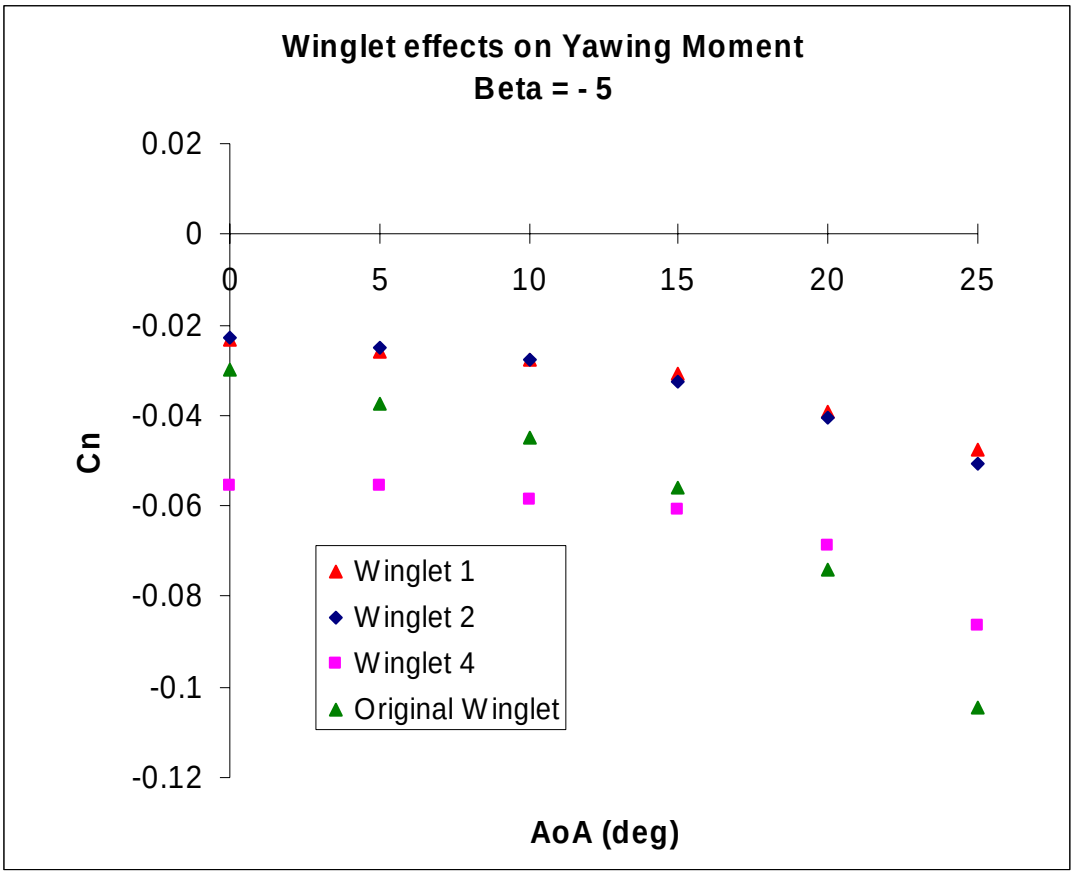

Figure 9.3 - Yawing Moment Produced at -5 degrees Sideslip

Due to this it became apparent that a large vertical surfaces would be needed. When comparing the amount of rolling moment and yawing moment produced by sideslip from the winglets studied to other aircraft an interesting trend was noted. Aircraft that had an equal ratio of rolling and yawing moment induced by sideslip tended to be more stable aircraft. A plot of this can be seen in the figure below.

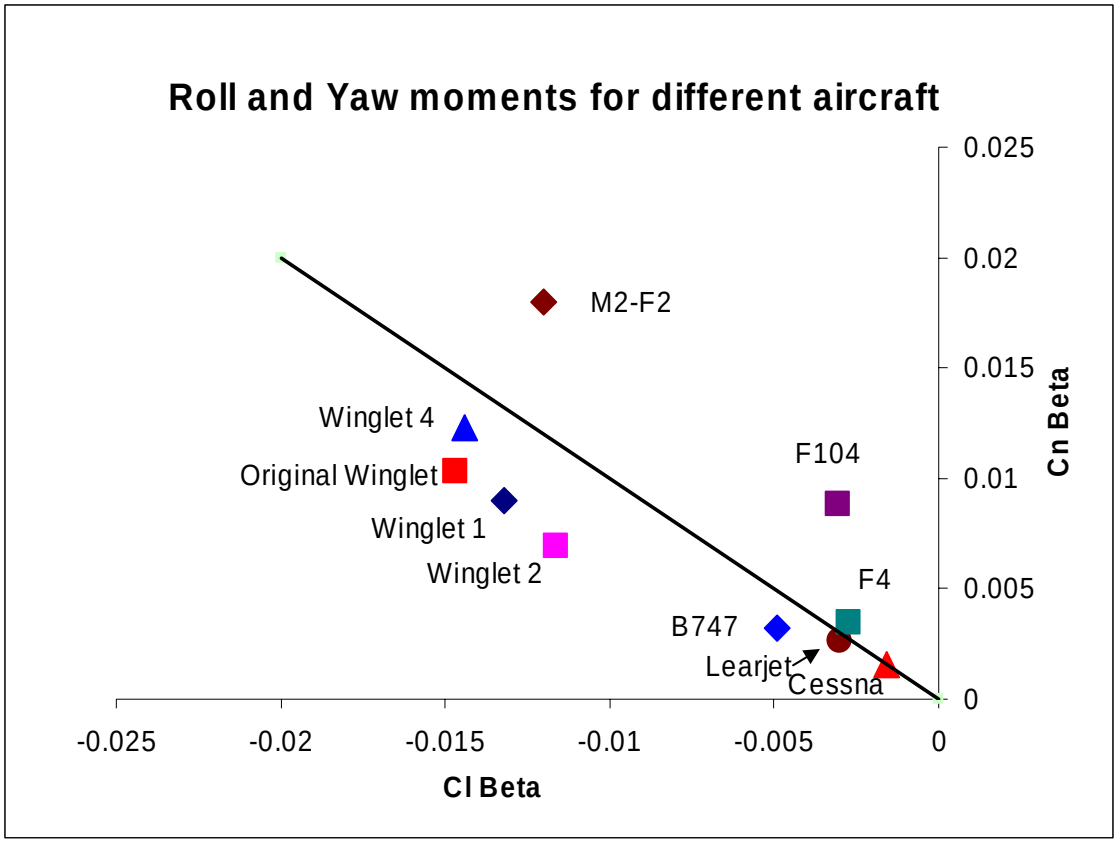

Figure 9.4 – Roll and Yaw Moments of Different Aircraft

It had already been considered that a winglet design such as winglet 4 would make a good choice for the aircraft. From the figure above, it was noted that with more vertical tail area, Cn Beta could be increased and thus falling on the line of equal ratio that the stable aircraft fell on. Although this is by no means the best way to guarantee a stable aircraft, it was the best that could be done in the short time available and without doing a full dynamic analysis.

Once the winglet size and shape was figured out, focus shifted to determining how to improve the controls of the aircraft. First the ailerons were investigated followed by the longitudinal control mechanisms.

From flight testing it was seen that roll control authority was a problem with the initial design. Due to the outward canted airfoil shaped winglets, the maximum span at the trailing edge of the aircraft was reduced by 4 inches. By changing to the flat plate winglets with no cant angle, this 4 inches could be regained allowing for a fixed center portion to be added. This change can be seen in figure 9.5.

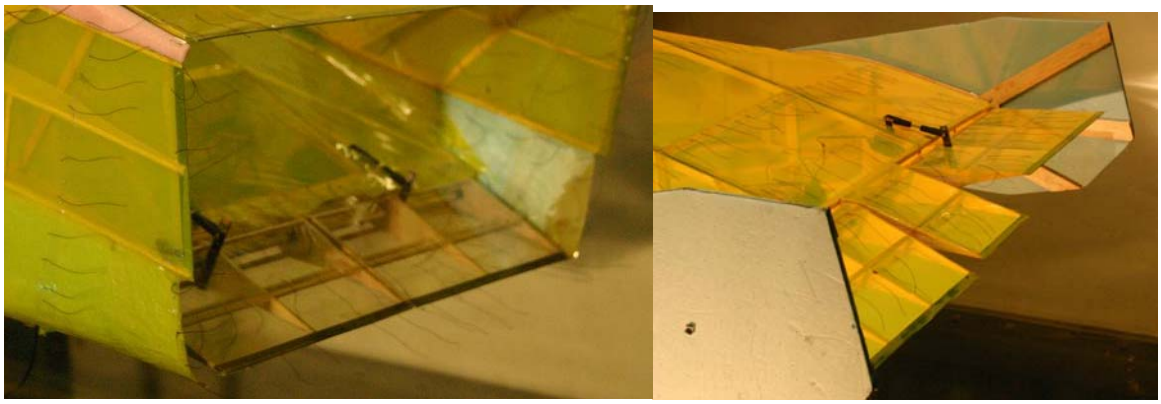

(a) (b)

Figure 9.5 - Aileron Configurations (a) Original (b) Spaced

It became of interest to see what the change was in control effectiveness and adverse yaw produced by the ailerons. The control effectiveness can be seen in figure 9.6.

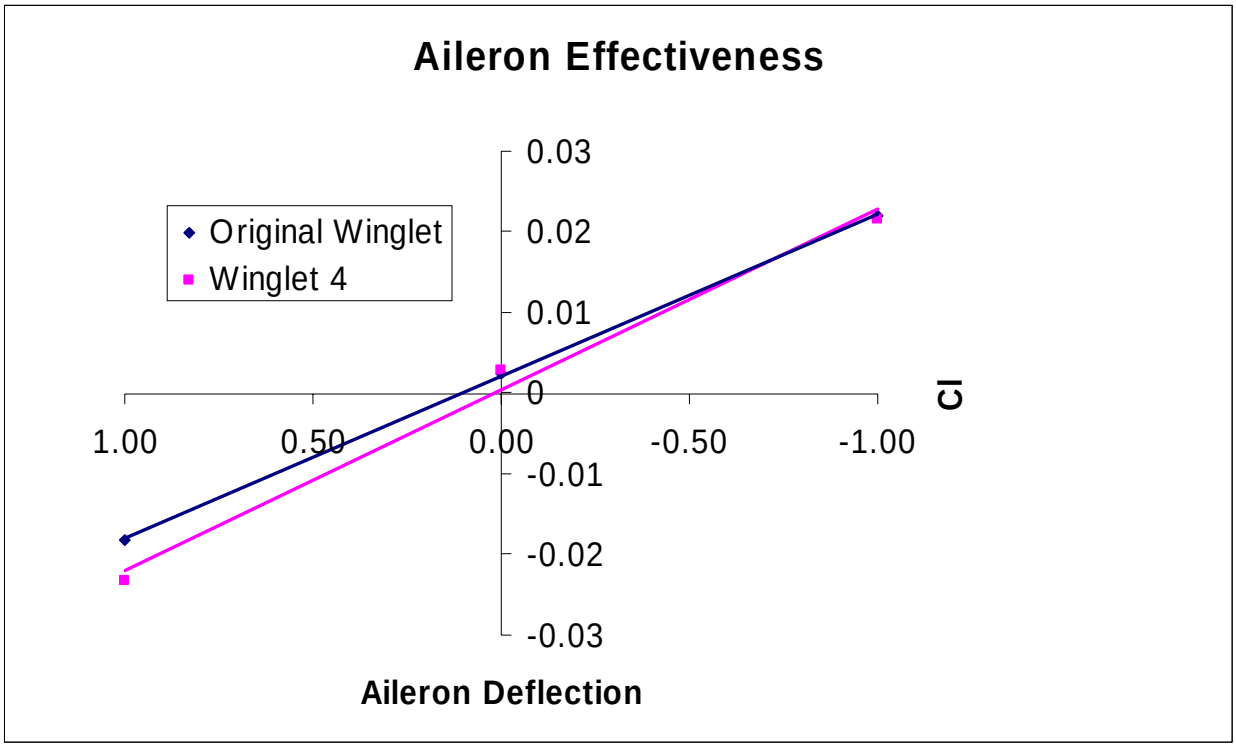

Figure 9.6 - Aileron Rolling Moment Produced by the Two Aileron Configurations

From figure 9.6 it can be seen that only a small increase in rolling authority was gained. The greatest difference was in the adverse yaw produced by the ailerons, as can be seen in figure 9.7.

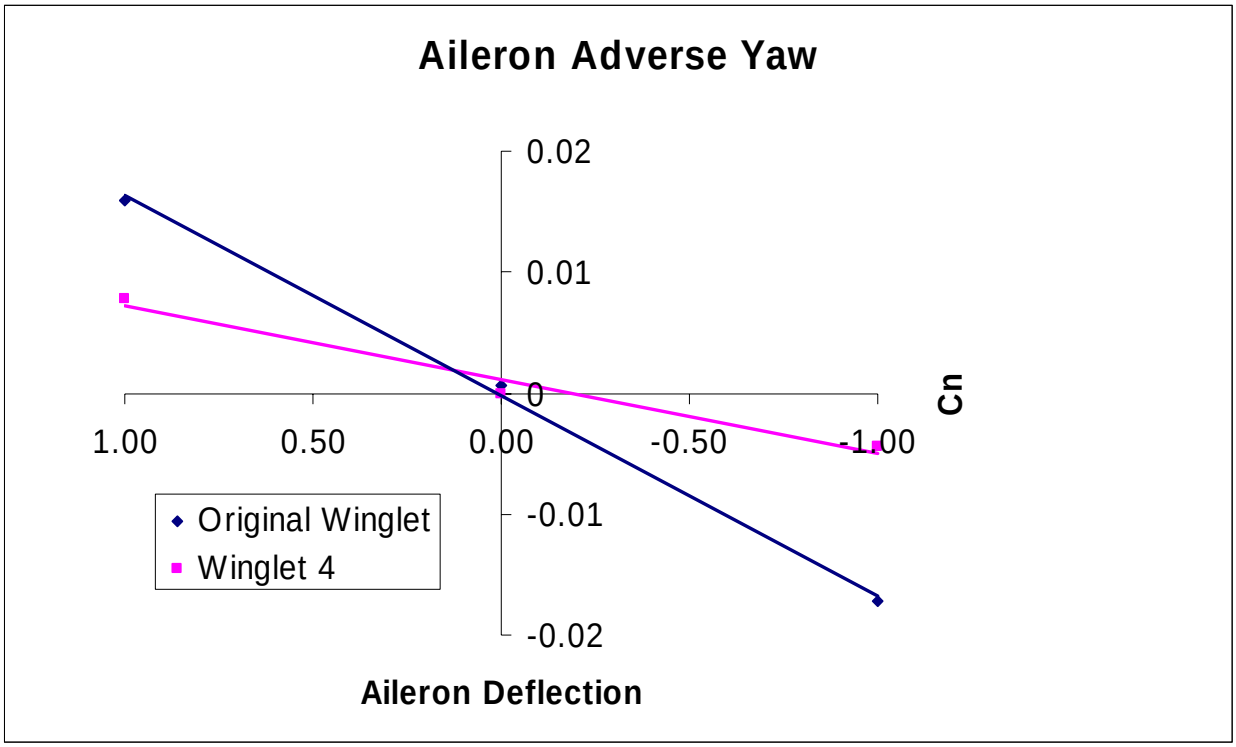

Figure 9.7 - Difference in Adverse Yaw of the two Aileron Configurations

As can be seen from figure 9.7, for nearly the same rolling moment produced, the spaced winglets produced less than half as much adverse yaw. This aids in the stability of the aircraft because rolling moment due to sideslip is not able to be reduced and thus sideslip must be kept to a minimum. Adverse yaw will cause the sideslip to increase and if large enough could result in a control reversal as seen in the initial flight tests. Due to this, it was determined to use a design similar to winglet 4 so that the spaced ailerons could be used. It would also help stability to add rudders to further minimize the yaw produced by aileron deflection and thus control sideslip.

Through the design process two longitudinal control methods were investigated; a full flying tail, better known as a stabilator, and elevons. The initial design called for the use of a stabilator as due to time restrictions insurance of stability with elevons was not able to be accomplished. The aircraft was designed with a modular configuration so that during wind tunnel tests the stabilator could be removed and the elevons could be tested. The setup of the two control methods can be seen in figures 9.8 and 9.9.

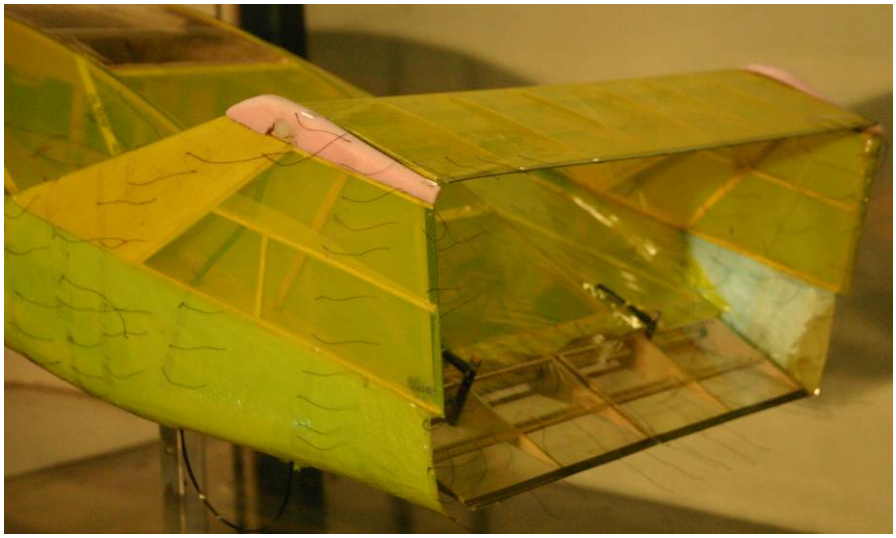

Figure 9.8 - Stabilator with Ailerons

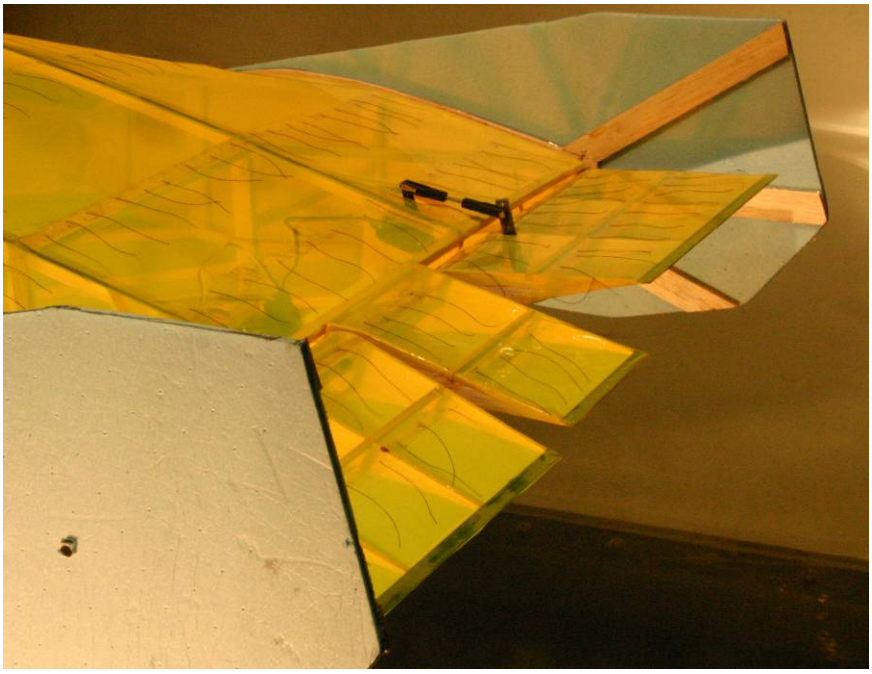

Figure 9.9 - Elevon Contorls

Each control setup was run through a full alpha sweep and the pitching moment produced by control deflection was measured at each angle of attack. From these tests, pitch trim diagrams were able to be created and can be seen in figure 9.10.

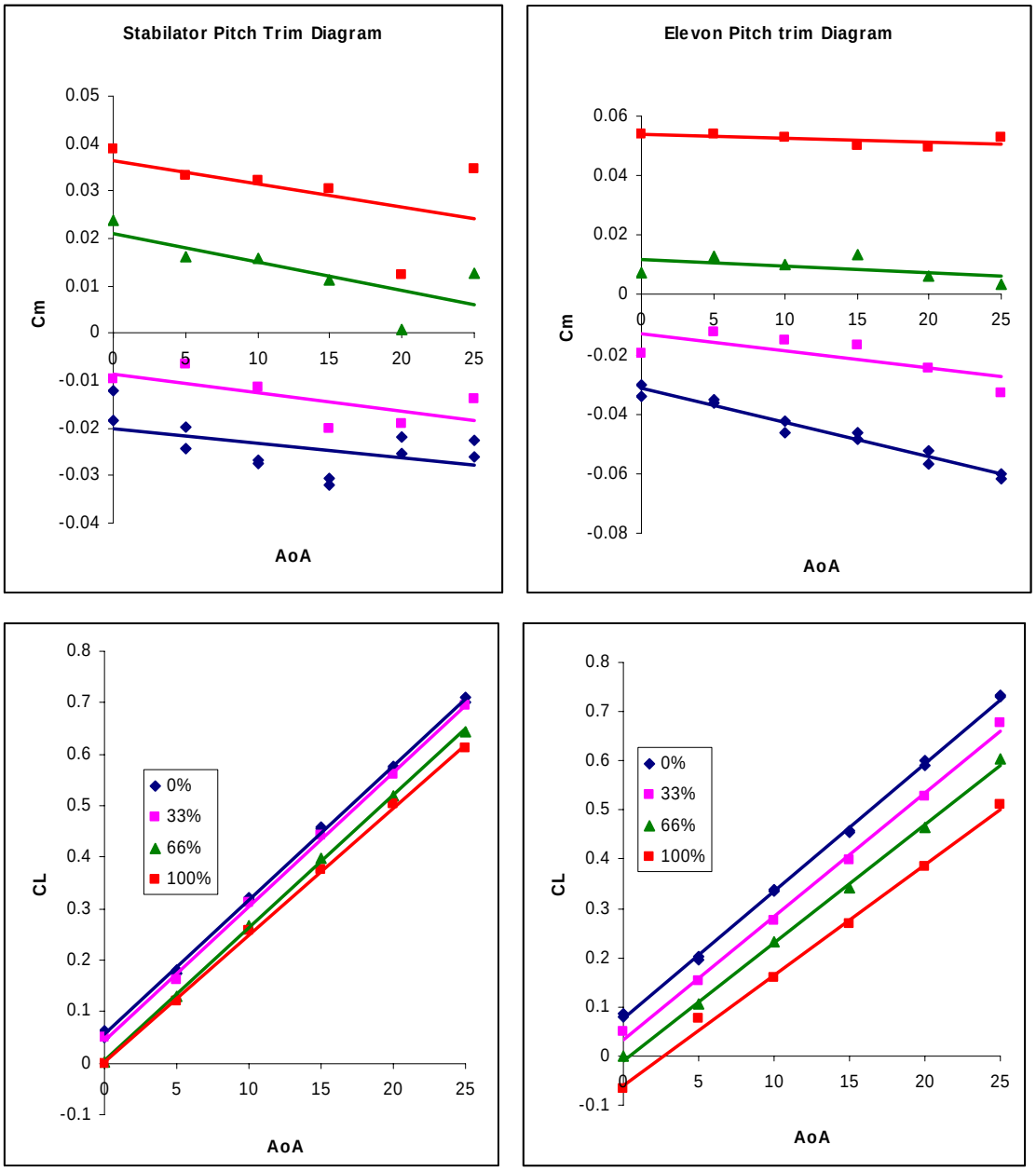

Figure 9.10 - Pitch Trim Diagrams for Stabilator and Elevon controls.
Note: Stabilator CG at 16 and Elevon CG at 14.25.

From the pitch trim diagrams it was determined that with proper CG placement adequate stability could be obtained as seen in the negative slope at all trim conditions in the top two graphs of figure 9.10. The penalty for using elevons is a slight decrease in CL due to deploying the control surface on the rear of the wing (acting as a negative flap for the wing). The result is a .05 to .1 reduction in CL for the same trimmed angle of attack. This results in a slight increase in drag. However, by eliminating the stabilator, the surface area and weight are reduced, resulting in a

decrease in drag. Also, the complexities of attaching the stabilator to the new thin winglets are avoided. It was decided to use elevenons instead of the stabilator because of this.

9.4 Flight Testing

Flight testing was conducted on the Facet Mobile and the Lifting Body designs. Accounts of the flight tests are documented below.

9.4.1 Facet Mobile Flight Testing

Flight 1 (No Payload)

The first flight, flown by the primary test pilot, proved that the Facet Mobile concept would fly with the low aspect ratio. Pitch stability was seen to be high and easily controllable. Roll stability was close to neutral and required a high pilot workload to control. The landing was successful with no damage to the aircraft.

Flight 2 (No Payload)

The second flight was flown by the secondary test pilot to get different input on the flight characteristics of the Facet Mobile design. The same stability and control characteristics were reported. During the final approach of this flight the right motor did not respond to the idle setting and thus the aircraft landed sideways. Only the landing gear was damaged.

Flight 3 (No Payload)

The handling characteristics were again analyzed and the intent of this test flight was to practice landing approaches. This flight was again flown by our secondary test pilot. After a single lap, the Facet Mobile was brought in for a landing. The power was cut and due to the poor gliding characteristics of the low aspect ratio Facet Mobile, the aircraft hit the ground hard. The landing gear was again damaged along with some of the internal structure.

9.4.2 Lifting Body Flight Testing

Flight 1 (No Payload)

The first Lifting Body test flight was flown in a single motor tractor configuration by our primary test pilot. Immediately after takeoff the aircraft rolled hard to the left and dove into the ground. The aircraft was destroyed leaving only small fragments of the airframe intact. It was suspected that the high torque of the single tractor motor may have torqued the aircraft to the left, making it uncontrollable for the pilot.

Flight 2 (No Payload)

The second Lifting Body flight was flown in a dual motor tractor configuration by the primary test pilot. The propellers were not counter-rotating. The second flight had very similar results to the

first flight. Immediately after takeoff the aircraft rolled to the right and dove into the ground. Again, the damage was severe.

Flight 3 (No Payload)

The third Lifting Body flight was flown in the same configuration as the second but without the horizontal tail and with rudders added to the winglets. The primary test pilot successfully took off and flew a lap. The aircraft was reported to be stable and easily controllable in pitch and neutrally stable and difficult to control in roll. The pilot attempted to land with power in order to prevent the aircraft from dropping too fast and ended up coming in too fast. The pilot lost control of the aircraft directly above the ground and the aircraft crashed.

Flight 4 (No Payload)

The fourth Lifting Body test flight, flown by the primary test pilot, was damaged during the takeoff roll and never became airborne. The landing gear mount failed and thus the aircraft was no longer supported.

Flight 5 (No Payload)

The fifth test flight exhibited an extremely short takeoff distance. The aircraft roll stability and control increased with the addition of a vertical surface and moving the rudder from the winglets to this center control surface. Also, the designed winglets were replaced by endplates. The primary pilot flew a perfect approach and landed very smoothly on a grass field into the wind. There was no damage to the aircraft. This was the first successful flight with the Lifting Body design.

Flight 6 (3 lb payload)

The first test flight with the 3 pound payload made the aircraft much less susceptible to disturbances and thus made it easier for the primary test pilot to fly. After flying 5 laps, the pilot flew the approach fast and ended up catching the landing gear on the surface before he was able to flare. The landing gear was ripped off and the payload was ejected. Control of the aircraft was lost and it crashed. Because of the coloring of the aircraft and the fading light, the pilot claimed to have misjudged the approach because it was difficult to see the aircraft.

Flight 7 (5 lb payload)

With the 5 pound payload, the aircraft took off within 100 feet. Again, with the increased weight, the aircraft was easier for the pilot to fly and became less susceptible to disturbances. The aircraft was flying very smooth for several laps before the primary test pilot decided to take the aircraft in for a landing. The approach was again flown a little bit fast and the aircraft hit the runway hard

enough to shear off a wheel from the landing gear. It seemed that the aircraft would skid to a halt but as it approached the edge of the runway, the gear without a wheel caught the mud and flipped the aircraft. The airframe and the leading edge were damaged.

Flight 8 (3 lb payload)

On the eighth Lifting Body test flight the aircraft was being flown in high winds. The primary test pilot struck a dirt mount on takeoff and broke carbon fiber landing gear.

Flight 9 (3 lb payload)

The ninth Lifting Body flight test was the first successful flight test with payload. After the primary test pilot took off and flew several laps he came in for several approaches. Once he was satisfied with his approaches he brought it in for landing. The new aluminum landing gear absorbed the load very well and the aircraft landed on the runway undamaged.

Flight 10 (5lb payload), Eagle Tree Flight 1

The tenth test flight was flown in windy conditions with 3 battery packs. After several successful laps and practice approaches, the aircraft was brought in for a successful landing on the runway. No damage was incurred. The flight lasted 3 minutes.

Flight 11 (5 lb payload) Eagle Tree Flight 2

In the eleventh flight test a fourth battery pack was introduced in an attempt to achieve the endurance necessary for the surveillance mission. With four battery packs the primary test pilot reported that the aircraft was not flying well and thus he brought it in for a landing. The aluminum landing gear absorbed the shock of the hard landing and the aircraft was minimally damaged.

Flight 12 (5 lb payload)

The twelfth and final flight test resulted in a crash during takeoff. The primary test pilot attempted to takeoff the aircraft in a fairly strong crosswind. On the takeoff roll the aircraft began to sideslip and immediately rolled over inches from the ground and crashed.

9.4.3 Battery Flight Testing

During flight testing, it was determined that, while three packs were sufficient for the ‘Dash’ mission, they were not able to provide the needed endurance for the four minute ‘Loiter’ mission. As shown in the graph below, the batteries drop off very suddenly and severely at about three minutes, forty seconds, short of the needed four minutes.

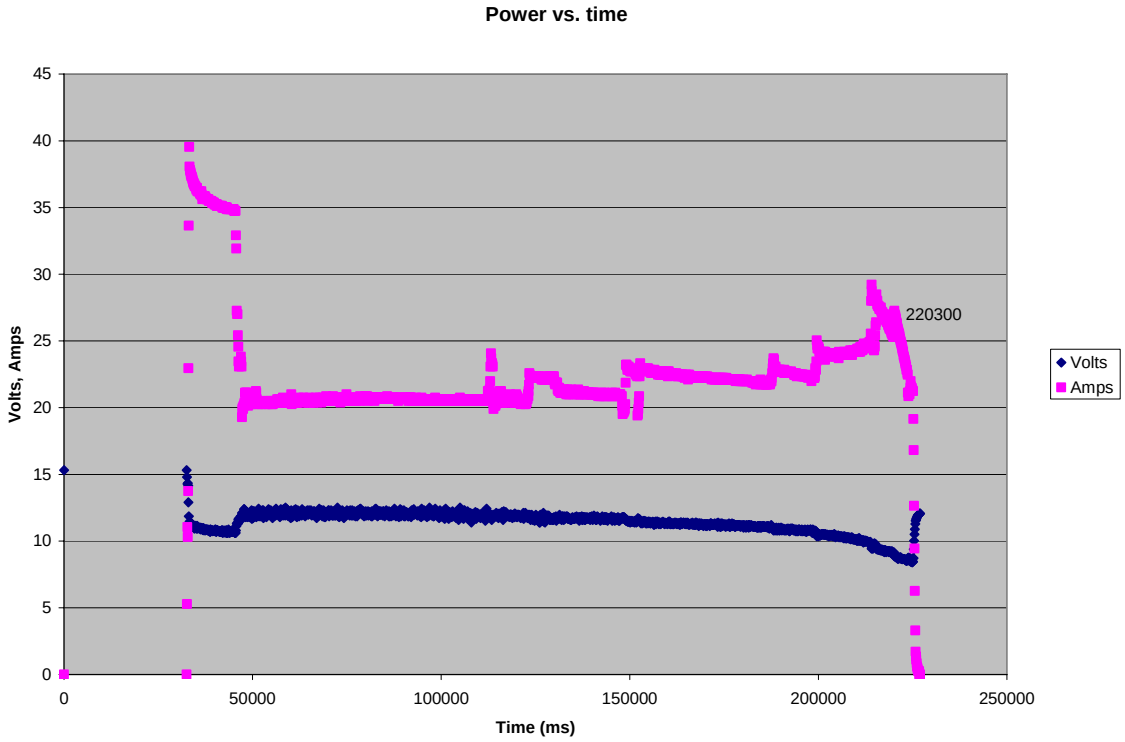

Figure 9.11 – Battery Endurance Test

It was decided that a fourth 11s pack would be added in order to achieve the required endurance. Calculations indicated that adding the fourth pack would ensure that we had sufficient endurance. However, at the competition we were still not able to stay aloft for four minutes, our final flight ending at 3 minutes, 45 seconds. This may be due to reduced capacity caused by overdrawing the batteries, and damaged battery cells caused by overheating and numerous crashes. The aircraft also turned out to require more power to maintain level flight than we had anticipated, taxing the batteries even more. We were not able to obtain another set of batteries, so every flight after a point was progressively worse.

9.4.4 Eagle Tree Flight Test Data

An eagle tree flight data recorder as well as power logger were installed for two flight tests at maximum payload. The first flight the payload was 5.5 lbs with a gross weight of approximetly 11 lbs, simulating the loiter mission. The battery setup was 3 parralel packs of Elite 1500 NiMH battery packs consisting of 11 cells. The data collected is seen below.

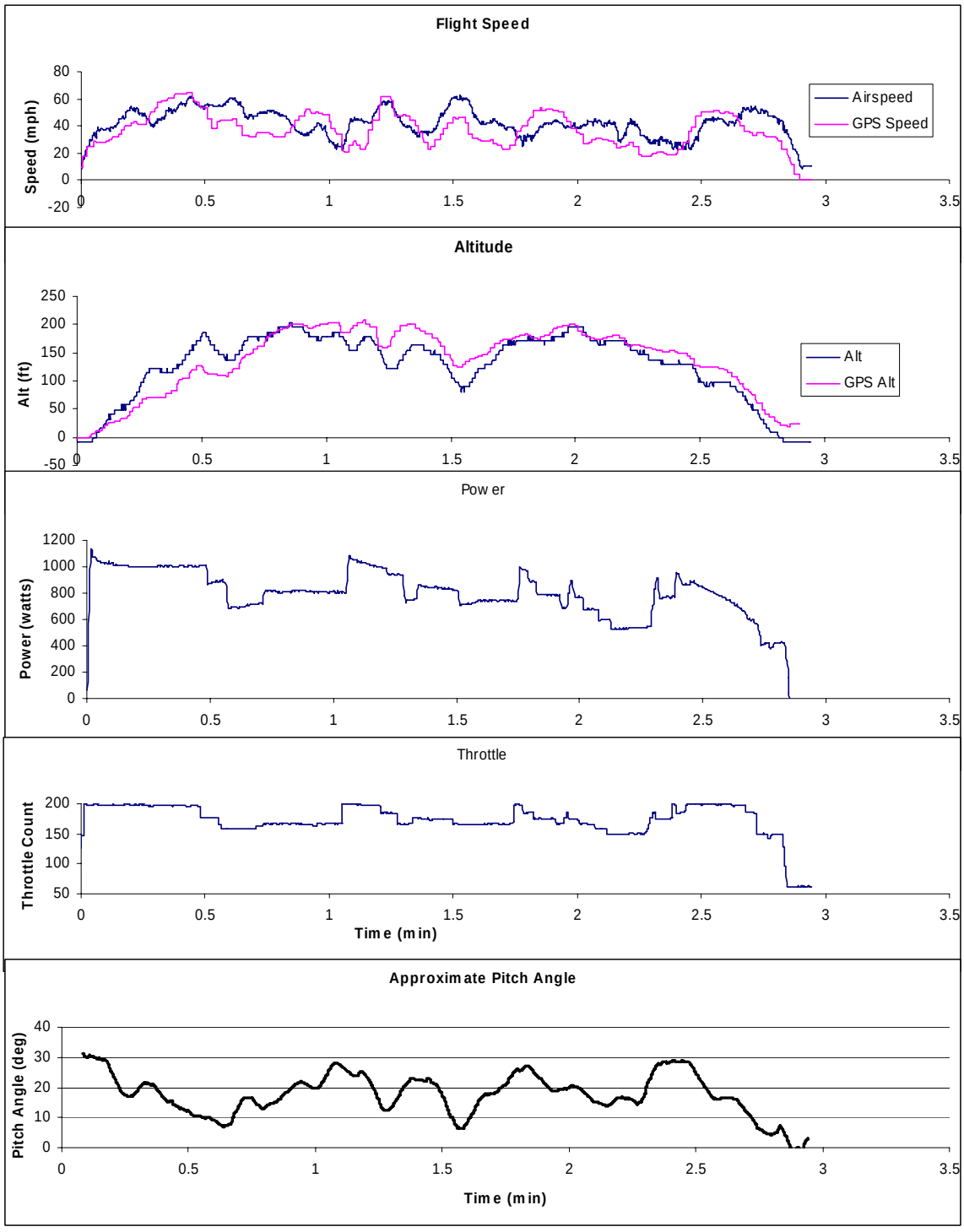

Figure 9.12 – Flight #1 Data

It was noted that on the first flight, only 3 minutes of flight was able to be achieved before loss of power necessitated a landing. The reason for this was the aircraft was using more power than expected. It was only expected to require approximately 500 watts of power, but instead was

using 700-800 watts. As a result, a 4th battery pack was added and the flight was tried again, seen in the figure below.

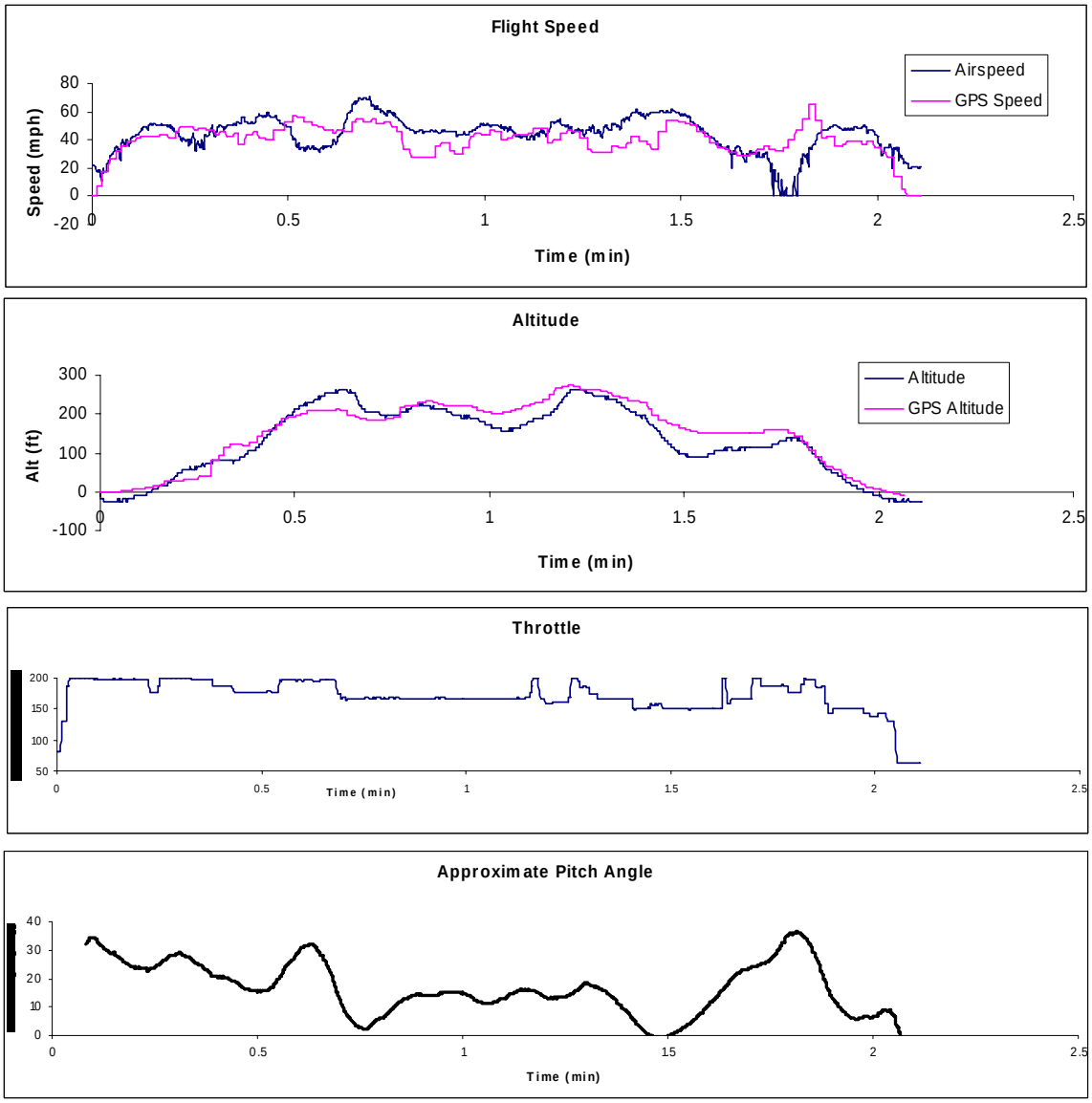

Figure 9.13 – Flight #2 Data

The aircraft was flying well during this flight and the throttle consumption was not much higher than that of the previous flight, however, due to either pilot error or wind gusts, the airspeed was allowed to get to low and the angle of attack too high, resulting in the pilot getting behind the power curve. As a result the aircraft entered a decent and thinking that there may be a problem, an emergency landing was made.

From the flight testing it was determined that a very small envelope exhisted to complete the endurance mission. However due to lack of flight testing time before competition, this problem was not able to be solved.

9.5 Competition

The competition this year in April '07 was held in Tucson, Az. Teams from all over the country and across the ocean brought their designs to compete. The designs varied from small to large but it was clearly evident from the number of teams that showed up with a 2 foot wing span, their designs were going to have an advantage in the final score. Some of the most common designs included a 2 foot biplane, 3 foot biplane, and a 3 foot high wing.

At the end of the day the designs that achieved the high scores, placing them in the top rank all shared similar characteristics. The following is a list of the teams and rank they received at the competition. The top ranking characteristics included; a wing span under 2 ft, an empty weight under 6 lbs, flying at least the 3 lb mission. For the teams that had a heavier airframe or a wingspan greater then 2ft, had to have flown the 5 lb mission to get in the top rankings.

The Purdue – AIAA DBF '07 team "Spirit of Amelia" obtained 3rd place in the overall competition. The design included a 22.75 in wingspan, a 5.7 lb airframe, and it had flown the 3 lb mission. The 5 lb mission was attempted but didn't succeed. The design for this years competition contained all the winning aircraft characteristics.

1st: MIT
2nd: OSU Orange
3rd: **Purdue**
4th: OSU Black
5th: Wichita State
6th: UT Austin (Chan 4 News)
7th: UC Boulder
8th: UIUC
9th: UCLA
10th: UFL (Investigator?)
11th: VT
12th: PSU
13th: ITU
14th: Purple Haze
15th: WVU Gold
16th: WVU Blue
17th: U. Arizona
18th: U. Strathclyde

Table 9.1 – Competition Results

The statistics of the top 4 aircrafts are shown in the table below. The winning characteristics are very evident in this table. The wingspan of the top for aircrafts was under 24 inches. Purdue had the smallest wing span in the competition by 0.05 in of the next smallest wing span. The second smallest wingspan aircraft could not complete the flying missions thus never achieving a score. The initial mission analysis done early on in the design process told us in order to obtain a high score the aircraft would have to have a wingspan of 2 feet. From the competition and the design statistics of the top aircrafts it is evident that the initial scoring analysis was validated.

Team	**Span**	**Empty Weight with batteries**	**Battery Weight**
Purdue	22.75 in	5.75 lbs	2.75 lbs
MIT	23.25 in	30 oz	?
OSU Orange	23.5 in	6.5 lbs	3 lbs
OSU Black	23.75 in	8.5 lbs	?

Table 9.2 – Aircraft Comparisons

The empty weight also played a large role as the winning team's aircraft had a total manufactured empty weight of 30 oz. This confirms the scoring analysis once again as the main factors were pointed out to be the wing span and the empty weight. Purdue had the 3rd lightest airframe in the competition and the second lightest to have flown.

Battery weight could not exceed 3 lbs and it was also included in the final empty weight. This played a large role in the capability of the aircraft to completer the flying missions. The top 4 teams all completed the 3 lb flying mission. The score was based on time and Purdue had flown the two laps in 1min 39 sec. The only team from the top 4 to complete the 5 lb mission was OSU Orange. From the stats it is seen that all 3 lbs were necessary to fly the 5 lb payload, some of the factors are most likely the high drag coming off of the not so aerodynamics bodies requiring more power.

The Report score also played a large role as it would multiply the score of the missions both ground and flying. The RAC was the factor that would divide the total score for the team and it was normalized to the lightest frame being MIT. The following table shows the Report Scores and the Normalized RAC. Purdue had the 5th highest report score of the competition.

Team	**RAC (Empty * Wing)** **Weight Span**	**Report Score**
Purdue	137	93.0
MIT	45	92.5
OSU Orange	166	95.0
OSU Black	185	87.0

Table 9.3 – Score Breakdown

The Total Scores of the top 4 teams of the competition were the following

Purdue	– 95
MIT	– 287
OSU Orange	– 125
OSU Black	– 66

Table 9.4 – Competition Scores

Purdue endeavor included the following break down of attempts. There were 5 flight attempts allowed for the 3 lb mission payload and the 5 lb mission payload.
The 3 lb and 5 lb missions corresponds to the air data probe payload and the camera ball payload respectively. The flying scores were normalized to the time and RAC of the top scoring team for that mission.

- **3lb Mission**
  - Scored on 1st attempt (1 of 5) : 00:01:39 sec
- **5lb Mission**
  - Crashed on 1st attempt (2 of 5)
    - **Cause: Large power spike**
  - Rebuilt -1 (overnight)
  - Crashed on 2nd attempt (3 of 5)
    - **Cause: too much throttle ran out of battery**
  - Rebuilt – 2 (in 4 hours)
  - Aircraft Damaged in pre flight (4 of 5)
  - Crashed on 3rd attempt (5 of 5)
    - **Cause: too long on 1st lap by 10 sec, short on 2nd lap by 15 sec**
    - **Not enough Battery**

- **Deployment Mission**
  - Scored 2st attempt : 9 sec
- **Reconfiguration Mission**
  - Scored 1st attempt : 16 sec

The key factors that drove the completion of the 5 lb mission were the battery. If Purdue had enough battery to completer the 5 lb mission it could have taken 2nd place in the overall competition. The unusual shape and small wing span not only increased the drag on the overall

aircraft drawing out more power but the small wing span also didn't provide any gliding, dropping the aircraft out of the air once power was lost.

Overall the competition drove the teams to explore opposite sites of the spectrum driving the designs to the extremes.

9.6 Financial Summary

The AIAA DBF project was fully funded by the College of Engineering – School of Aeronautics and Astronautics at Purdue University. Two separate awards were given: a project fund and a travel fund.

9.6.1 Project Budget

A fund in the amount of $5,000.00 was awarded to the team for the AIAA project. This fund was used for all project and related expenses. All building supplies, electronics, batteries, propulsion systems, and other related items for all test aircraft and competition aircraft were purchased using the project fund.

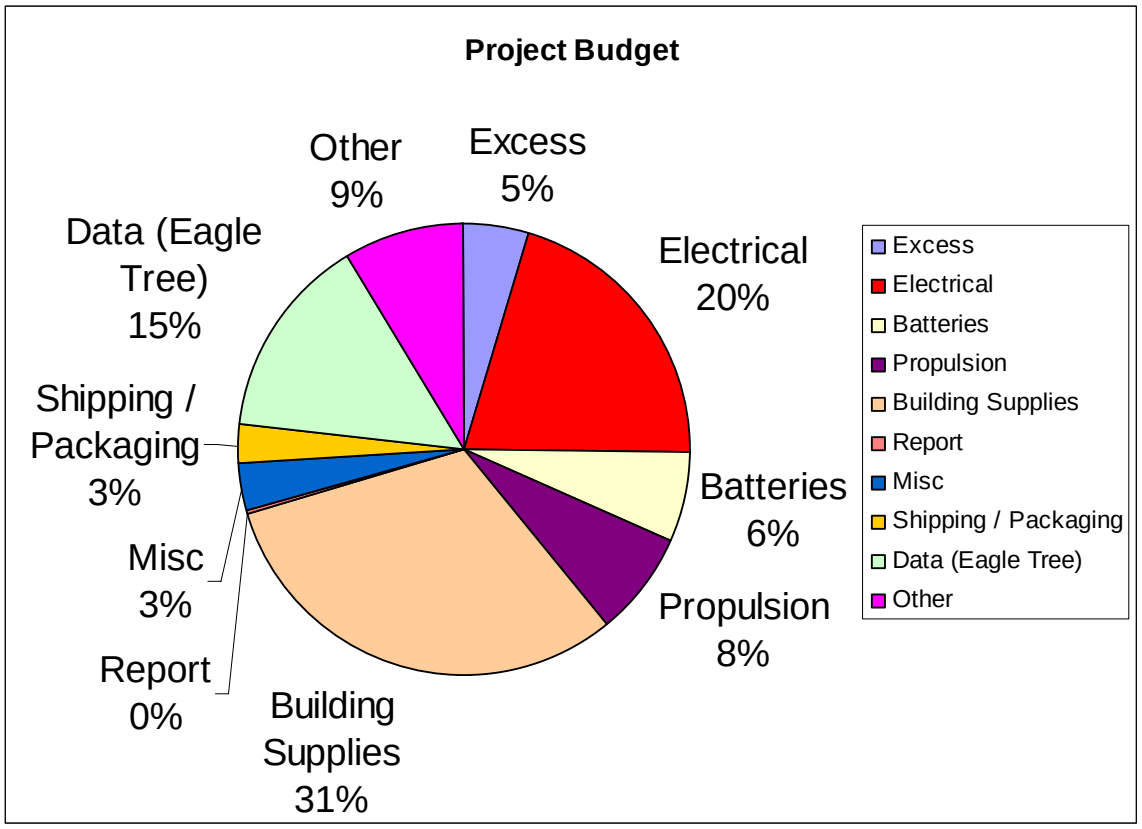

Figure 9.14 – Construction Budget

Expenses for the project were categorized so that a cost breakdown analysis could be conducted as a forecasting tool and as a post project budget summary. An expense breakdown by category shows that building supplies, electrical, and data collection utilities (Eagle Tree) were the largest expenses. There was an excess of $241.80 at the end of the project.

Category	Amount ($)
Excess	241.80
Electrical	1023.92
Batteries	311.95
Propulsion	384.78
Building Supplies	1552.01
Report	15.58
Misc	169.58
Shipping / Packaging	136.20
Data (Eagle Tree)	727.93
Other	436.25
Total	5000.00

Table 9.5 – Construction Cost

The project fund of $5000.00 allowed for the construction of multiple test aircraft and ample supplies for repairs to the Competition aircraft. Additionally, data collecting utilities (i.e. eagle tree) were purchased from the fund which can be used for other related projects. At the end of the project, an excess in funding of only 5% shows that our original necessary funding for the project approximation was close, but very conservative. Towards the end of the project, much care had to be taken so that the project did not run over budget. Additional funding in this area, in terms of an increase of ~10%, would allow for more flexibility in the spending.

9.6.2 Travel Budget

A separate fund was awarded to the team for the travel expenses to/from the competition in the amount of $6,600.00. The competition was held in Tucson, Arizona. The team traveled, by commercial airlines, to Tucson from Indianapolis. The duration of the trip was 5 days. Three hotel rooms and two rental cars were required for the team during the stay in Tucson. A cost breakdown (Fig X.X.2) shows that travel, lodging, and rental car were the major expenses in the travel budget.

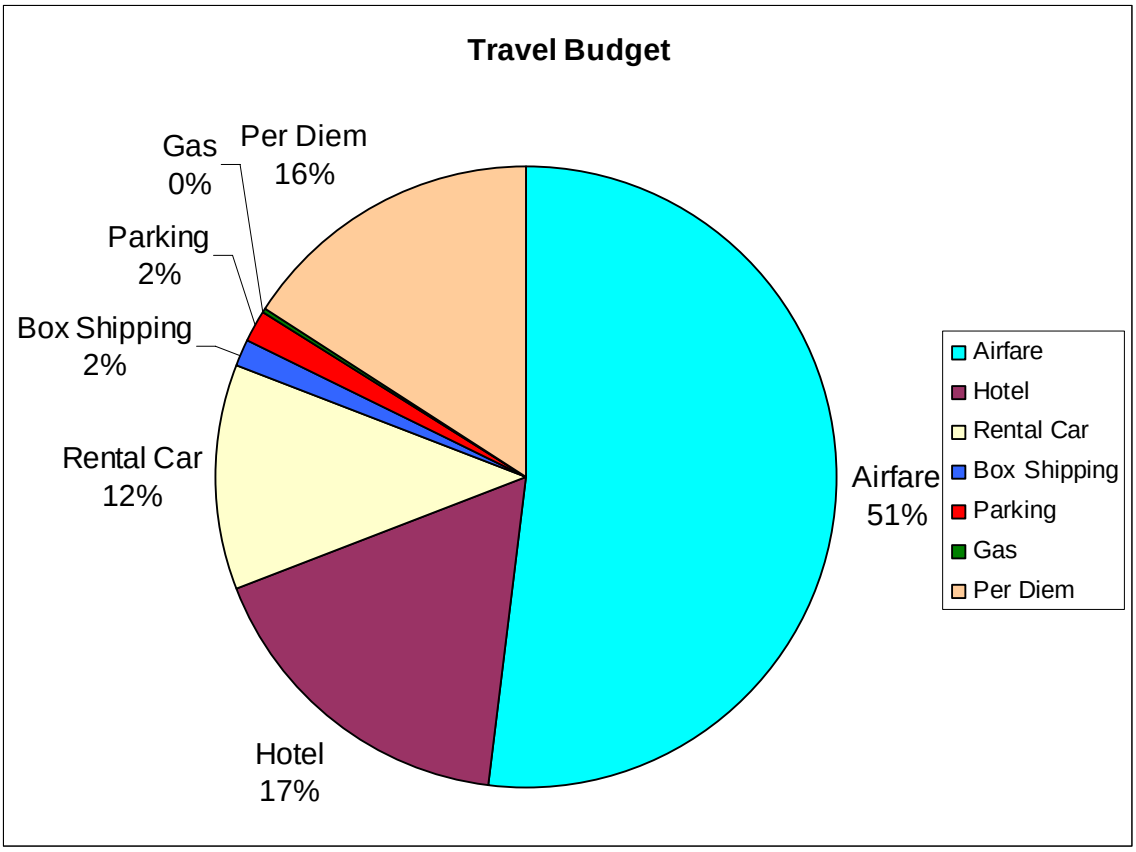

Figure 9.15 – Travel Budget

After all travel expenses were deducted from the account, the remaining money was divided equally among the participating members as a per diem. The per diem for each member (11) was $94.45.

Category	Amount ($)
Airfare	3426.60
Hotel	1131.48
Rental Car	769.45
Box Shipping	100.00
Parking	105.00
Gas	28.52
Per Diem	1038.95
Total:	6600.00

Table 9.6 – Travel Costs

Ample funds were provided for the teams travel to the competition. Originally, an estimate of $600.00 per person for travel was decided upon. This estimate proved to be very accurate for the travel expenses for the team.

9.7 Recommendations for Next Year

Preliminary Design

Consolidating the preliminary analysis and sizing codes to evaluate different configurations would expedite this initial process. The integration of the performance code as well would give one preliminary design tool that iterates for an optimized design. The performance code needs to be validated using this year's results and corrected to better match the test data.

CAD

Next year, parametric models should be developed that are ready for CFD and structural analysis. Some difficulties were experienced importing the CAD files in Gambit and ANSYS, requiring the models to be altered several times.

Aerodynamics

CFD should be used much more next year for the aircraft optimization. The efforts this year consisted largely of learning how to use the tool, and it is expected that in the future CFD will play a more integral role in the design process. Wind tunnel testing would be used primarily for CFD verification and the investigation of any unforeseen problems.

Propulsion

Static tests on top of a moving vehicle were attempted this year, but the cold weather prevented the batteries from working properly. This should be done early in the first semester of next year. Earlier and more frequent flight tests are also a goal so that there is more time to correct any unanticipated problems with the analyses. Purchasing new batteries before the competition should be considered, along with the appropriate number of times to cycle them. An electrical engineer has been recruited for next year's team who ought to be a valuable resource.

Stability

More research of historical data would have been extremely beneficial to establish the problem areas of different designs. CFD data can be used for stability analysis, and should be worked to its full potential next year. Also, roll data should be obtained in the initial wind tunnel tests to avoid wasting time in remounting and re-running the tests. Finally, X-plane cannot be relied upon as a valid stability check.

Structures

A more detailed analysis on the landing gear and the associated structures should be performed, as it was built too firm and kept ripping through the plane on landing. Criteria need to be developed to determine the acceptability of the building material qualities, as much of the balsa used on the aircraft was substandard. Also, a weight reduction analysis could help in lessening unnecessary weight without compromising the aircraft's structural integrity.

Building

Once the design is finalized, a new jig should be developed. This will help maintain the precision and can be more exact and fixed than a jig used while the design is still evolving. An increased use of CAM should be evaluated, as it will always be more precise but comes with at the expense of money and time. The payload integration should be given more thought next year with respect to adding the weight and moving the cg, as this year's configuration required that the payload be disassembled for these tasks.

Test Flight

The Eagle Tree system should be used as soon as the aircraft is flight worthy to provide in-flight data for further analysis. Also, an overbuilt flight test aircraft should be designated so that the pilot can gain experience with the aircraft without requiring frequent rebuilding.

Report

Weekly progress reports should be maintained, which can then be compiled for the final report. Another goal is to have more professors look over only the specific section of the report that deals with their specialization. That way, they will be able to focus on a smaller section and critique it with more attention to detail.

General

In general, hard deadlines need to be kept to assure that the project stays on track and all goals are met. Another aim is to increase Purdue faculty involvement